1974

Computation of electric fields for EHV and UHV transmission lines

Harshad Jagmohandas Parekh
Iowa State University

Computation of electric fields for EHV and UHV transmission lines

by

Harshad Jagmohandas Parekh

A Dissertation Submitted to the
Graduate Faculty in Partial Fulfillment of
The Requirements for the Degree of
DOCTOR OF PHILOSOPHY

Major: Electrical Engineering

Approved:

Signature was redacted for privacy.

In Charge of Major Work

Signature was redacted for privacy.

For the Major Department

Signature was redacted for privacy.

For the Graduate College

Iowa State University
Ames, Iowa

1974

TABLE OF CONTENTS

TABLE OF CONTENTS
(Continued)

1. INTRODUCTION

A. Preamble

With the growing demand for the electrical energy, the possibility of transmitting large blocks of this power at ultra high voltage (UHV-1000kv and above) level is being investigated in major industrialized countries of the world. U.S.A., Canada, U.S.S.R., Britain, France and Italy all have experimental experience with transmission at extra high voltage (EHV-500kv to 1000kv) level of around 750kv. The majority of the problems associated with transmission lines operated at UHV level would appear to be solved and the justification for such lines is envisaged as a technological and economical probability within the next decade at any rate in North America and in the U.S.S.R. (1).

Some of the problems associated with the UHV lines are due to the appearance of extremely high electric field near the conductor surface as well as on the ground. Due to the extremely high electric field, the radio interference and the audible noise generated may reach levels higher than the admissible. This problem is of great importance especially in the region where the UHV lines cross urban areas (2).

UHV lines influence their surroundings remarkably by the induced electric field on the ground in the neighborhood of the lines. In spite of the great height of the lines, the values of the electric field intensity might be two or three times higher than that of the present 500kv lines. As a consequence of these electric fields, the induced current flowing through the bodies of people near a UHV line might produce undesirable effects (3).

Another important problem associated with UHV lines is the appearance of corona around the conductor surface (4-5). Corona is regarded as the partial breakdown of air surrounding the conductor. This is caused by the extremely high electric field which appears on the conductor surface as well as in the region closely surrounded by the conductor. The electric power used in ionizing the air surrounding the conductor is known as corona loss. The corona loss represents a loss of revenue and therefore it must be minimized for economical reasons.

The standard way of reducing the corona loss, radio interference and audible noise is to use bundle conductors. A bundle conductor is a group of subconductors all of which operate in parallel to transmit electrical power. The bundle conductor reduces the intensity of electric field on the conductor surface as well as in the space surrounding the conductor. The bundles of eight and more subconductors have been proposed to avoid excessive radio interference and audible noise on UHV lines. This performance can be improved further by using split-bundle conductors in which each subbundle is composed of several subconductors (6-7).

Thus, the knowledge of accurate electric field distribution around conductors of high voltage transmission lines is required to predict the corona loss, radio interference and audible noise levels (8-10). This knowledge is of great help to the designers of EHV and UHV transmission lines.

B. Statement of Problem

The purpose of this dissertation is to compute the electric field distribution around bundle conductors used on practical high voltage

transmission lines. This dissertation describes the extension of the work done by Abou-Seada (11).

Abou-Seada calculated the electric field and potential distribution around a twin-subconductor unipolar and bipolar line by using a charge simulation method. His work was complicated and required trial and error testing to achieve better accuracy of results. Moreover, his work was not applicable for the electric field computation around a bundle of more than two subconductors.

In this dissertation, a method is described which is much simpler and gives better accuracy of the results than that obtained by Abou-Seada. Moreover, this method does not require trial and error testing and is applicable for a bundle of up to eight cylindrical subconductors.

In this dissertation, the section on the electric field computation is divided into five parts. The first part describes a charge simulation method to compute accurately the electric field and potential distribution around high voltage direct current (HVDC) transmission line having smooth cylindrical bundle conductors. The second part describes a method to compute accurately the electric field and potential distribution around split-bundle cylindrical conductors proposed to be used on future UHV lines. The third part describes a computer program which plots very efficiently the equipotential and equigradient lines in the vicinity of bundle conductors used on high voltage transmission lines. The fourth part describes the application of the charge simulation method to compute the electric field and potential distribution around a stranded twin-subconductor bundle. The fifth part describes an analytical method to compute accurately the electric field and potential distribution around a stranded conductor

enclosed by a cylinder. The results obtained by the charge simulation method and the analytical method are compared to check the accuracy of the charge simulation method which is comparatively much easier than the analytical method.

II. REVIEW OF LITERATURE

A. Smooth Cylindrical Conductors

The use of bundle conductors to transmit electric power was first suggested by Thomas in 1909 (12-13). His purpose was to reduce inductance and increase capacitance so that greater power can be transmitted at a given permissible voltage drop.

The calculation of electric field around bundle conductors was first attempted by Crary, reported by Clarke in the thirties (14). He assumed the electric field due to subconductors of other phases negligible and the field produced by other subconductors of the same phase uniform in the region of the subconductor under consideration. His formula for the maximum electric field on the conductor surface of the N-subconductors bundle was

$$E_{ml} = 4q\left\{\sqrt{\left[\sum_{p=1}^{N} \frac{1}{r_{lp}} \cos \phi_{lp}\right]^2 + \left[\sum_{p=1}^{N} \frac{1}{r_{lp}} \sin \phi_{lp}\right]^2} + \frac{1}{d}\right\} \qquad 2.1$$

where

E_{ml} = maximum electric field on the surface of subconductor 1

q = line charge per unit length

r_{lp} = the distance between subconductor 1 and subconductor p in the same phase

ϕ_{lp} = the angle between a line joining the centers of subconductors 1 and p in the same phase and the horizontal line

d = diameter of subconductor 1

Crary's formula was found to give correct values of the maximum electric field only for a ratio of spacing to diameter of subconductors

equal to or greater than five.

Using complex variables and the transformation techniques, Poritsky, reported by Clarke, developed formulas for computing the electric field, potential, and complex potential at any point for a twin-subconductor bundle (14). His formula for the maximum electric field on the conductor surface was

$$E_m = 2\pi q \frac{\sqrt{s}}{rg\sqrt{s+d}} \cdot \frac{1 + 3t^{1.2} - 5t^{2.3} - 7t^{3.4} + 9t^{4.5}}{1 - t^{1.2} - t^{2.3} + t^{3.4} + \ldots\ldots} \qquad 2.2$$

where

q = line charge per unit length

2s = spacing of subconductors

d = diameter of each subconductor

$$g = \log_e \frac{\sqrt{s+d} + \sqrt{s}}{\sqrt{s+d} - \sqrt{s}} \qquad 2.3$$

$$t = e^{-\pi/2g} \qquad 2.4$$

Poritsky's formula is not applicable for a bundle of more than two subconductors. Moreover, Poritsky neglected the effect of the ground.

Adams calculated the electric field for a 3-phase ac transmission line considering only one conductor per phase (15). He represented the charge on each conductor by a single line charge at the center of the conductor. The effect of the ground was taken into consideration by placing an image of each line charge below the ground plane. He calculated first the values of the line charges by solving simultaneous equations which relate the line charges with the potentials on the

conductors. These equations were

$$\begin{aligned} V_1 &= P_{11}q_1 + P_{12}q_2 + \text{-- -- -- -- --} + P_{1N}q_N \\ V_2 &= P_{21}q_1 + P_{22}q_2 + \text{-- -- -- -- --} + P_{2N}q_N \\ &\text{-- -- -- -- -- -- -- -- -- -- -- -- --} \\ &\text{-- -- --- -- -- -- -- -- -- -- -- -- --} \\ V_N &= P_{N1}q_1 + P_{N2}q_2 + \text{-- -- -- -- --} + P_{NN}q_N \end{aligned} \qquad 2.5$$

where

N = number of conductors

V_N = potential of conductor N to ground

P = potential coefficient

q_N = line charge per unit length on conductor N

The values of the potential coefficient were obtained by

$$P_{jj} = \frac{1}{2\pi\epsilon_o} \log_e \frac{2h}{r} \qquad 2.6$$

$$P_{jk} = \frac{1}{2\pi\epsilon_o} \log_e \frac{S_{jk}'}{S_{jk}} \qquad 2.7$$

where

h = height of conductor above ground

ϵ_o = permittivity of free space

r = radius of conductor

S_{jk} = distance between conductors j and k

S_{jk}' = distance between conductor j and the image of conductor k

Since the values of the potential and the potential coefficients were known, the values of the line charges were calculated by solving equation 2.5. Once these values were obtained, the electric field at any desired point was obtained by superimposing the contributions due to the

individual line charges.

Miller used the same method as proposed by Adams and developed formulas to calculate the maximum electric field on the conductor surface for various geometries of smooth cylindrical conductors (16). His formula for the maximum electric field on the surface of a 4-subconductor bundle arranged in a square form was

$$E_m = \frac{2\sqrt{2}}{S} q_1 + \left(\frac{\sqrt{2}}{S} + \frac{4}{d}\right) q_2 \qquad 2.8$$

where

$$q_1 = \frac{B - C}{AB - C^2} \qquad 2.9$$

$$q_2 = \frac{A - C}{AB - C^2} \qquad 2.10$$

$$A = P_{11} + P_{12} \qquad 2.11$$

$$B = P_{33} + P_{34} \qquad 2.12$$

$$C = P_{13} + P_{14} \qquad 2.13$$

$$P_{11} = 2\log_e \frac{4(h + S)}{d} \qquad 2.14$$

$$P_{33} = 2\log_e \frac{4(h - S)}{d} \qquad 2.15$$

$$P_{12} = 2 \log_e \frac{(h + S)}{S} \qquad 2.16$$

$$P_{13} = 2 \log_e \frac{h}{\sqrt{S}} \qquad 2.17$$

$$P_{14} = 2 \log_e \frac{h}{S} \qquad 2.18$$

$$P_{34} = 2 \log_e \frac{(h - S)}{S} \qquad 2.19$$

where

2S = subconductor spacing

d = diameter of subconductor

h = height of subconductors above ground

Based on the work done by Adams and Miller, Reichman calculated the values of the conductor voltage which produced electric field of 16.65 kv per cm. on the conductor surface for different geometrical parameters of bundle conductors used on ac transmission lines (17). The electric field 16.65 kv per cm. was chosen following extensive literature surveys and field tests on the high voltage lines of Hydro-Electric Power Commission of Ontario. It was thought that lines operated at or below this gradient would not produce excessive radio noise in fair weather conditions.

The results obtained by Adams, Miller and Reichman were not accurate because of the fact that the equipotential surfaces resulting from the line charges (assumed to be at the centers of the subconductors) did not coincide with the subconductor surfaces. This meant that one of the boundary conditions which required that the subconductor surfaces be equipotential surfaces was not satisfied. This was the source of error in the results obtained by Adams, Miller and Reichman.

King proposed a method of calculating the electric field near a bundle conductor by replacing the N subconductors of the bundle by N equivalent line charges of very small radius which was negligible in comparison with the spacing between the subconductors (18). These equivalent line charges were displaced from the centers of the subconductors by such an amount that one set of equipotential points coincided with the points of the maximum and the minimum electric fields

at the subconductor surfaces.

The displacement of the equivalent line charges from the centers of the subconductors was given by

$$\sigma = \frac{d}{2}\sqrt{\left\{\frac{1}{2}\left[\left(\frac{D}{d}+1\right)^N + \left(\frac{D}{d}-1\right)^N\right]\right\}} - \frac{D}{2} \qquad 2.20$$

where

d = diameter of subconductor

D = diameter of bundle circle

N = number of subconductors in a bundle

King's method gave accurate values of the maximum electric field on the conductor surface but considerable deviation of the equipotential points from the corresponding points on the conductor surface occurred in the region between the maximum and the minimum electric fields. King neglected the effect of the ground.

Sreenivasan gave formulas to plot the equipotential and the equigradient lines in the vicinity of a bundle of two subconductors (19). He represented the actual charge on each subconductor by an axial line charge positioned at a small distance from the center of the subconductor. His formula for this small displacement was

$$\sigma = \frac{(r^2/2S)}{1 + (r/S) - (r^2/2S^2)} \qquad 2.21$$

where

r = radius of subconductor

2S = spacing of subconductors

Sreenivasan assumed very small ratio of subconductor radius to subconductor spacing and neglected the effect of the ground. Moreover, his

work was not applicable for a bundle of more than two subconductors.

Timascheff proposed a method to plot equipotential and flux lines around a bundle of any number of subconductors by using the method of conformal mapping (20). He considered a single thin conductor of radius α at point $(1, j0)$ in the complex W plane. This conductor was transformed into Z plane by using a transformation

$$Z^N = W \qquad 2.22$$

where N was the number of subconductors in the bundle. The transformed conductor in the Z plane was made to coincide with one of the subconductors of the bundle. Timascheff's formula to calculate the suitable value of α from the known values of the subconductor spacing 2S, the subconductor radius r and the number of subconductors N was

$$\frac{S}{r} = \sin\left(\frac{\pi}{N}\right) \cdot \frac{\sqrt[N]{1+\alpha} + \sqrt[N]{1-\alpha}}{\sqrt[N]{1+\alpha} - \sqrt[N]{1-\alpha}} \qquad 2.23$$

In his analysis, Timascheff assumed very small ratio of the subconductor radius to the subconductor spacing and neglected the effect of the ground. Moreover, his method failed to give any generalized solution to find the electric field at any point on the conductor surface or in the interelectrode space.

Timascheff extended the application of his method to find the electric field at any point in the vicinity of bundle conductors and plot equigradient lines (21). His formula to calculate the relative electric field at any point (x, y) was

$$\lambda = \frac{E}{E_{max}} = \left[\frac{\alpha}{(1+\alpha)^{(N-1)/N}}\right] \cdot \frac{1}{\rho} \cdot (1 + 2\rho\cos\phi + \rho^2)^{N-(1/2N)} \qquad 2.24$$

where α was obtained from the equation 2.23 and

$$\rho = |Z|^N \sin N\beta / \sin\phi \qquad 2.25$$

$$\phi = \tan^{-1}[|Z|^N \sin N\beta / (|Z|^N \cos N\beta - 1)] \qquad 2.26$$

$$|Z| = \sqrt{x^2 + y^2} \qquad 2.27$$

$$\beta = \tan^{-1}(y/x) \qquad 2.28$$

In this work too, Timascheff assumed very small ratio of the subconductor radius to the subconductor spacing and neglected the effect of the ground.

Sarma and Janischewskyj used the method of successive images (22-25) to calculate the electrostatic field of a system of parallel cylindrical conductors. Their method was based on the concept of representing the distributed charge on the conductor's surface by a system of line charges inside the conductor's surface in such a way that one of the equipotential surfaces resulting from the line charges coincided with the conductor surface. The well known fact that the electric field of long line charge +q C/m placed parallel to a long conducting cylinder can be calculated by representing the induced charge on the cylinder's surface by a long line charge -q C/m placed at a distance σ from the center of the cylinder, was used in their method. The displacement σ was given by

$$\sigma = r^2/2S \qquad 2.29$$

where

r = radius of cylinder

2S = distance between line charge +q C/m and the center of the cylinder

Using the above fact in the process of successive imaging, Sarma and Janischewskyj calculated the electric field around the bundle conductors. The effect of the ground was taken into consideration by placing images of the line charges below the ground plane. In general, for N parallel conductors system, at the end of the first order imaging process, 2N - 1 line charges were placed inside each conductor. At the end of the second order imaging process, there were $(2N - 1)^2$ line charges inside each conductor. As the order of the imaging process became higher, the accuracy of the results became better. At the end of the K^{th} order imaging process, there were $(2N - 1)^K$ number of line charges inside each conductor. The order of the imaging process required to attain any desired degree of accuracy depended on r/2S ratio. If this ratio was smaller, the order of the imaging process was lower.

The values of the electric field obtained by Sarma and Janischewskyj were accurate but for higher ratios of r/2S, the number of the line charges required to simulate the parallel conductors system became very large. This made their method complicated to use for the electric field computation for bundle conductor transmission line.

Abou-Seada and Nasser used the method of charge simulation to calculate the electric field and potential around a twin-subconductor bundle (26-27). In this method, the actual charge distribution on each subconductor surface was represented by several fictitious line charges placed inside each subconductor. These line charges of unknown magnitudes were placed on a fictitious cylinder whose radius was half of the subconductor radius. The correct angular positions of these line

charges on the fictitious cylinder were determined by trial and error testing to achieve better accuracy of the results.

The values of the potential (due to all the fictitious line charges and their images below the ground) at few selected points on the subconductor surface were calculated and equated to one unit which was the assumed potential of each subconductor. The first, second and the fourth derivatives of these potentials with respect to the angular coordinate were calculated and equated to zero to obtain the subconductor surface as an equipotential surface. This process yielded a set of simultaneous equations in terms of the unknown line charges and when solved with the digital computer, gave the values of the fictitious line charges. Once the values of the line charges were known, potentials at many other points on the conductor surface were calculated to check if the subconductor surface resulted in an equipotential surface. If this was the case, then the values of the potential and the electric field at any desired point on the conductor surface or in interelectrode space were calculated by superimposing the contribution due to the individual line charges and their images. If this was not the case, then the angular positions of the line charges on the fictitious cylinder were changed until the subconductor surface resulted in an equipotential surface.

The results obtained by Abou-Seada and Nasser gave an error of about one percent in the values of the direction of electric field. Moreover, their method was complicated to use, required trial and error testing and was applicable only for the case of a twin-subconductor bundle.

Thanassoulis and Comsa proposed a dipole method to calculate the

maximum electric field on the surface of an N-subconductor bundle (28, b). In this method, each charged subconductor of the bundle was represented by a line charge of q C/m placed at its center, plus N - 1 pairs of line charges of equal magnitude but of opposite sign. These line charges were separated by a small distance σ so that they formed an electric dipole of moment $\overline{P} = q\,\overline{\sigma}$. Then the maximum electric field on the surface of the subconductor under consideration was calculated by taking the vector sum of all the electric fields due to the line charges and the dipoles. This method was also used to calculate the maximum electric field on the surface of a split-bundle conductor in which each subbundle was divided into several subconductors.

The dipole method did not give accurate values of the maximum electric field because of many simplifying assumptions made in the theoretical analysis. In this method, the effect of the ground was neglected. In the case of the split-bundle conductor, the field produced by the subconductors in other subbundles was assumed uniform in the region of the subbundle with the subconductor under consideration. Moreover, the subconductors of the subbundle were assumed to be placed on the circumference of a circle and the centers of the subbundles were assumed to lie on the circumference of a bigger circle.

The dipole method failed to give the values of the electric field in the interelectrode space. These values are necessary for the theoretical analysis of dc corona losses on practical high voltage transmission lines (29-30).

B. Stranded Conductors

In all the researches described above, the bundle conductors were assumed to be perfectly smooth and cylindrical. Since the practical transmission lines consist of stranded bundle conductors, the problem of electric field computation for these conductors is of practical importance. Almost no attempt has been made to solve this problem because of the complexity involved in the problem.

The usual procedure to predict the maximum electric field on the surface of the stranded conductors is to use strand factors which are determined experimentally. The strand factor is defined as the ratio of the electric field of a smooth cylindrical conductor to that of a stranded conductor of the same radius. Since the values of the electric field on the surface of the stranded conductor vary from the maximum at the tips to zero at the discontinuity points (where two strands intersect each other), the values of the strand factor vary at different points on the conductor surface. Moreover, the values of the strand factor also depend on the number of strands in the stranded conductor.

Only recently the problem of electric field computation around an isolated stranded conductor has been attempted by Andrews and Shrapnel (31). They calculated semi-analytically the distribution of electric field by solving Laplace's equation in the space surrounding the stranded conductor.

The effect of ground was neglected in the above method and it was not applicable for bundle conductors as used in practical EHV transmission lines. Thus, the problem of electric field computation for practical transmission lines having stranded bundle conductors yet remains to be solved.

III. COMPUTATION OF ELECTRIC FIELD AND POTENTIAL

This section describes mainly the charge simulation method for computing accurately the electric field and potential distribution around bundle conductors used on high voltage transmission lines. This section is divided into five parts. Part A describes the charge simulation method for computing the electric field and potential distribution around HVDC bipolar transmission lines. Part B describes the computation of electric field and potential distribution around split-bundle transmission lines. Part C describes a computer program to plot equipotential and equigradient lines in the vicinity of HVDC bipolar and split-bundle transmission lines. Part D describes the application of the charge simulation method for computing the electric field and potential distribution around a stranded two-subconductor bundle. The last part E describes an analytical method for computing accurately the electrical field distribution around a stranded conductor enclosed by a cylinder. In this part, the results obtained by the charge simulation method are compared with those obtained by the analytical method to check the accuracy of the charge simulation method.

A. HVDC Bipolar Transmission Lines

1. General

HVDC transmission lines are being increasingly used to transmit large blocks of power over long distances. This is attributed to the economical and electrical advantages it offers over conventional high

voltage ac transmission lines (32-33). For transmission schemes envisaged within the next decade, HVDC application of the bipolar line would require voltages of the order of ±600 kv (34). The knowledge of the electric field and potential distribution around HVDC bipolar lines is essential to predict corona onset voltage, corona loss and the radio interference (30).

2. Method of computation

The method employed for computing the electric field and potential distribution around HVDC bipolar lines is known as charge simulation method. In this method, the actual charge distribution on the conductor surface is represented by several fictitious line charges inside the conductor surface and their images represent the effect of the ground. These unknown line charges can be placed at any desired position inside the conductor surface. To satisfy the boundary condition at the conductor surface, one of the equipotential surfaces resulting from the fictitious charges and their images must coincide with the conductor surface.

Potential at any point is given by the sum of the potentials due to the individual unknown fictitious line charges. Obtaining the potentials at various points on the conductor surface where the values of the potential are all equal and which are the same as the conductor potential, yields a number of simultaneous equations in terms of the unknown line charges. These equations, when solved with a digital computer, give the values of the line charges. Once the values of these charges are known, potentials at many other points on the conductor surface are computed to check if the conductor surface results in an equipotential

surface. If this is the case, then electric field and potential at any point on the conductor surface can be easily computed.

3. Mathematical formulas of simulation

The various configurations of the HVDC bipolar transmission line considered in this section are shown in Figures 3.1-3.3. Figure 3.1 shows the bipolar line with four positive subconductors and four negative subconductors. Figure 3.2 shows the bipolar lines with two positive subconductors and two negative subconductors. Figure 3.3 shows a simple bipolar line with one positive and one negative conductor. Since the bipolar lines of Figures 3.2 and 3.3 are the special cases of the bipolar line of Figure 3.1, the mathematical formulation for only the more general case of Figure 3.1 is explained here. The bipolar lines of Figure 3.2 are obtained from the general case of Figure 3.1 by letting B = 0 [horizontal arrangement of Figure 3.2 (a)] or A = 0 [vertical arrangement of Figure 3.2 (b)]. The simple bipolar line of Figure 3.3 is obtained from the general case of Figure 3.1 by letting A = 0 and B = 0 simultaneously.

As shown in Figure 3.4, the actual charge distribution on the surface of the positive conductor is represented by axial line charges of unknown magnitudes Q(K), where K = 1,2,3,-----,N. These charges are placed symmetrically on a coaxial cylinder of radius RQ inside each positive subconductor. The locations of these line charges are given by angles measured from the horizontal plane in counter clockwise direction. These angles are designated

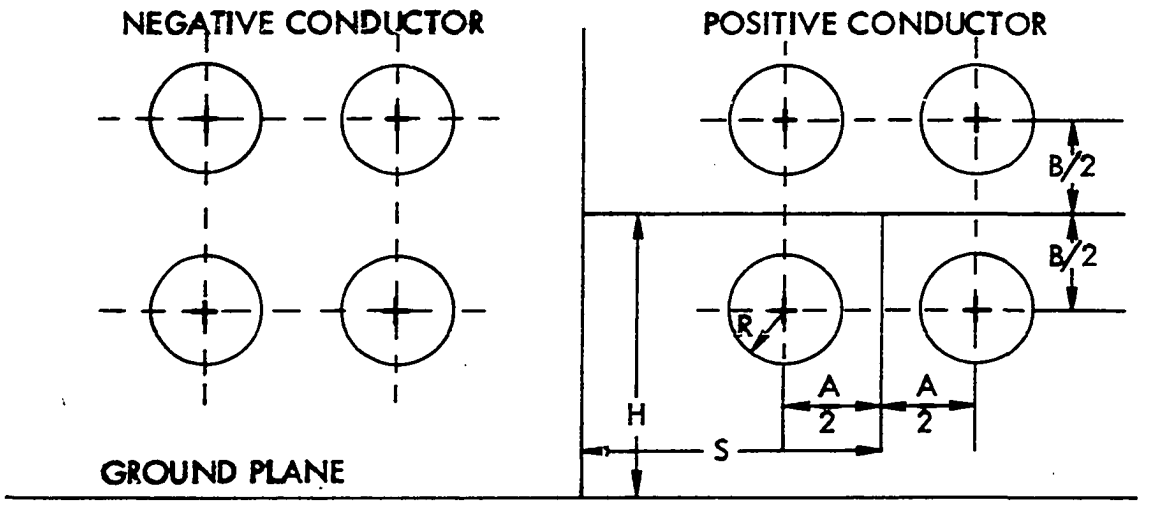

Figure 3.1. Bipolar line with four positive and four negative subconductors.

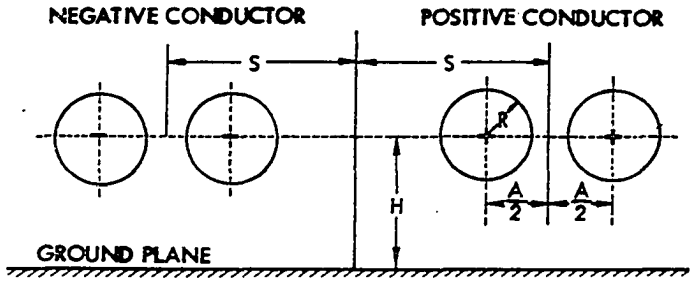

(a)

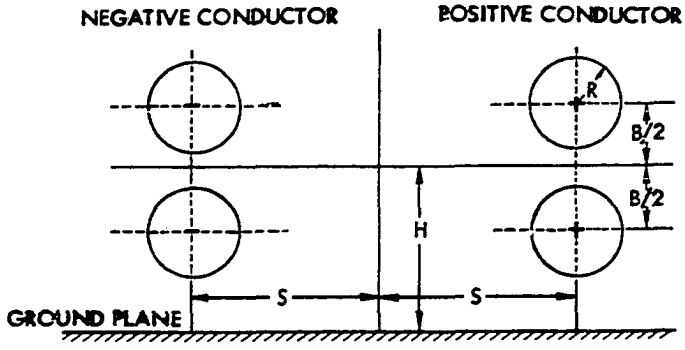

(b)

Figure 3.2. Bipolar line with two positive and two negative sub-conductors.
(a) horizontal arrangement
(b) vertical arrangement

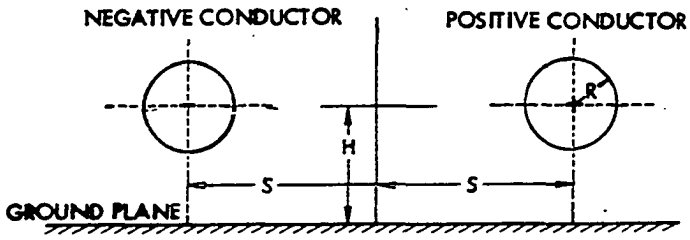

Figure 3.3. Simple bipolar line with one positive and one negative subconductor.

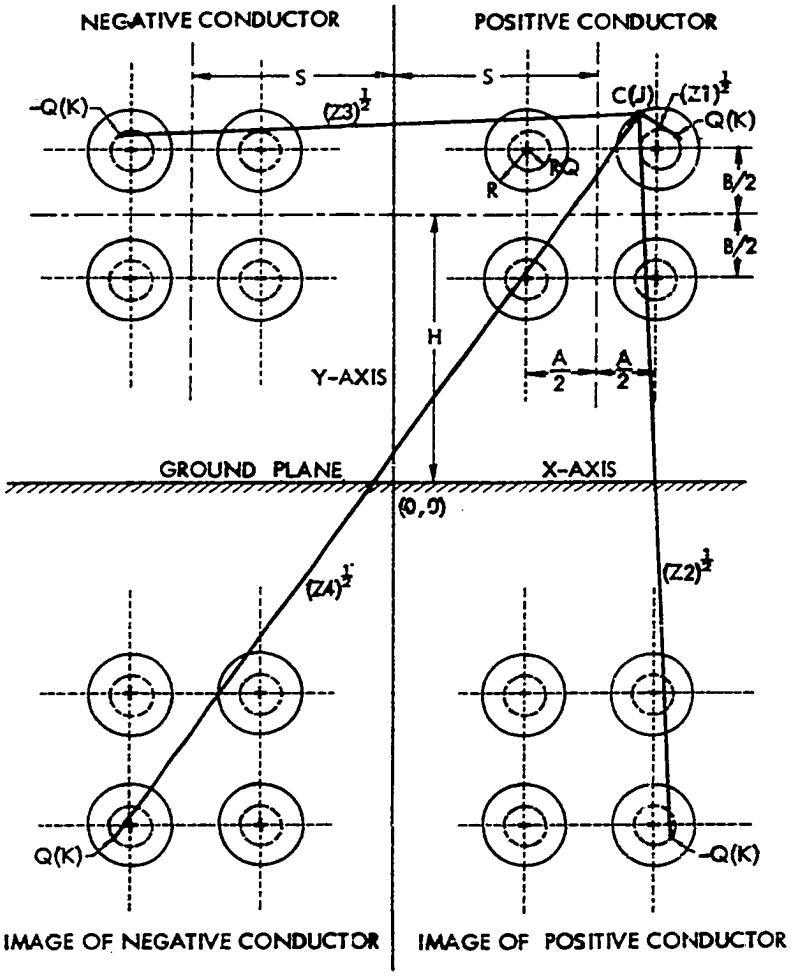

Figure 3.4. Charge representation of bipolar transmission line.

$$\alpha(K) = (K-1)\cdot(360/NN),\ K = 1,2,3,.....,NN \qquad 3.1$$

where

$$NN = N/4 \qquad 3.2$$

The X and Y coordinates of the axial line charges placed inside positive subconductors are given by

$$XQ(K1) = S + (A/2) + RQ.\cos[\alpha(K1)] \qquad 3.3$$

$$YQ(K1) = H + (B/2) + RQ\cdot\sin[\alpha(K1)] \qquad 3.4$$

where

$$K1 = 1,2,3,.....,NN \qquad 3.5$$

and

$$XQ(K2) = S - (A/2) + RQ\cdot\cos[\alpha(K1)] \qquad 3.6$$

$$YQ(K2) = YQ(K1) \qquad 3.7$$

where

$$K1 = 1,2,3,.....,NN \qquad 3.5$$

$$K2 = K1 + NN \qquad 3.8$$

and

$$XQ(K3) = XQ(K2) \qquad 3.9$$

$$YQ(K3) = H - (B/2) + RQ\cdot\sin[\alpha(K1)] \qquad 3.10$$

where

$$K1 = 1,2,3,.....,NN \qquad 3.5$$

$$K2 = K1 + NN \qquad 3.8$$

$$K3 = K1 + (2\cdot NN) \qquad 3.11$$

and

$$XQ(K4) = XQ(K1) \qquad 3.12$$

$$YQ(K4) = YQ(K3) \qquad 3.13$$

where

$$K1 = 1,2,3,.....,NN \qquad 3.5$$

$$K3 = K1 + (2 \cdot NN) \qquad 3.11$$

$$K4 = K1 + (3 \cdot NN) \qquad 3.14$$

The magnitudes and positions of the axial line charges inside the negative conductor are obtained by taking images (of the positive conductor's charges) with respect to the Y-axis. Image charges of both the positive and the negative conductor charges are placed on the other side of the ground which is assumed to be of zero potential.

The potential at any point on the conductor's surface must be equal to the assumed value of one unit. To satisfy this boundary condition, points C(J), J = 1,2,3,....,N are chosen on the positive conductor's surface and the potentials at these points are calculated and equated to one unit. The X and Y coordinates of the points C(J) are designated XC(J) and YC(J). These coordinates are given by Equations 3.3-3.14 except the radius RQ is replaced by the subconductor radius R.

The potential $\emptyset[C(J)]$ at any point C(J) on the conductor surface is given by

$$\emptyset[C(J)] = \sum_{K=1}^{N} \frac{Q(K)}{2\pi\epsilon_o} \cdot \tfrac{1}{2} \log_e \frac{(Z2 \cdot Z3)}{(Z1 \cdot Z4)} = 1.0 \qquad 3.15$$

where ϵ_o is the permittivity of the free space, J = 1,2,3,...., N and the square of the distances Z1, Z2, Z3, and Z4 are as shown in Figure 3.4 and given by

$$Z1 = X1 \cdot X1 + Y1 \cdot Y1 \qquad 3.16$$

$$Z2 = X1 \cdot X1 + Y2 \cdot Y2 \qquad 3.17$$

$$Z3 = X2 \cdot X2 + Y1 \cdot Y1 \qquad 3.18$$

$$Z4 = X2 \cdot X2 + Y2 \cdot Y2 \qquad 3.19$$

where

$$X1 = XC(J) - XQ(K) \qquad 3.20$$

$$X2 = XC(J) + XQ(K) \qquad 3.21$$

$$Y1 = YC(J) - YQ(K) \qquad 3.22$$

$$Y2 = YC(J) + YQ(K) \qquad 3.23$$

where

$$J = 1,2,3,.....,N$$

$$K = 1,2,3,.....,N$$

Equation 3.15 represents a set of simultaneous equations which can be solved with a digital computer to obtain the values of the axial line charges Q(K). Once the values of the line charges are known, potential and electric field at any desired point on the conductor surface or in the outside space can be easily computed. The Equations necessary to compute the potential and the electric field in X and Y direction at any point (x,y) are given by

$$\phi(x,y) = \sum_{K=1}^{N} \frac{Q(K)}{2\pi\epsilon_o} \cdot \tfrac{1}{2} \cdot \log_e \frac{(Z2 \cdot Z3)}{(Z1 \cdot Z4)} \qquad 3.24$$

$$E_X(x,y) = \sum_{K=1}^{N} \frac{Q(K)}{2\pi\epsilon_o} \cdot \left[\frac{X1}{Z1} + \frac{X2}{Z4} - \frac{X1}{Z2} - \frac{X2}{Z3} \right] \qquad 3.25$$

$$E_Y(x,y) = \sum_{K=1}^{N} \frac{Q(K)}{2\pi\epsilon_o} \cdot \left[\frac{Y1}{Z1} + \frac{Y2}{Z4} - \frac{Y2}{Z2} - \frac{Y1}{Z3} \right] \qquad 3.26$$

where Equations 3.16-3.23 can be used with XC(J) and YC(J) replaced by x and y respectively.

4. Programming

A computer program is written for computing the electric field and potential distribution for the dc bipolar line shown in Figure 3.4. The computer program is written in FORTRAN IV language for the IBM 360 computer available at the computation center, Iowa State University. Double precision arithmetic is used throughout the main program and the subroutine. The simultaneous equations 3.15 representing the boundary conditions are solved using a subroutine which operates on the method of Gauss elimination with complete pivotting.

The main computational steps are illustrated in the flow chart of Figure 3.5. The radius RQ of the fictitious cylinder on which the line charges are placed is taken as 0.5 R. The total number of the axial line charges N is taken as 60. These values of RQ and N give accurate results. The solution of the simultaneous equations 3.15 gives the values of the unknown line charges. These are used in computing the potential and the field anywhere on the conductor's surface and in the outside space. The computer program is given in Appendix A.

5. Results

Results are obtained for the bipolar line with four positive subconductors and four negative subconductors. The following values of the geometrical parameters are chosen to illustrate the results:

subconductor radius = 2.0 cm.

conductor height = 1500 cm.

subconductor separation = 50 cm.

conductor separation = 1000 cm.

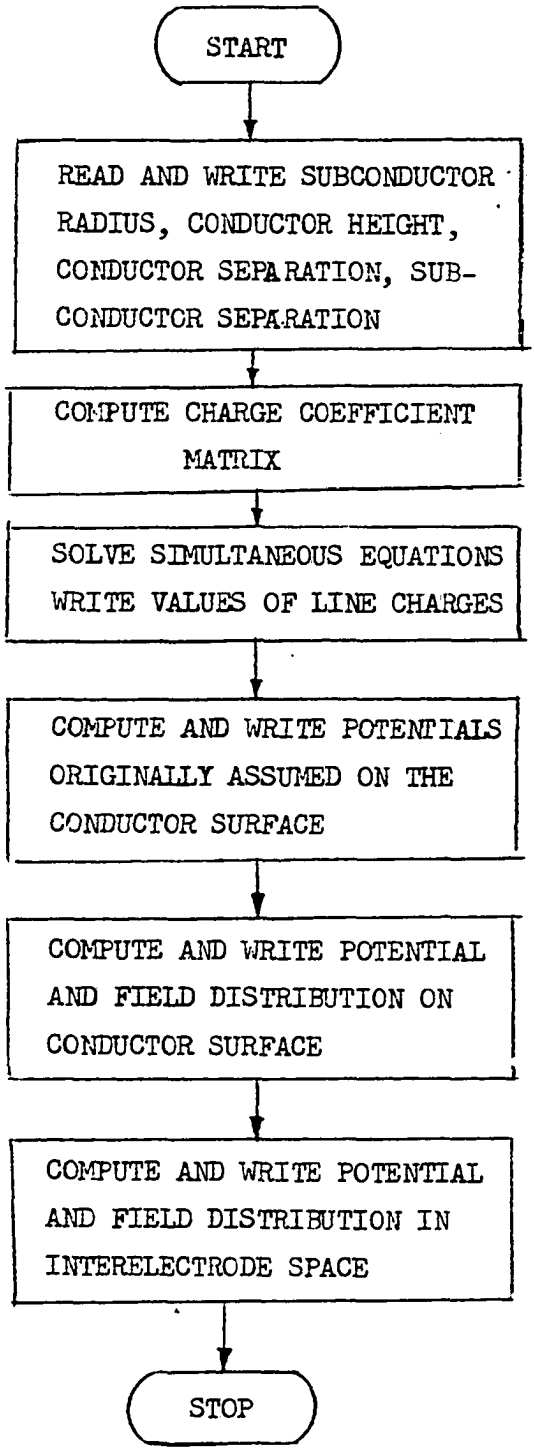

Figure 3.5. Main flow chart.

The values of the line charges obtained by solving the simultaneous equations 3.15 are shown in Table 3.1. Since the conductor potential is assumed to be of one unit, the value of capacitance between the positive conductor and the ground is obtained simply by summing the values of all the line charges shown in Table 3.1 and multiplying the sum by $2\pi\epsilon_o$. The value of the capacitance for the case considered is 0.15205×10^{-10} Farad/meter.

Using the values of the line charges shown in Table 3.1, potential and electric field at 120 points on each positive subconductor are computed. The values of the potential at these points are found to be one unit and the directions of the electric field are found to be perpendicular to the conductor surface. This means that the boundary conditions are satisfied very well. For the purpose of simplicity, the values of the potential and the electric field at only 8 points on each subconductor are shown in Figure 3.6 with Table 3.2.

As seen from Table 3.2, the values of the electric potential on the conductor surface are one unit and the directions of the electric field are perpendicular to the conductor surface. The highest electric field intensity on the conductor's surface appears at point 6 of SW subconductor. This value is 0.041081 (volt/cm) per volt. While calculating the values of the electric field at many points on the conductor's surface, it was found that the actual location of the maximum electric field was at few degrees above point 6 of SW subconductor, although the difference in magnitudes of the field at these points was very small. The actual location of the maximum electric field is affected by the geometrical parameters of the bipolar line.

Table 3.1. Values of line charges obtained by solving the simultaneous Equations 3.15 -- [(Coulomb/m /volt)]/$2\pi\epsilon_o$

Q(1)	0.005425	Q(21)	0.006180	Q(41)	0.006194
Q(2)	0.005750	A(22)	0.006245	Q(42)	0.005884
Q(3)	0.005861	Q(23)	0.006055	Q(43)	0.005367
Q(4)	0.005745	Q(24)	0.005628	Q(44)	0.004718
Q(5)	0.005411	Q(25)	0.005023	Q(45)	0.004046
Q(6)	0.004901	Q(26)	0.004338	Q(46)	0.005435
Q(7)	0.004293	Q(27)	0.003703	Q(47)	0.004934
Q(8)	0.003697	Q(28)	0.003240	Q(48)	0.004333
Q(9)	0.003231	Q(29)	0.003033	Q(49)	0.003737
Q(10)	0.002983	Q(30)	0.003114	Q(50)	0.003261
Q(11)	0.002993	Q(31)	0.003477	Q(51)	0.002995
Q(12)	0.003260	Q(32)	0.003118	Q(52)	0.002986
Q(13)	0.003736	Q(33)	0.003035	Q(53)	0.003237
Q(14)	0.004330	Q(34)	0.003241	Q(54)	0.003707
Q(15)	0.004927	Q(35)	0.003704	Q(55)	0.004305
Q(16)	0.003469	Q(36)	0.004340	Q(56)	0.004917
Q(17)	0.004035	Q(37)	0.005027	Q(57)	0.005428
Q(18)	0.004705	Q(38)	0.005635	Q(58)	0.005762
Q(19)	0.005352	Q(39)	0.006064	Q(59)	0.005877
Q(20)	0.005868	Q(40)	0.006258	Q(60)	0.005763

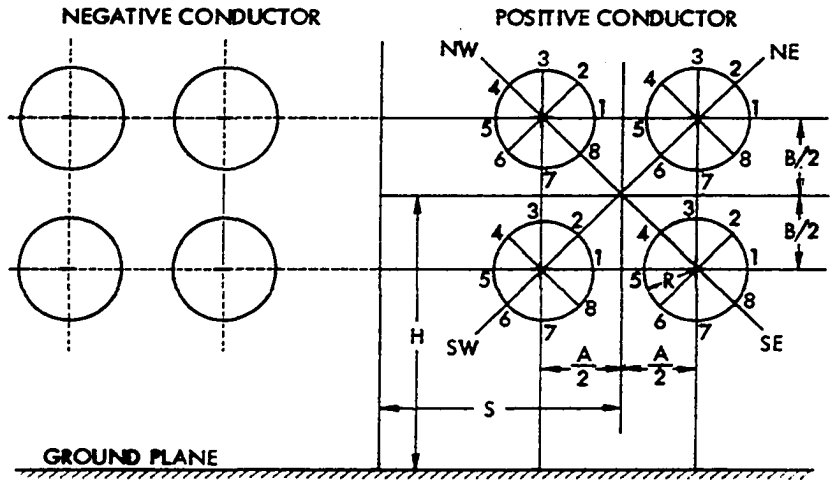

Figure 3.6. Configuration for bipolar line.
R=2 cm, H=1500 cm, A=50 cm, B=50 cm, S=500 cm.

Table 3.2. Distribution of potential and electric field on positive conductor's surface (Potential was "1.000000" on all entries)

Positive subconductor number	Point number	Electric field in x-direction	Electric field in y-direction	Electric field magnitude	Angle of electric field
NE	1	0.036977	0.000000	0.036977	0.000289
"	2	0.027349	0.027349	0.038677	44.998532
"	3	0.000001	0.037299	0.037299	89.997938
"	4	-0.023722	-0.023723	0.033549	134.998991
"	5	-0.029558	0.000000	0.029558	-179.999741
"	6	-0.019627	-0.019628	0.027758	-134.999199
"	7	0.000001	-0.029251	0.029251	-89.998649
"	8	0.023409	-0.023407	0.033104	-44.998470
NW	1	0.030513	0.000000	0.030513	0.000411
"	2	0.024585	0.024584	0.034768	44.999145
"	3	0.000001	0.039081	0.039081	89.998007
"	4	-0.028991	0.028993	0.041001	134.998493
"	5	-0.039488	-0.000000	0.039488	-179.999850
"	6	-0.024978	-0.024979	0.035325	-134.998535
"	7	0.000001	-0.030893	0.030893	-89.998729
"	8	0.020424	-0.020423	0.028883	-44.999252
SW	1	0.030571	-0.000000	0.030571	-0.000413
"	2	0.020452	0.020452	0.028923	44.999179
"	3	0.000001	0.030926	0.030926	89.998658
"	4	-0.025007	0.025009	0.035367	134.998464
"	5	-0.039548	0.000000	0.039548	179.999776
"	6	-0.029048	-0.029049	0.041081	-134.998565
"	7	0.000001	-0.039169	0.039169	-89.998077
"	8	0.024641	-0.024640	0.034847	-44.999216
SE	1	0.037048	-0.000000	0.037048	-0.000292
"	2	0.023443	0.023441	0.033152	44.998398
"	3	0.000001	0.029288	0.029288	89.998579
"	4	-0.019658	0.019659	0.027801	134.999127
"	5	-0.029620	0.000000	0.029620	179.999667
"	6	-0.023783	-0.023784	0.033635	-134.999063
"	7	0.000001	-0.037397	0.037397	-89.998009
"	8	0.027414	-0.027413	0.038768	-44.998604

Table 3.2 illustrates the wide variation of the electric field on the conductor's surface. For the results shown in Table 3.2, the ratio of the minimum to the maximum electric field on the surface of each subconductor is approximately equal to 0.71.

The potential and the electric field distribution for the bipolar line of two subconductors arranged horizontally [Figure 3.2(a)] is obtained by letting B = 0 in the computer program written for the bipolar line of four subconductors. The values of the electric field and the potential at eight points on each subconductor are shown in Figure 3.7 with Table 3.3.

As seen from Table 3.3, the values of the electric potential on the conductor surface are one unit and the directions of the electric field are perpendicular to the conductor surface. This indicates that the boundary conditions are well satisfied. The highest electric field intensity on the conductor's surface appears at point 5 of W subconductor. This value is 0.060270 (volt/cm) per volt. For the geometrical parameters of Figure 3.7, the ratic of the minimum to the maximum electric field on the surface of E subconductor is 0.049920/0.058064 = 0.86. This ratio for W subconductor is 0.050791/0.060270 = 0.845.

The actual location of the maximum electric field is near point 5 but its magnitude is only slightly greater than that at point 5. The maximum electric field for this case is about 46.8 percent higher than the corresponding value for the four subconductor bipolar line.

The potential and the electric field distribution for the bipolar line of two subconductors arranged vertically [Figure 3.2(b)] is obtained by letting A = 0 in the computer program written for the bipolar line of

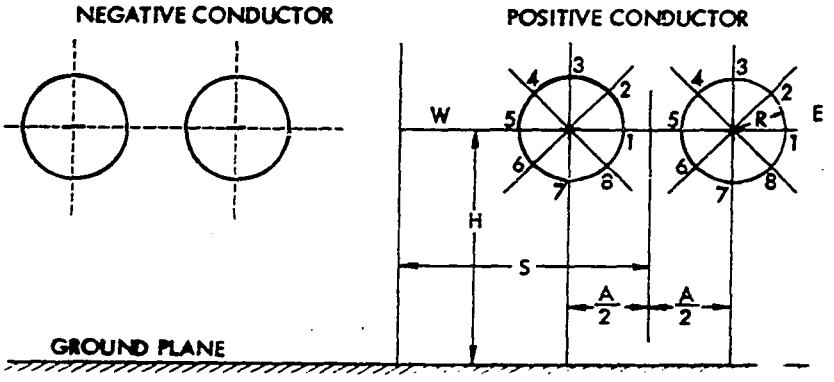

Figure 3.7. Configuration for twin-bundle dc bipolar line (horizontal arrangement) R = 2.0 cm, H = 1500 cm, A = 50 cm, S = 500 cm.

Table 3.3. Distribution of potential and electric field on positive conductor's surface (The potential was "1.000000" on all entries)

Positive subconductor number	Point number	Electric field in x-direction	Electric field in y-direction	Electric field magnitude	Angle of electric field
E	1	0.058064	-0.000000	0.058064	-0.000001
"	2	0.040326	0.040324	0.057027	44.998595
"	3	0.000002	0.054330	0.054330	89.998190
"	4	-0.036266	0.036268	0.051289	134.998976
"	5	-0.049920	0.000000	0.049920	179.999999
"	6	-0.036282	-0.036282	0.051311	-134.999048
"	7	0.000002	-0.054360	0.054360	-89.998260
"	8	0.040341	-0.040339	0.057049	-44.998668
W	1	0.050791	-0.000000	0.050791	-0.000001
"	2	0.037019	0.037018	0.052352	44.999058
"	3	0.000002	0.055861	0.055861	89.998237
"	4	-0.041743	0.041745	0.059035	134.998592
"	5	-0.060270	0.000000	0.060270	179.999999
"	6	-0.041757	-0.041759	0.059054	-134.998664
"	7	0.000002	-0.055889	0.055889	-89.998308
"	8	0.037033	-0.037032	0.052372	-44.999130

four subconductors. The values of the electric field and the potential at eight points on each subconductor of the positive subconductor are shown in Figure 3.8 with Table 3.4.

As seen from Table 3.4, the values of the electric potential on the conductor surface are one unit and the directions of the electric field are perpendicular to the conductor surface. This indicates that the boundary conditions are well satisfied. The highest electric field intensity on the conductor surface appears at point 7 of S subconductor. This value is 0.059165 volt/cm per volt. For the geometrical parameters of Figure 3.8, the ratio of the minimum to the maximum electric field on the surface of N subconductor is 0.050342/0.059083 = 0.85. This ratio for S subconductor is 0.050374/0.059165 = 0.85.

The actual location of the maximum electric field is near point 7 of S subconductor although its magnitude is only slightly greater than at point 7. The maximum electric field for this case is about 44 percent higher than the corresponding value for the four subconductor bipolar line.

The potential and the electric field distribution for the simple bipolar line with one positive conductor and one negative conductor (Figure 3.3) is obtained by letting A = 0 and B = 0 in the computer program written for the general case with few changes. The values of the electric field and potential at eight points on the positive conductor are shown in Figure 3.9 with Table 3.5.

As seen from Table 3.5, the boundary conditions on the conductor surface are well satisfied. The highest electric field intensity appears

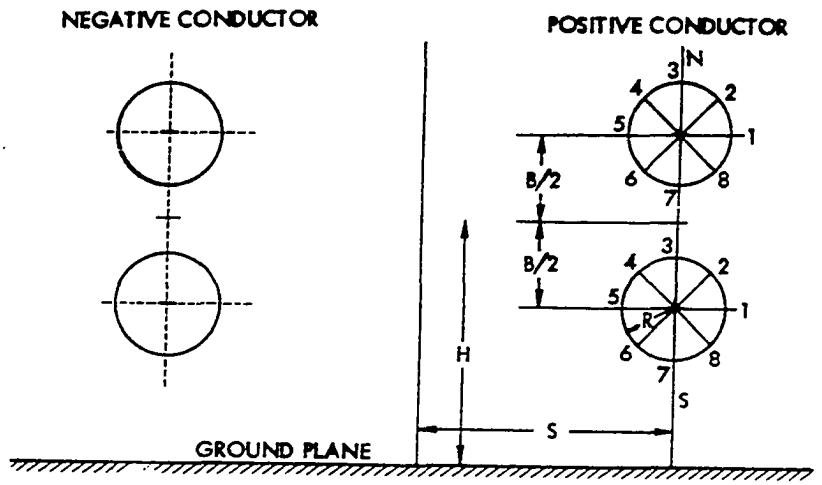

Figure 3.8. Configuration for twin-bundle dc bipolar line (vertical arrangement). R = 2.0 cm, H = 1500 cm, B = 50 cm, S = 500 cm.

Table 3.4. Distribution of potential and electric field on positive conductor's surface (The potential was "1.000000" on all entries)

Positive subconductor number	Point number	Electric field in x-direction	Electric field in y-direction	Electric field magnitude	Angle of electric field
N	1	0.054672	0.000000	0.054672	0.000225
"	2	0.040795	0.040793	0.056792	44.998771
"	3	0.000002	0.059083	0.059083	89.998715
"	4	-0.041186	0.041188	0.058247	134.998715
"	5	-0.055458	-0.000000	0.055458	-179.999895
"	6	-0.036830	-0.036832	0.052087	-134.998805
"	7	0.000001	-0.050342	0.050342	-89.998608
"	8	0.036438	-0.036437	0.051531	-44.998790
S	1	0.054730	-0.000000	0.054730	0.000227
"	2	0.036467	0.036465	0.051571	44.998718
"	3	0.000001	0.050374	0.050374	89.998537
"	4	-0.036857	0.036859	0.052126	134.998733
"	5	-0.055513	0.000000	0.055513	179.999822
"	6	-0.041238	-0.041240	0.058321	-134.998787
"	7	0.000002	-0.059165	0.059165	-89.998164
"	8	0.040848	-0.040847	0.057767	-44.998843

at point 5 of the positive conductor. This value is 0.081434 volt/cm per volt and it is about 98 percent higher than the corresponding value for the bipolar line of four subconductors, about 37.7 percent higher than the corresponding value for the bipolar line of two subconductors of Figure 3.8 and about 35 percent higher than the corresponding value for the bipolar line of two subconductors of Figure 3.7.

The knowledge of the maximum electric field occurring at the conductor surface and the value of capacitance is important in the design of high voltage transmission lines. The advantage of using the charge simulation method is that the capacitance of a conductor is obtained simply by summing the values of all the fictitious line charges obtained by solving the simultaneous Equations 3.15.

Figures 3.10-3.13 illustrate the effect of geometrical parameters on the maximum electric field and the capacitance for the different configurations of the dc bipolar lines.

Figure 3.10 illustrates the variation of the maximum electric field and the capacitance with subconductor radius. As the radius increases, the electric field decreases but the capacitance increases. Moreover, by increasing the number of subconductors, the electric field is reduced but the capacitance is increased.

Figure 3.11 illustrates the variation of the maximum electric field and the capacitance with conductor height. It can be seen that the effect of the conductor height on the maximum electric field and the capacitance is negligible. The difference in the value of the maximum electric field for two different heights of 10 m and 20 m is about 2 percent.

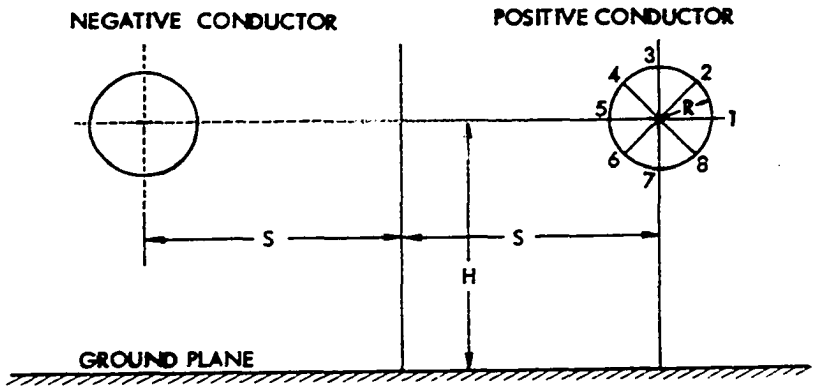

Figure 3.9. Configuration for simple dc bipolar line. R = 2.0 cm, H = 1500 cm, S = 500 cm.

Table 3.5. Distribution of potential and electric field on positive conductor's surface

Point number	Potential	Electric field in x-direction	Electric field in y-direction	Electric field magnitude	Angle of electric field
1	1.000000	0.080854	-0.000000	0.080854	-0.000001
2	1.000000	0.057228	0.057226	0.080931	44.998774
3	1.000000	0.000002	0.081132	0.081132	89.998755
4	0.999999	-0.057515	0.057518	0.081341	134.998755
5	0.999999	-0.081434	0.000000	0.081434	180.000000
6	0.999999	-0.057526	-0.057528	0.081356	-134.998827
7	1.000000	0.000002	-0.081154	0.081154	-89.998324
8	1.000000	0.057239	-0.057237	0.080946	-44.998846

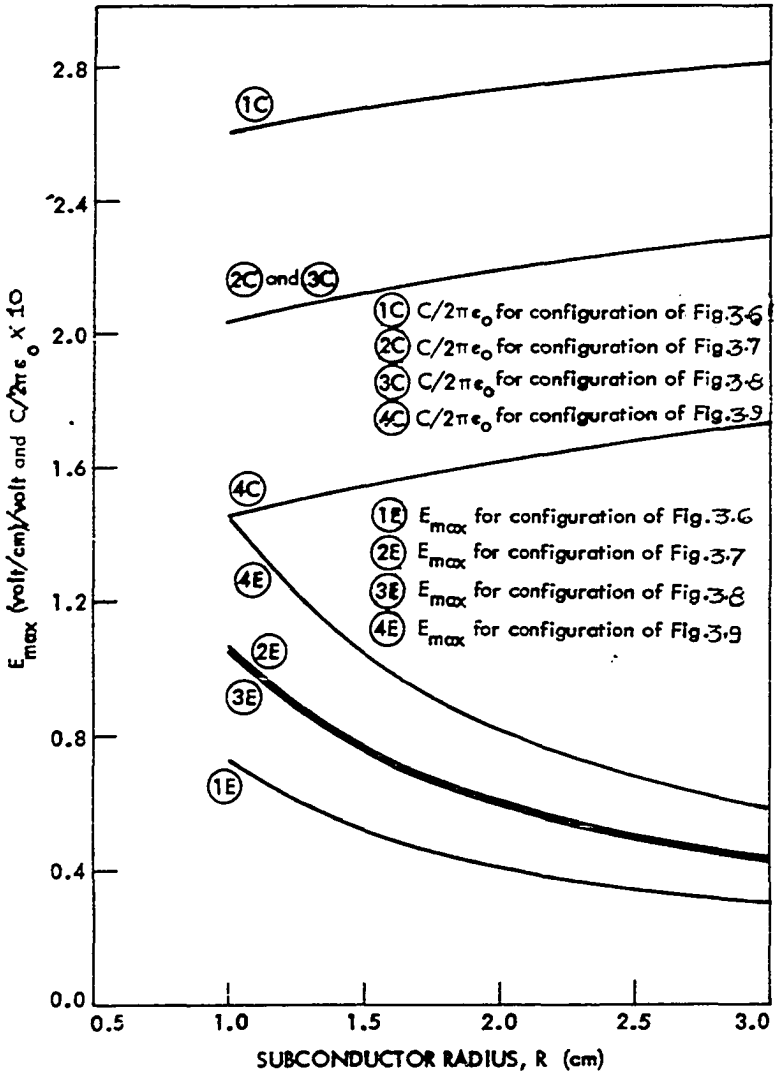

Figure 3.10. Variation of maximum electric field and capacitance with subconductor radius for different configurations of dc bipolar lines. H = 1500 cm, S = 500 cm, A = B = 50 cm.

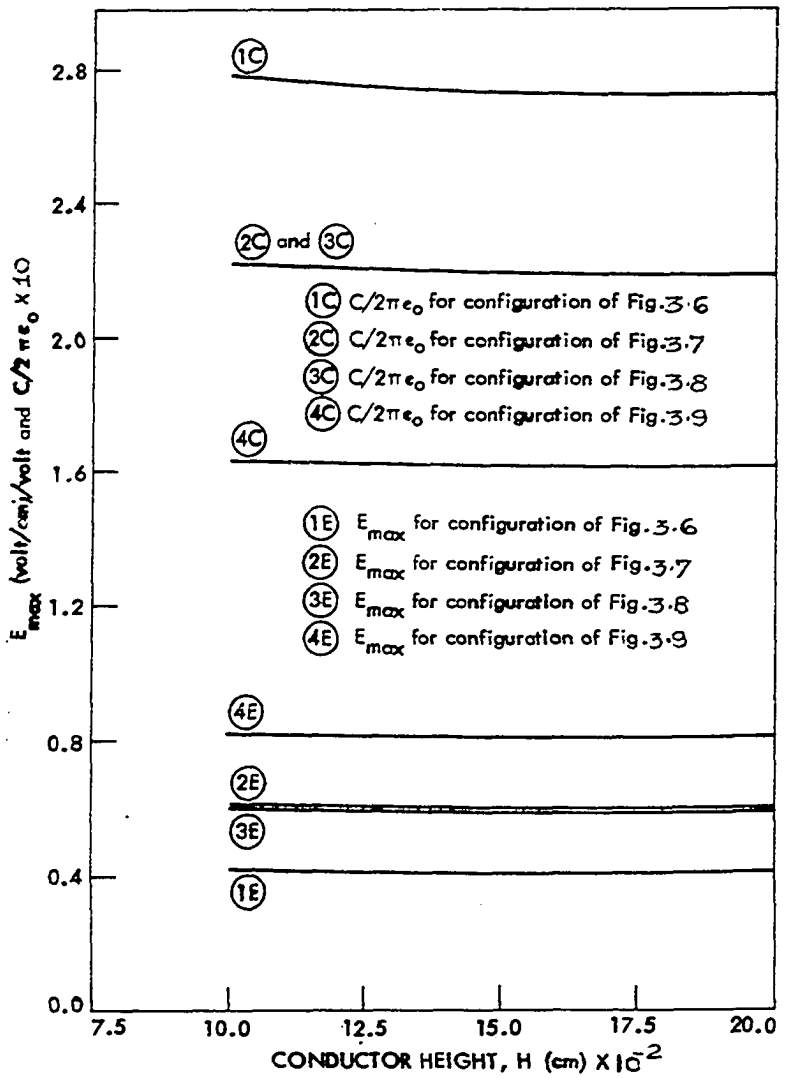

Figure 3.11. Variation of maximum electric field and capacitance with conductor height for different configurations of dc bipolar lines. R = 2.0 cm, A = B = 50 cm, S = 500 cm.

Figure 3.12 illustrates the variation of the maximum electric field and the capacitance with conductor separation. As the conductor separation increases, the maximum electric field and the capacitance decreases.

Figure 3.13 illustrates the variation of the maximum electric field and the capacitance with subconductor separation. As the subconductor separation increases, the maximum electric field increases slightly but the capacitance increases appreciably.

Figures 3.10-3.13 illustrate that the values of the electric field for the bipolar line of two subconductors arranged vertically are about 1.87 percent less than those for the line with the subconductors arranged horizontally although the values of the capacitance remain the same for the two cases.

6. Conclusions

(1) The computer program written for computing the electric field and potential distribution for HVDC bipolar lines is simple and gives very accurate results.

(2) Accurate values of capacitance are obtained simply by summing the values of all the line charges which represent the actual charge distribution on the conductor surface.

(3) The effect of the ground plane which should not be neglected is included in the program.

(4) Although the cases of three, five and more number of subconductors in a bundle are not discussed in this section, the electric field and potential distribution for such cases can be obtained easily by the same

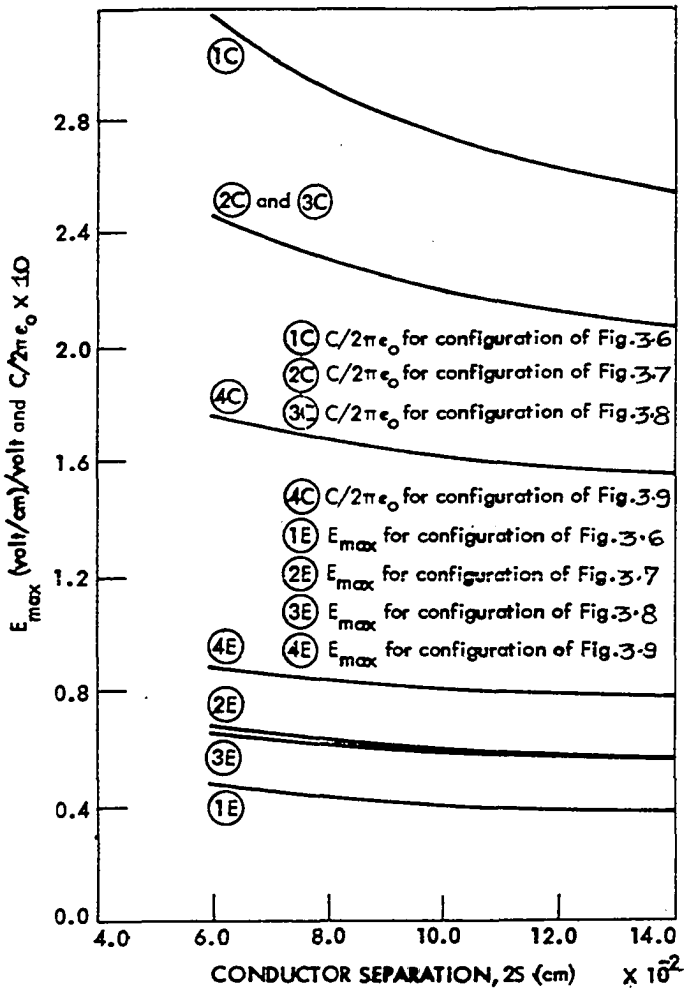

Figure 3.12. Variation of maximum electric field and capacitance with conductor separation for different configuration of dc bipolar lines. R = 2.0 cm, H = 1500 cm, A = B = 50 cm.

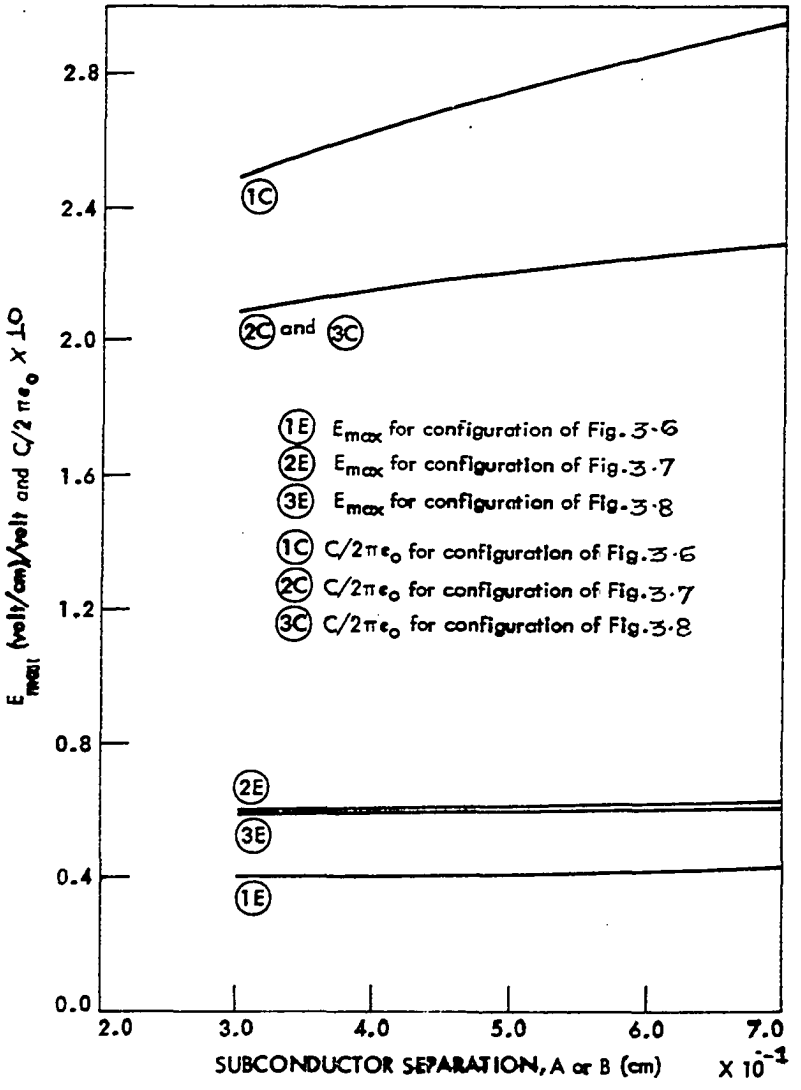

Figure 3.13. Variation of maximum electric field and capacitance with subconductor separation for different configuration of dc bipolar lines. R = 2.0 cm, H = 1500 cm, S = 500 cm.

computer program with few changes.

(5) The computer program written can also be used for the computation of electric field for an unipolar split-bundle dc line. The results obtained for these lines are discussed in the following section.

B. Split-Bundle Transmission Lines

1. General

With the growing demand for electric energy, the possibility of transmitting large blocks of this power at ultra high voltage (UHV) level is the most economical. Some of the problems associated with the UHV lines are due to the corona loss and radio interference. In the early days of the high voltage transmission, the corona had to be avoided because of the energy loss associated with it. Currently, however, the radio interference aspect of the corona has become more important.

The standard way of reducing the corona is by using bundle conductors. The bundle conductors reduce the intensity of the electric field on the conductor surface as well as in the region surrounding the conductor. The high electric field is responsible for the appearance of the corona and the radio interference. The corona performance can be improved by using split-bundle conductor in which each subbundle is composed of several subconductors.

A recent paper described a method known as the "dipole method" to calculate the maximum electric field on the surface of the split-bundled conductor (6, 28). The limitations of this method are:

(1) In the theoretical studies of the corona losses, it is essential to know the exact distribution of the electric field and potential every-

where on the conductor surface as well as in the interelectrode space. This is not possible with the dipole method.

(2) The effect of the ground should not be neglected as has been done in the theoretical analysis of the dipole method. The height of the conductor above the ground plays an important role in determining the values of the electric field. This is described in detail in a later section.

(3) The electric field produced by the subconductors in other subbundles can not be considered uniform (as has been assumed) in the region of the subbundle with the subconductor under consideration.

In this section, a method is described for computing accurately the electric field and potential at any desired point for the split-bundle conductor without the above limitations.

2. Method of computation

The method of computation is known as the charge simulation method which has been described in a previous section.

3. Mathematical formulation

The various configurations of the split-bundle transmission line considered in this section are shown in Figures 3.14-3.16. Figure 3.14 shows the split-twin-bundle line with four subconductors in bundle I and four subconductors in bundle II. Figure 3.15 shows the split-twin-bundle line with two subconductors in each subbundle. Figure 3.16 shows a simple twin-bundle line. Since the transmission lines of Figures 3.15 and 3.16 are the special cases of the line of Figure 3.14, the mathematical

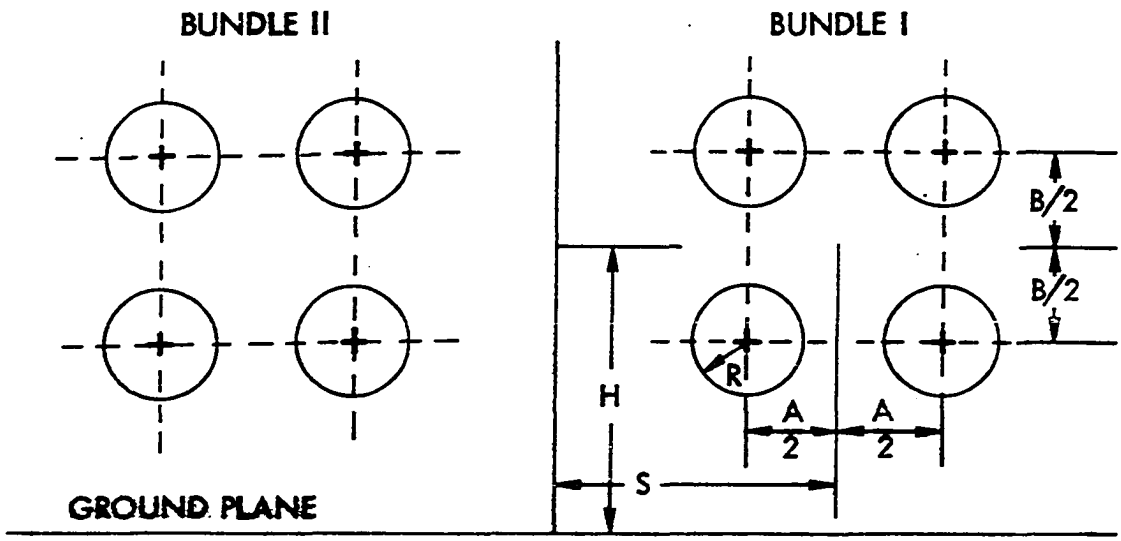

Figure 3.14. Split-twin-bundle line with four subconductors in each subbundle.

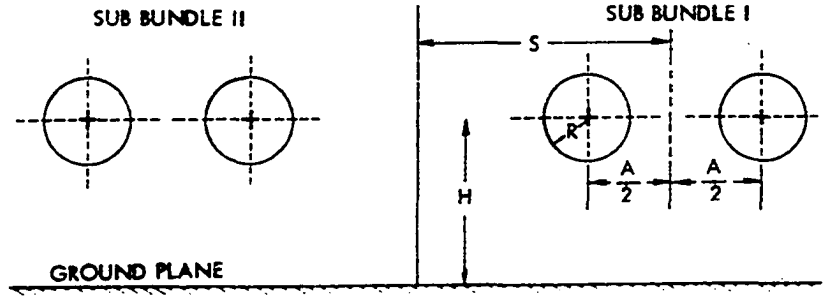

(a)

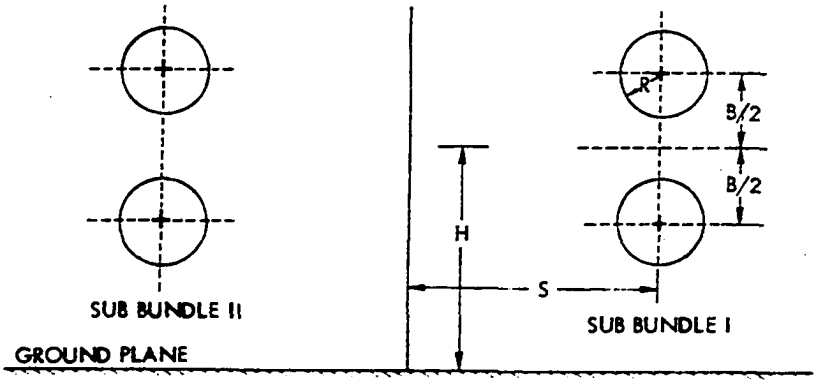

(b)

Figure 3.15. Split-twin-bundle line with two subconductors in each subbundle.
(a) horizontal arrangement
(b) vertical arrangement

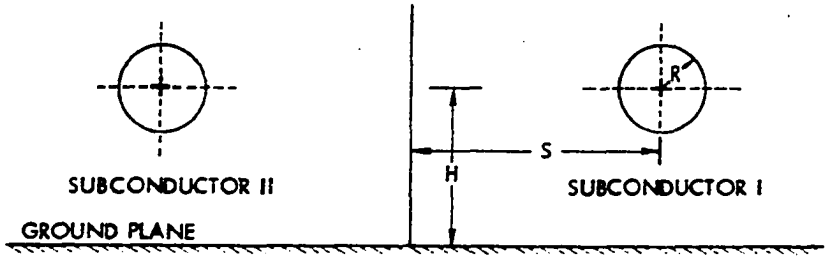

Figure 3.16. Simple twin-bundle line.

formulation for only the more general case of Figure 3.14 is explained here. The lines of Figure 3.15 are obtained from the general case of Figure 3.14 by letting B = 0 [horizontal arrangement of Figure 3.15(a)] or A = 0 [vertical arrangement of Figure 3.15(b)]. The simple twin-bundle line of Figure 3.16 is obtained from the general case of Figure 3.14 by letting A = 0 and B = 0 simultaneously.

As shown in Figure 3.17, the actual charge distribution on the surface of the subconductors of bundle I is represented by axial line charges of unknown magnitudes Q(K), where K = 1,2,3,.....,N. These line charges are placed symmetrically on a coaxial cylinder of radius RQ inside each subconductor. The locations of these line charges are given by the angles measured from the horizontal plane in counter clockwise direction. These angles are designated

$$\alpha(K1) = (K1 - 1)\circ(360/NN), \quad K1 = 1,2,3,\ldots,NN \tag{3.27}$$

where

$$NN = N/4 \tag{3.28}$$

The X and Y coordinates of the axial line charges, Q(K), placed inside each subconductor of subbundle I are given by

$$XQ(K1) = S + (A/2) + RQ\circ\cos[\alpha(K1)] \tag{3.29}$$

$$YQ(K1) = H + (B/2) + RQ\circ\sin[\alpha(K1)] \tag{3.30}$$

where

$$K1 = 1,2,3,\ldots,NN \tag{3.31}$$

and

$$XQ(K2) = S - (A/2) + RQ\circ\cos[\alpha(K1)] \tag{3.32}$$

$$YQ(K2) = YQ(K1) \tag{3.33}$$

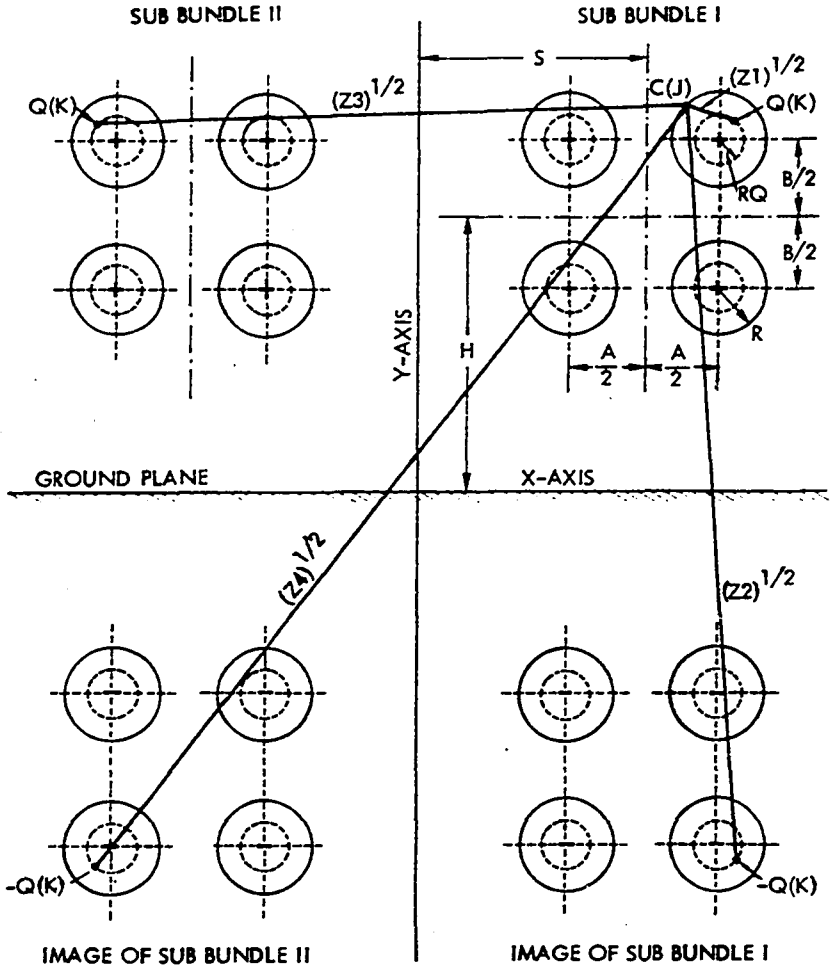

Figure 3.17. Charge representation for the split-bundle transmission line with four subconductors in each subbundle.

where

$$K1 = 1,2,3,\ldots\ldots,NN \qquad 3.31$$

$$K2 = K1 + NN \qquad 3.34$$

and

$$XQ(K3) = XQ(K2) \qquad 3.35$$

$$YQ(K3) = H - (B/2) + RQ\cdot\sin[\alpha(K1)] \qquad 3.36$$

where

$$K1 = 1,2,3,\ldots\ldots,NN \qquad 3.31$$

$$K2 = K1 + NN \qquad 3.34$$

$$K3 = K1 + (2\cdot NN) \qquad 3.37$$

and

$$XQ(K4) = XQ(K1) \qquad 3.38$$

$$YQ(K4) = YQ(K3) \qquad 3.39$$

where

$$K1 = 1,2,3,\ldots\ldots,NN \qquad 3.31$$

$$K3 = K1 + (2\cdot NN) \qquad 3.37$$

$$K4 = K1 + (3\cdot NN) \qquad 3.40$$

The magnitudes and positions of the axial line charges placed inside the subconductors of subbundle II are equal and symmetric to those of subbundle I about the Y axis. Image charges of all these line charges (inside subconductors of subbundle I and II) are placed on the other side of the ground plane which is assumed to be of zero potential.

The potential at any point on the conductor's surface must be equal to one unit which is the assumed conductor potential with respect to the ground. To satisfy this boundary condition, points C(J),

J = 1,2,3,.....,N are chosen on the surface of subconductors of sub-bundle I and the potential at these points are calculated and equated to one unit. The X and Y coordinates of these points are designated XC(J) and YC(J). These coordinates are given by Equations 3.29-3.40 except the radius RQ is replaced by the subconductor radius R.

The potential $\phi[C(J)]$ at any point C(J) on the conductor surface is given by

$$\phi[C(J)] = \sum_{K=1}^{N} \frac{Q(K)}{2\pi\epsilon_o} \cdot \tfrac{1}{2} \cdot \log_e \frac{(Z2 \cdot Z4)}{(Z1 \cdot Z3)} = 1.0 \qquad 3.41$$

where J = 1,2,3,.....,N and distances square Z1, Z2, Z3, and Z4 are as shown in Figure 3.17 and are given by

$$Z1 = X1 \cdot X1 + Y1 \cdot Y1 \qquad 3.42$$

$$Z2 = X1 \cdot X1 + Y2 \cdot Y2 \qquad 3.43$$

$$Z3 = X2 \cdot X2 + Y1 \cdot Y1 \qquad 3.44$$

$$Z4 = X2 \cdot X2 + Y2 \cdot Y2 \qquad 3.45$$

where

$$X1 = XC(J) - XQ(K) \qquad 3.46$$

$$X2 = XC(J) + XQ(K) \qquad 3.47$$

$$Y1 = YC(J) - YQ(K) \qquad 3.48$$

$$Y2 = YC(J) + YQ(K) \qquad 3.49$$

where

J = 1,2,3,.....,N

K = 1,2,3,.....,N

Equation 3.41 represents a set of simultaneous equations which can be solved with a digital computer to obtain the values of the axial line

charges Q(K). Once the values of these line charges are known, the potential and the electric field at any point on the conductor surface or in the outside space can be easily computed. The equations necessary to compute the potential and electric field in X and Y direction at any point (x,y) are given by

$$\phi(x,y) = \sum_{K=1}^{N} \frac{Q(K)}{2\pi\epsilon_o} \cdot \tfrac{1}{2} \cdot \log_e \frac{(Z2 \cdot Z4)}{(Z1 \cdot Z3)} \qquad 3.50$$

$$E_X(x,y) = \sum_{K=1}^{N} \frac{Q(K)}{\pi\epsilon_o} \cdot \tfrac{1}{2} \cdot \left[\frac{X1}{Z1} + \frac{X2}{Z3} - \frac{X1}{Z2} - \frac{X2}{Z4}\right] \qquad 3.51$$

$$E_Y(x,y) = \sum_{K=1}^{N} \frac{Q(K)}{\pi\epsilon_o} \cdot \tfrac{1}{2} \cdot \left[\frac{Y1}{Z1} + \frac{Y1}{Z3} - \frac{Y2}{Z2} - \frac{Y2}{Z4}\right] \qquad 3.52$$

where Equations 3.42-3.49 are used with XC(J) and YC(J) replaced by x and y respectively.

4. Programming

A computer program is written for computing the electric field and potential distribution for the split-bundle line shown in Figure 3.14. The computer program is written in FORTRAN IV language for the IBM 360 computer available at the Computation Center, Iowa State University. Double precision arithmetic is used throughout the main program and the subroutine. The simultaneous equations 3.41 representing the boundary conditions are solved using a subroutine which operates on the method of Gauss elimination with complete pivotting.

The main computational steps are the same as shown in Figure 3.5. The radius RQ of the fictitious cylinder on which the line charges are placed is taken as 0.5 R. The total number of the axial line charges N

is taken as 60. The solution of the simultaneous equations 3.41 gives the value of the unknown line charges. These are used in computing the potential and the field anywhere on the conductor's surface and in the outside space. The computer program is given in Appendix B.

5. Results

Results are obtained for the split-twin-bundle line with four subconductors in each subbundle. The following values of the geometrical parameters are chosen to illustrate the results:

subconductor radius = 2.0 cm.

conductor height = 2000 cm.

subconductor separation = 24 cm.

subbundle separation = 60 cm.

The values of the line charges obtained by solving the simultaneous Equations 3.41 are shown in Table 3.6. Since the conductor potential is assumed to be of one unit, the value of capacitance between the subbundle and the ground is obtained simply by summing the values of all the line charges shown in Table 3.6 and multiplying the sum by $2\pi\epsilon_o$. The value of the capacitance for the case considered is 0.56846×10^{-11} Farad / meter.

Using the values of the line charges shown in Table 3.6, potential and electric field at 120 points on each subconductor of subbundle I are computed. The values of the potential at these points are found to be one unit and the directions of the electric field are found to be perpendicular to the conductor surface. This means that the boundary conditions

Table 3.6. Values of line charges obtained by solving the simultaneous equations [(Coulomb/m/volt)/$2\pi\epsilon_o$]

Q(1)	0.003467	Q(21)	0.002146	Q(41)	0.002207
Q(2)	0.003707	Q(22)	0.001801	Q(42)	0.002392
Q(3)	0.003698	Q(23)	0.001393	Q(43)	0.002337
Q(4)	0.003452	Q(24)	0.001016	Q(44)	0.002036
Q(5)	0.002994	Q(25)	0.000721	Q(45)	0.001570
Q(6)	0.002374	Q(26)	0.000516	Q(46)	0.003497
Q(7)	0.001680	Q(27)	0.000406	Q(47)	0.002997
Q(8)	0.001048	Q(28)	0.000400	Q(48)	0.002311
Q(9)	0.000616	Q(29)	0.000502	Q(49)	0.001569
Q(10)	0.000455	Q(30)	0.000718	Q(50)	0.000945
Q(11)	0.000569	Q(31)	0.001090	Q(51)	0.000563
Q(12)	0.000953	Q(32)	0.000724	Q(52)	0.000455
Q(13)	0.001575	Q(33)	0.000499	Q(53)	0.000628
Q(14)	0.002310	Q(34)	0.000393	Q(54)	0.001075
Q(15)	0.002984	Q(35)	0.000398	Q(55)	0.001725
Q(16)	0.001071	Q(36)	0.000512	Q(56)	0.002434
Q(17)	0.001534	Q(37)	0.000725	Q(57)	0.003063
Q(18)	0.001984	Q(38)	0.001033	Q(58)	0.003521
Q(19)	0.002274	Q(39)	0.001426	Q(59)	0.003759
Q(20)	0.002326	Q(40)	0.001850	Q(60)	0.003754

are satisfied very well. For the purpose of simplicity, the values of the potential and the electric field at only eight points on each subconductor of subbundle I are shown in Figure 3.18 with Table 3.7.

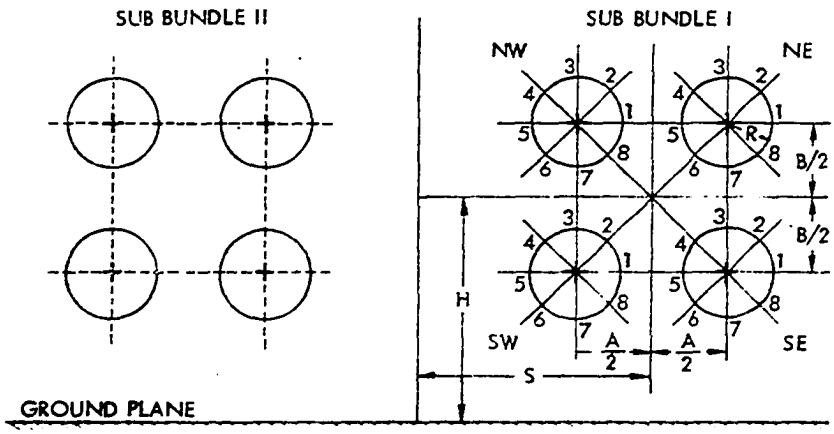

Figure 3.18. Configuration for split-twin-bundle line. R = 2.0 cm, H = 2000 cm, A = B = 24 cm, S = 30 cm.

Table 3.7. Distribution of electric field on subbundle subconductors' surface (Potential computed at each point is "1.000000").

Subbundle I subconductor number	Point number	Electric field in x-direction	Electric field in y-direction	Electric field magnitude	Angle of electric field
NE	1	0.020931	0.000000	0.020931	0.000388
"	2	0.015564	0.015563	0.022010	44.998172
"	3	0.000001	0.019687	0.019687	89.997647
"	4	-0.010725	0.010725	0.015167	134.999418
"	5	-0.010995	-0.000000	0.010995	-179.999220
"	6	-0.006875	-0.006875	0.009723	-135.000044
"	7	0.000000	-0.012142	0.012142	-89.999117
"	8	0.011931	-0.011931	0.016873	-44.997781
NW	1	0.008978	0.000000	0.008978	0.001197
"	2	0.008401	0.008401	0.011881	44.999004
"	3	0.000001	0.013248	0.013248	89.997286
"	4	-0.008522	0.008522	0.012052	134.998786
"	5	-0.009391	0.000000	0.009391	-179.999209
"	6	-0.004969	-0.004969	0.007027	-134.998943
"	7	0.000000	-0.005991	0.005991	-89.999534
"	8	0.004713	-0.004713	0.006665	-44.999112
SW	1	0.009156	0.000000	0.009156	-0.001218
"	2	0.004776	0.004775	0.006754	44.999046
"	3	0.000000	0.006051	0.006051	89.999496
"	4	-0.005039	0.005040	0.007127	135.001122
"	5	-0.009587	0.000000	0.009587	179.999120
"	6	-0.008733	-0.008733	0.012350	-135.001144
"	7	0.000001	-0.013587	0.013587	-89.997348
"	8	0.008603	-0.008603	0.012166	-44.999080
SE	1	0.021152	0.000000	0.021152	-0.000407
"	2	0.012012	0.012011	0.016987	44.997716
"	3	0.000000	0.012208	0.012208	89.999065
"	4	-0.006940	0.006940	0.009814	135.000029
"	5	-0.011177	0.000000	0.011177	179.999132
"	6	-0.010933	-0.010933	0.015462	-135.000519
"	7	0.000001	-0.020045	0.020045	-89.997707
"	8	0.015794	-0.015794	0.022336	-44.998253

As seen from Table 3.7, the values of the electric potential on the conductor surface are one unit and the directions of the electric field are perpendicular to the conductor surface. The highest electric field intensity on the conductor's surface appears at point 8 of SE subconductor. This value is 0.022336 volt/cm per volt. While calculating the values of the electric field at many points on the conductor's surface, it was found that the actual location of the maximum electric field was at a few degrees above the point 8 of SE subconductor, although the difference in magnitudes of the field at these two points was very small. The actual location of the maximum electric field is affected by the geometrical parameters of the split-bundle line.

Table 3.7 shows the wide variation of the electric field on the conductor's surface. For the results shown in Table 3.7, the ratio of the minimum to the maximum electric field on the surface of each subconductor is approximately equal to 0.445.

The potential and the electric field distribution for the split-twin-bundle line with two subconductors in each subbundle arranged horizontally [Figure 3.15(a)] is obtained by letting B = 0 in the computer program for the split-bundle line with four subconductors in each subbundle. The values of the electric field and potential at eight points on each subconductor of subbundle I are shown in Figure 3.19 with Table 3.8.

As seen from Table 3.8, the values of the electric potential on the conductor's surface are one unit and the directions of the electric field are perpendicular to the conductor surface. The highest electric field intensity on the conductor's surface appears at point 1 of E subconductor.

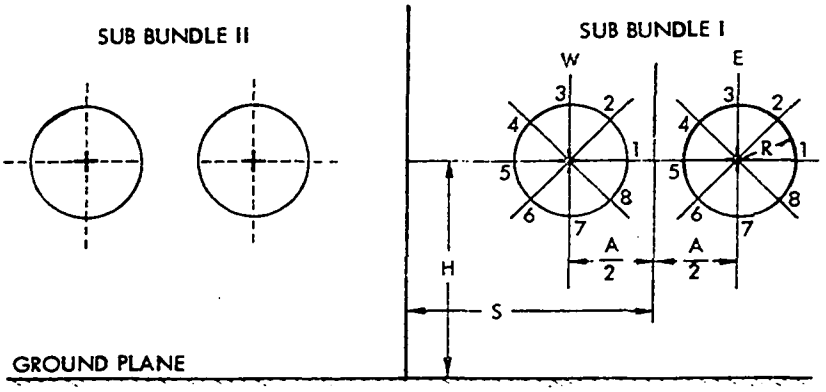

Figure 3.19. Configuration for split-twin-bundle transmission line. R = 2.0 cm, H = 2000 cm, A = 24 cm, S = 30 cm.

Table 3.8. Distribution of electric field on subbundle I subconductors' surface Potential computed at each point "1.000000".

Subbundle I subconductor number	Point number	Electric field in x-direction	Electric field in y-direction	Electric field magnitude	Angle of electric field
E	1	0.033118	0.000000	0.033118	-0.000009
"	2	0.022364	0.0022362	0.031626	44.998345
"	3	0.000001	0.027770	0.027770	89.998055
"	4	-0.016460	0.016461	0.023279	134.999455
"	5	-0.021213	0.000000	0.021213	179.999990
"	6	-0.016554	-0.016554	0.023411	-134.999522
"	7	0.000001	-0.027958	0.027958	-89.998111
"	8	0.022458	-0.022456	0.031759	-44.998420
W	1	0.018721	-0.000000	0.018721	-0.000015
"	2	0.013724	0.013723	0.019408	44.999140
"	3	0.000001	0.020280	0.020280	89.997928
"	4	-0.014214	0.014215	0.020102	134.998890
"	5	-0.019792	-0.000000	0.019792	179.999989
"	6	-0.014308	-0.014308	0.020234	-134.998960
"	7	0.000001	-0.020467	0.020467	-89.997979
"	8	0.013817	-0.013817	0.019540	-44.999212

This value is 0.033118 volt/cm per volt. For the geometrical parameters of Figure 3.19, the ratio of the minimum to the maximum electric field on the surface of E subconductor is 0.021213/0.033118 = 0.64. This ratio for W subconductor is 0.018721/0.020467 = 0.92.

The actual location of the maximum electric field is near point 1 of E subconductor but its magnitude is only slightly greater than that at point 1. The maximum electric field for this case is about 48.3 percent higher than the corresponding value for the split-twin-bundle line of Figure 3.14.

The potential and the electric field distribution for the split-twin-bundle line with two subconductors in each subbundle arranged vertically [Figure 3.15(b)] is obtained by letting A = 0 in the computer program written for the split-twin-bundle line with four subconductors in each subbundle. The values of the electric field and potential at eight points on each subconductor of subbundle I are shown in Figure 3.20 with Table 3.9.

As seen from Table 3.9, the values of the electric potential on the conductor's surface are one unit and the directions of the electric field are perpendicular to the conductor's surface. The highest electric field intensity on the conductor's surface appears at point 8 of S subconductor. This value is 0.029126 volt/cm per volt. For the geometrical parameters of Figure 3.20, the ratio of the minimum to the maximum electric field on the surface of N subconductor is 0.018484/0.028798 = 0.64. This ratio for S subconductor is 0.018597/0.029126 = 0.64.

The actual location of the maximum electric field is near point 8 of S subconductor, although its magnitude is only slightly greater than that

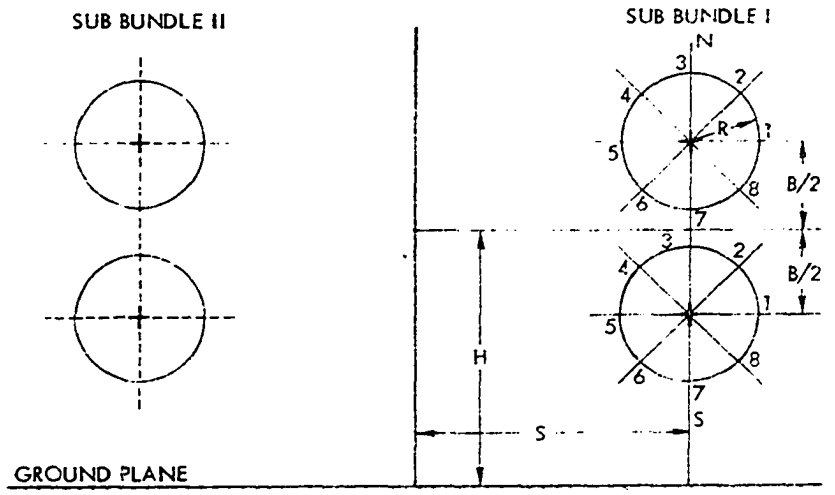

Figure 3.20. Configuration for split-twin-bundle transmission line. R = 2 cm, H = 2000 cm, B = 24 cm, S = 30 cm.

Table 3.9. Distribution of electric field on subbundle I subconductors' surface (Potential computed at each point is "1.000000".)

Subbundle I subconductor number	Point number	Electric field in x-direction	Electric field in y-direction	Electric field magnitude	Angle of electric field
N	1	0.026830	0.000000	0.026830	0.000405
"	2	0.020364	0.020363	0.028798	44.998466
"	3	0.000001	0.027848	0.027848	89.997885
"	4	-0.017483	0.017483	0.024725	134.998964
"	5	-0.020980	-0.000000	0.020980	-179.999617
"	6	-0.013070	-0.013070	0.018484	-134.999104
"	7	0.000000	-0.018997	0.018997	-89.999163
"	8	0.016029	-0.016028	0.022667	-44.998209
S	1	0.027049	-0.000000	0.027049	-0.000419
"	2	0.016110	0.016109	0.022783	44.998140
"	3	0.000000	0.019071	0.019071	89.999105
"	4	-0.013150	0.013150	0.018597	134.999034
"	5	-0.021195	0.000000	0.021195	179.999533
"	6	-0.017712	-0.017712	0.025049	-134.999033
"	7	0.000001	-0.028221	0.028221	-89.997947
"	8	0.020595	-0.020595	0.029126	-44.998543

at point 8. The maximum electric field for this case is about 30.4 percent higher than the corresponding value for the split-twin-bundle line with four subconductors in each subbundle.

The potential and electric field distribution for the simple twin-bundle line (Figure 3.16) is obtained by letting A = 0 and B = 0 in the computer program written for the general case of Figure 3.14 with few changes. The values of the electric field and potential at eight points on subconductor I are shown in Figure 3.21 with Table 3.10.

As seen from Table 3.10, the boundary conditions are satisfied very well on the conductor surface. The highest electric field intensity appears at point 1 of subconductor I. This value is 0.045106 volt/cm per volt. It is about 102 percent higher than the corresponding value for the line of Figure 3.18, about 36.2 percent higher than the corresponding value for the line of Figure 3.19 and about 55 percent higher than the corresponding value for the line of Figure 3.20.

Figures 3.22-3.29 illustrate the effect of the geometrical parameters on the maximum electric field and the capacitance for different configurations of the split-twin-bundle line.

Figure 3.22 illustrates the variation of the maximum electric field with the subconductor radius. As the radius increases, the electric field decreases. The electric field is also reduced by increasing the number of subconductors in each subbundle.

Figure 3.23 illustrates the variation of the maximum electric field with the conductor height. This figure indicates that the effect of the conductor height on the electric field should not be neglected since

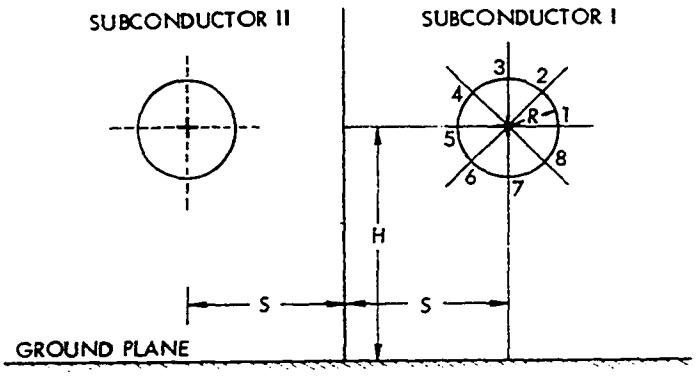

Figure 3.21. Configuration for twin-bundle line. R = 2 cm, H = 2000 cm, S = 30 cm.

Table 3.10. Distribution of electric field on subconductor I surface. (Potential computed at each point is "1.000000".)

Subconductor number	Point number	Electric field in x-direction	Electric field in y-direction	Electric field magnitude	Angle of electric field
I	1	0.045106	-0.000000	0.045106	-0.000000
"	2	0.031331	0.031330	0.044308	44.998606
"	3	0.000001	0.042383	0.042383	89.998209
"	4	-0.028511	0.028512	0.040321	134.998948
"	5	-0.039455	0.000000	0.039455	179.999995
"	6	-0.028595	-0.028596	0.040441	-134.999018
"	7	0.000001	-0.042553	0.042553	-89.998271
"	8	0.031416	-0.031415	0.044428	-44.998679

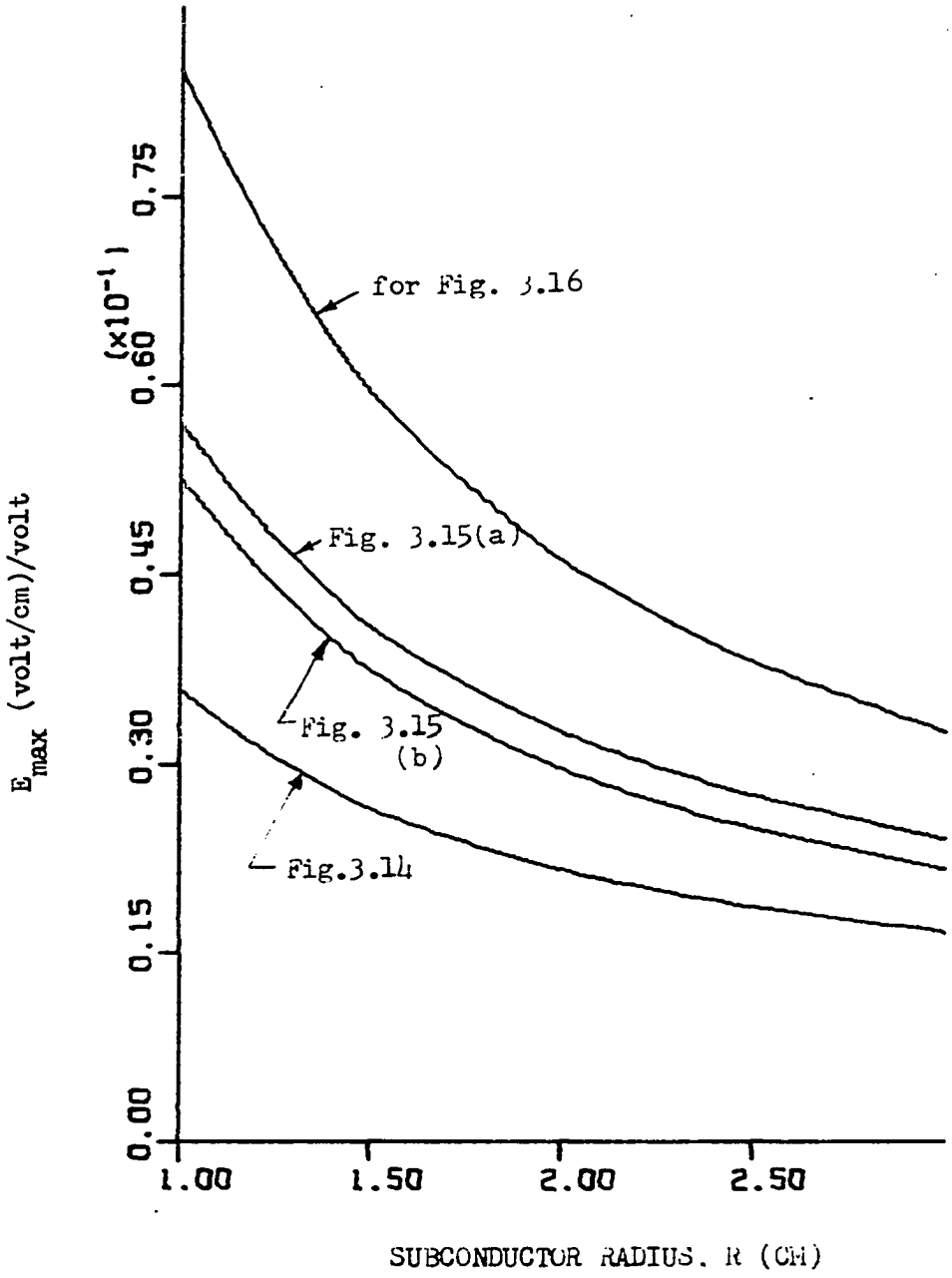

Figure 3.22. Variation of maximum electric field with subconductor radius for different configuration of split-bundle lines. H = 2000 cm, S = 50 cm, A = B = 24 cm.

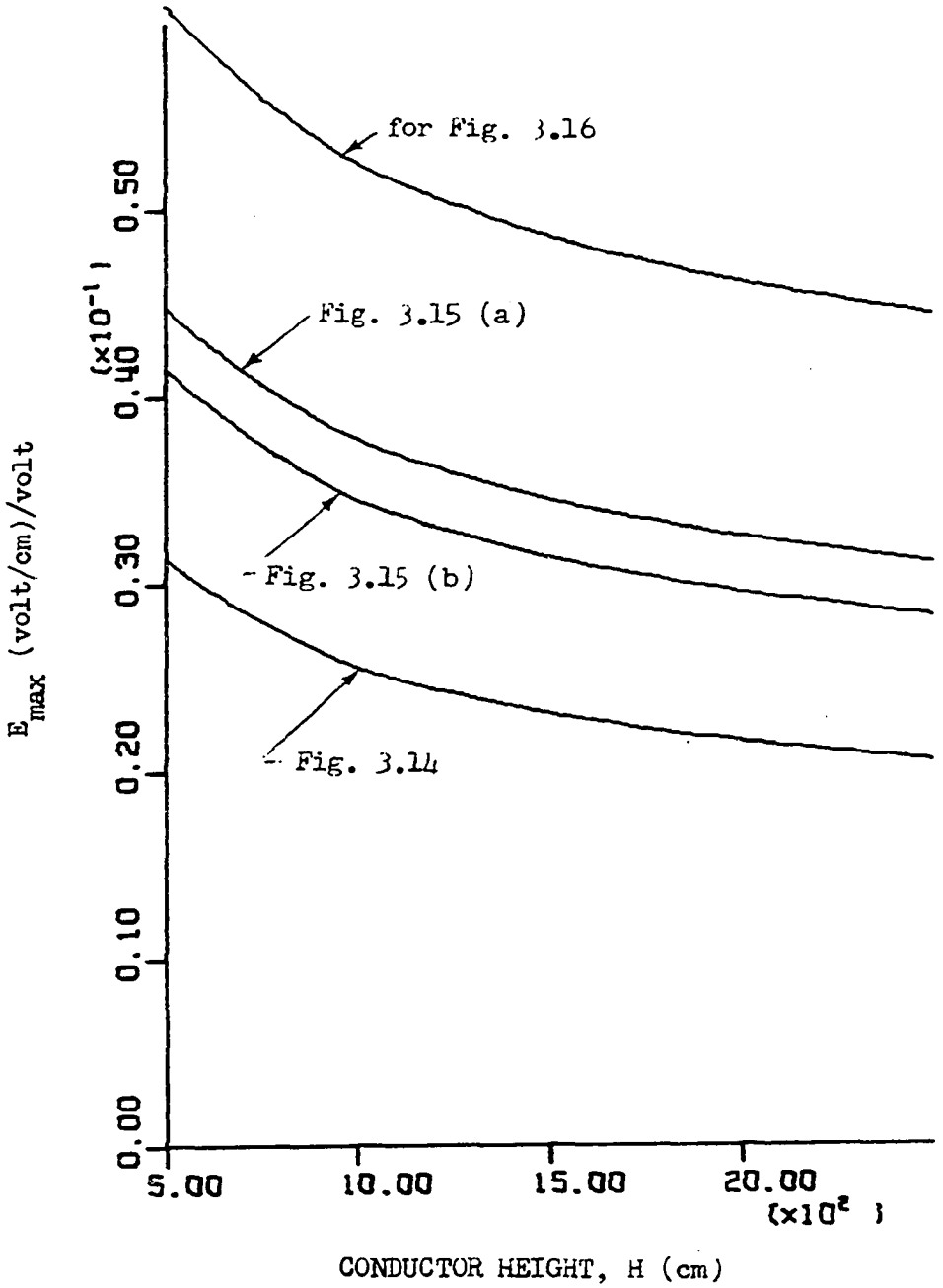

Figure 3.23. Variation of maximum electric field with conductor height for different configurations of split-bundle lines. R = 2 cm, A = B = 24 cm, S = 50 cm.

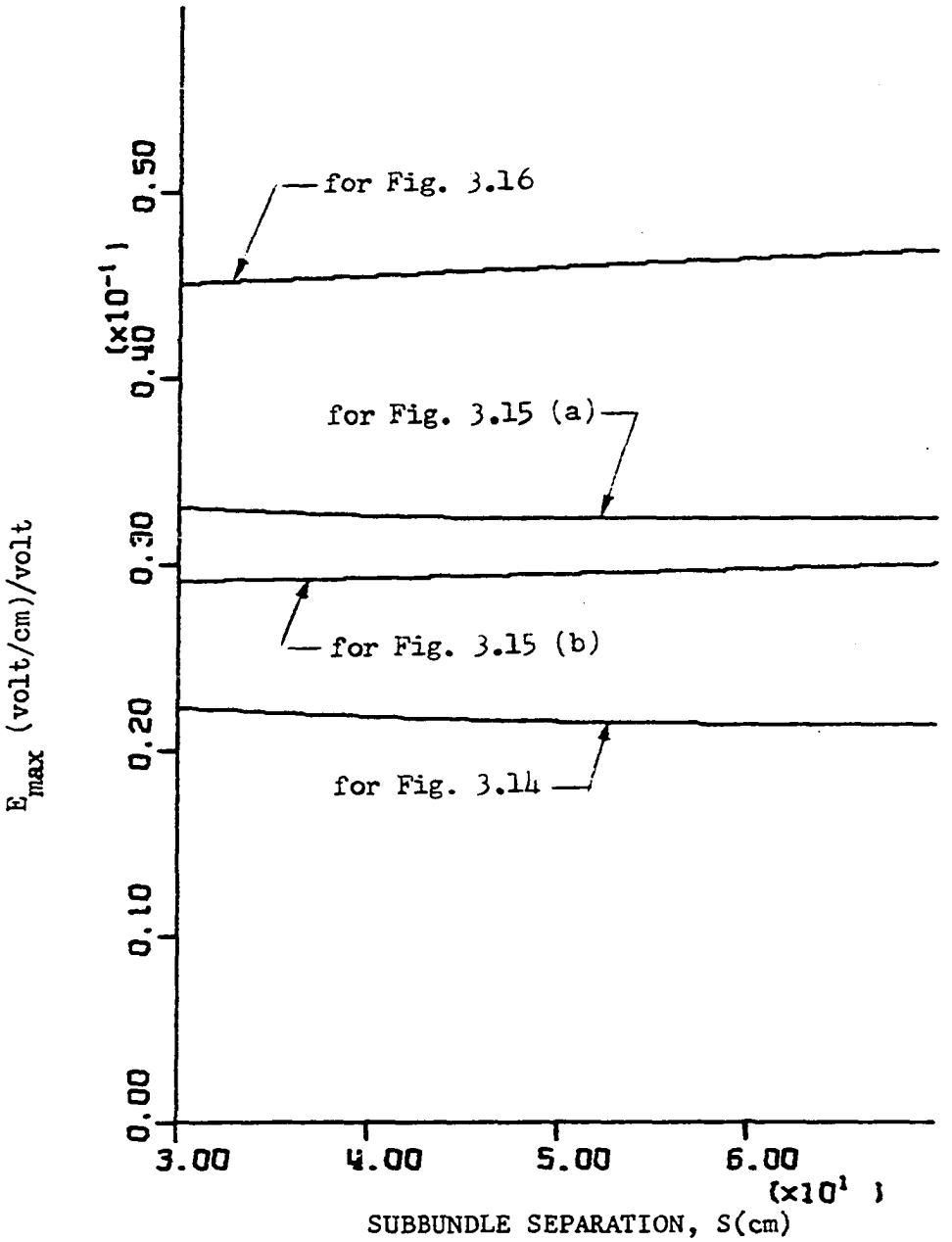

Figure 3.24. Variation of maximum electric field with subbundle separation for different configurations of split-bundle lines. R = 2 cm, H = 2000 cm, A = B = 24 cm.

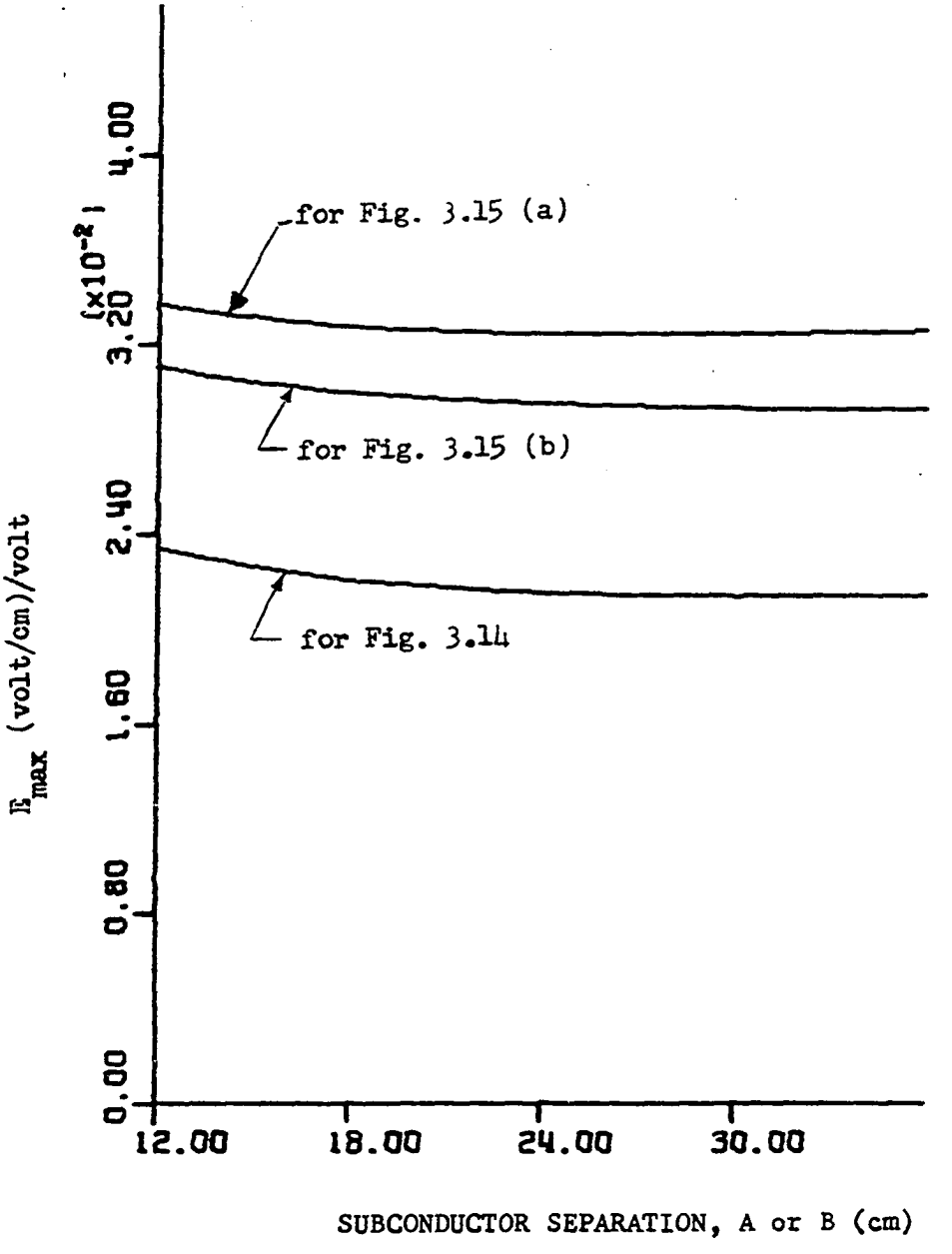

Figure 3.25. Variation of maximum electric field with subconductor separation for different configurations of split-bundle lines. R = 2 cm, H = 2000 cm, S = 50 cm.

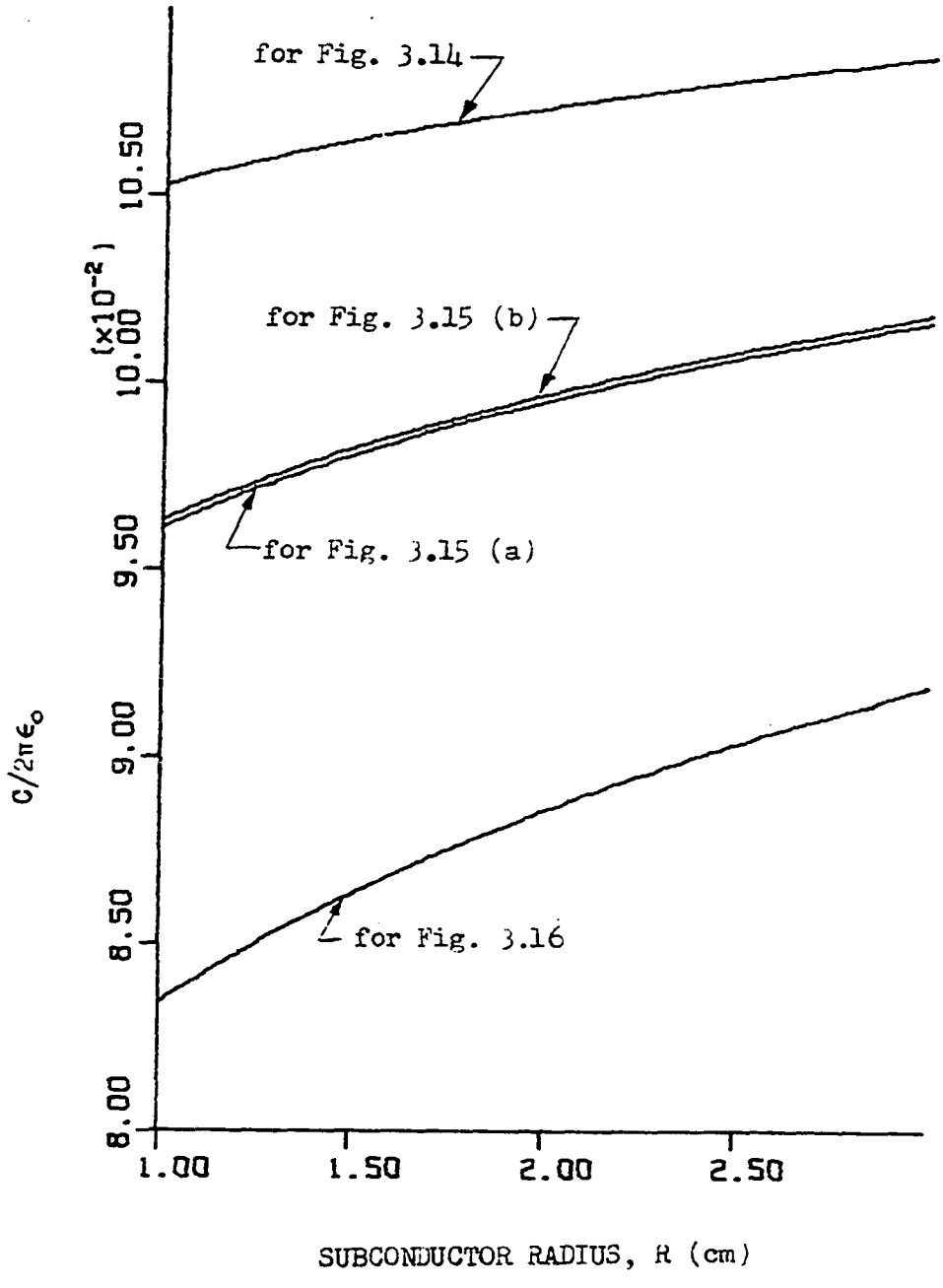

Figure 3.26. Variation of capacitance with subconductor radius for different configurations of split-bundle lines. H = 2000 cm, A = B = 24 cm, S = 50 cm.

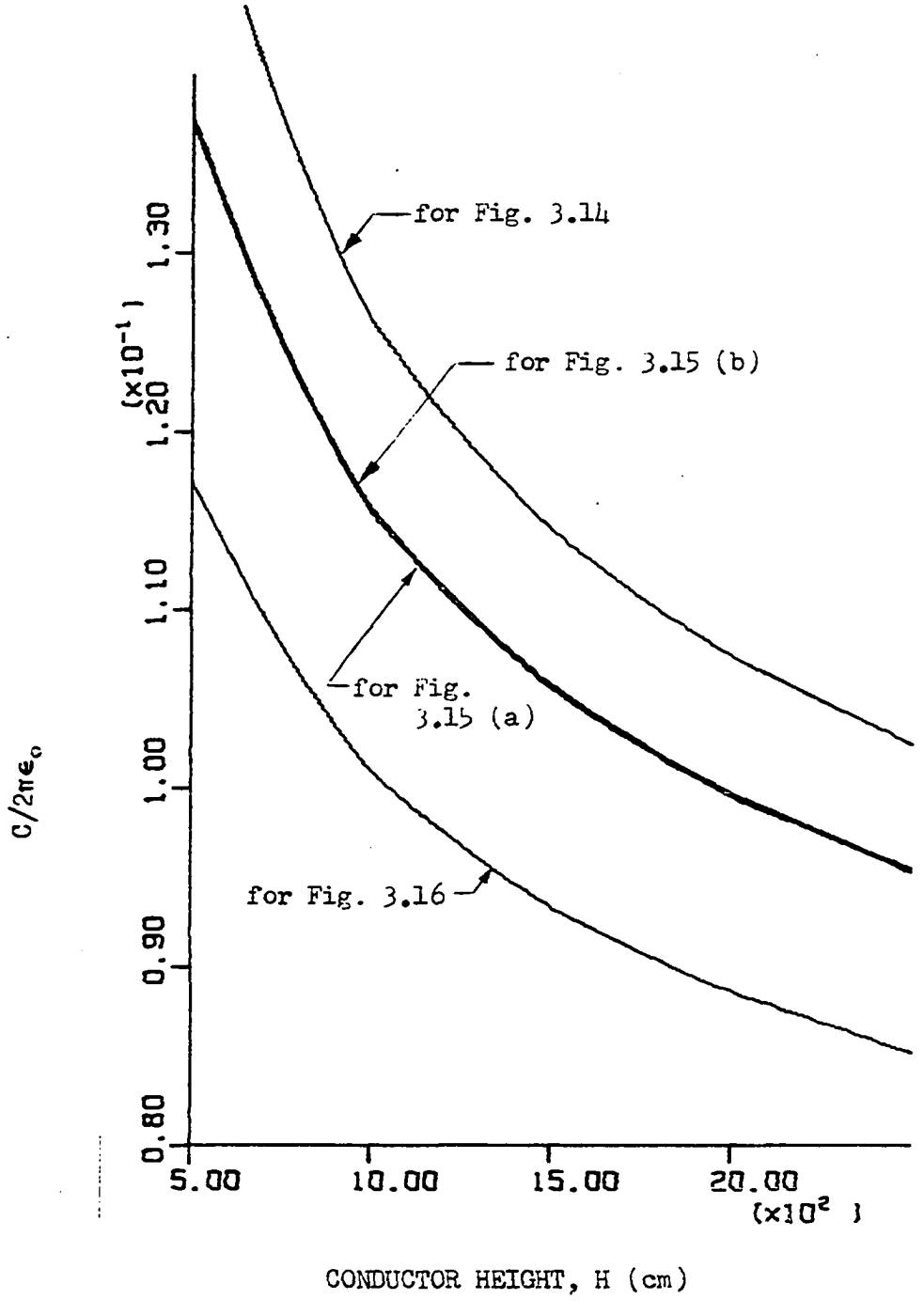

Figure 3.27. Variation of capacitance with conductor height for different configurations of split-bundle lines. R = 2 cm, S = 50 cm, A = B = 50 cm.

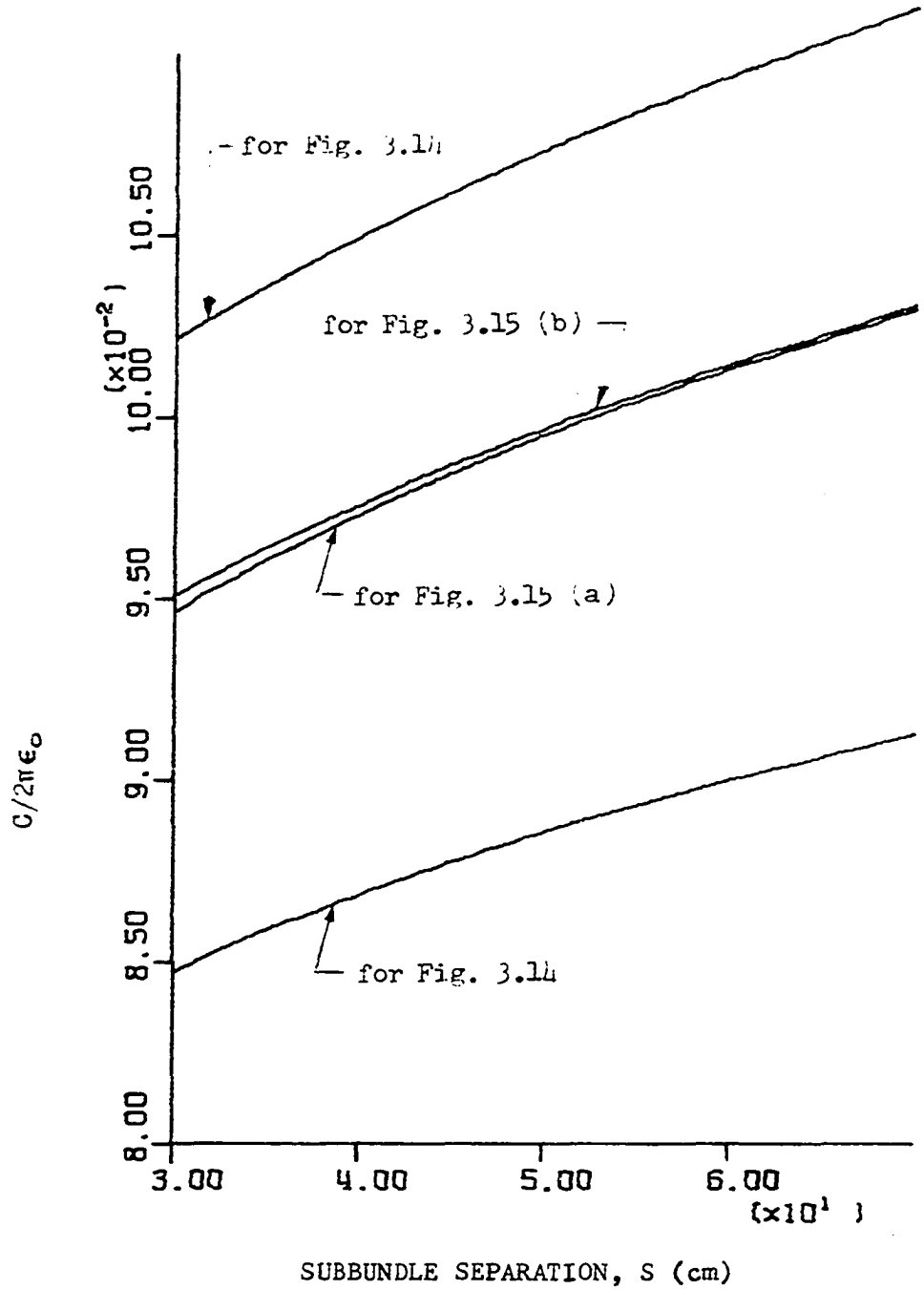

Figure 3.28. Variation of capacitance with subbundle separation for different configurations of split-bundle lines. R = 2 cm, H = 2000 cm, A = B = 24 cm.

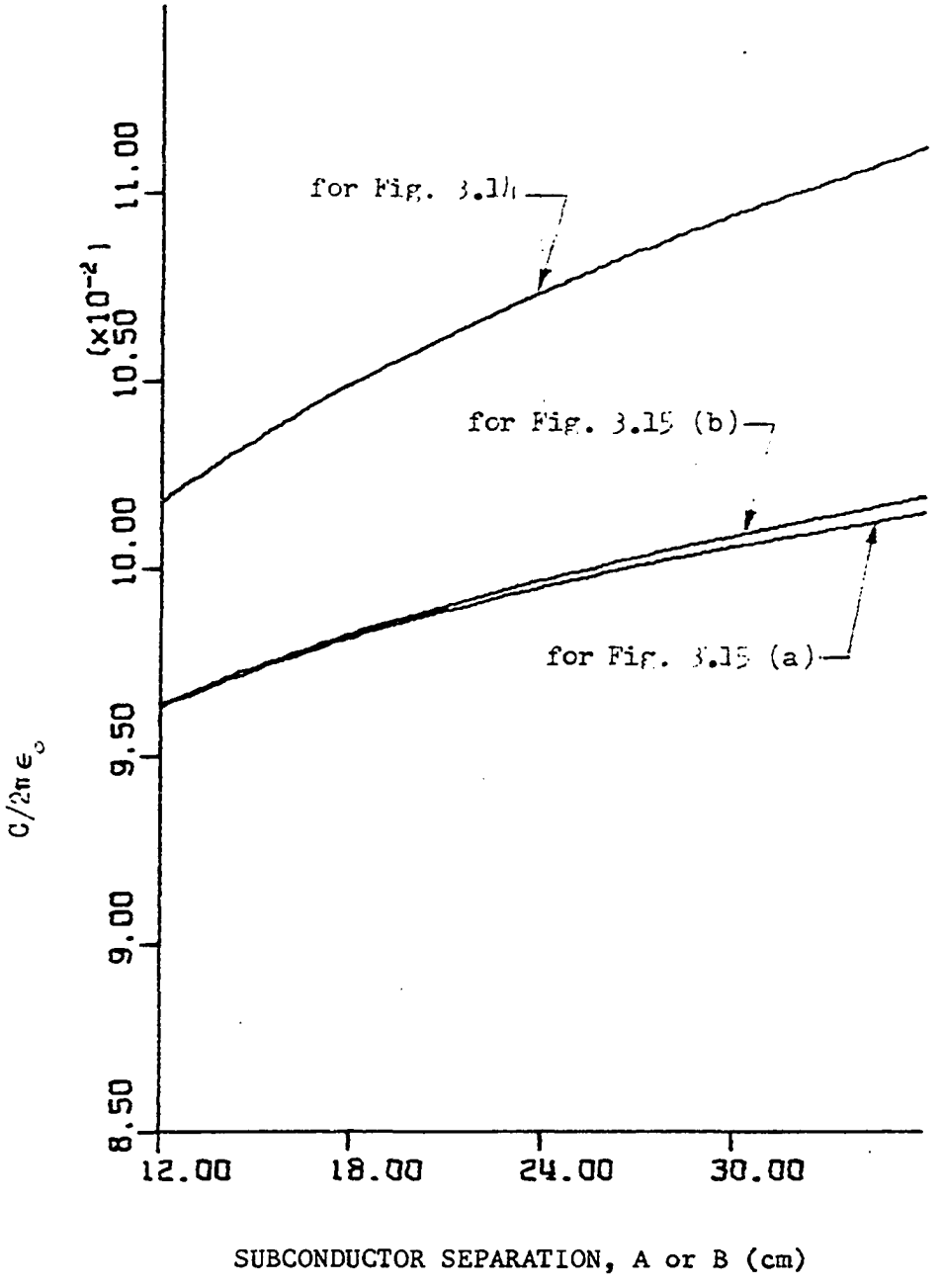

Figure 3.29. Variation of capacitance with subconductor separation for different configurations of split-bundle lines. R = 2 cm, S = 50 cm, H = 2000 cm.

the conductor height influences the electric field very much.

Figure 3.24 illustrates the variation of the maximum electric field with the subbundle separation. This figure indicates that the effect of the subbundle separation on the electric field is very small. As the subbundle separation increases, the electric field increases slightly. This is because of the reduced effect of the proximity.

Figure 3.25 illustrates the variation of the maximum electric field with the subconductor separation. This figure indicates that the effect of the subconductor separation on the electric field is slight. As the subconductor separation increases, the electric field decreases.

Figure 3.26 illustrates the variation of the capacitance with the subconductor radius. The capacitance increases with the subconductor radius and the number of subconductors in each subbundle.

Figure 3.27 illustrates the variation of the capacitance with the conductor height. The conductor height has a very high effect on the capacitance. The capacitance decreases with the increase in the conductor height.

Figure 3.28 illustrates the variation of the capacitance with the subbundle separation. The capacitance increases with the subbundle separation.

Figure 3.29 illustrates the variation of the capacitance with the subconductor separation. The capacitance increases with the subconductor separation.

In order to compare the results obtained by the method described in this section with those obtained by Comsa and Thanassoulis (6, 28),

the values of the maximum electric field are calculated for different subbundle separation.

Figure 3.30 illustrates the variation of the maximum electric field with the subbundle separation, 2S, for different ratios of A/d where A is the subconductor separation and d is the diameter of each subconductor. The value of d is chosen such that the total sum of the cross-sectional areas of all subconductors [eight subconductors of Figure 3.30(a)] is equal to that of a single conductor of diameter D = 3.5". The bundle configuration of Figure 3.30(b) is obtained by letting A = 0 and the subconductor diameter d' is such that its cross-sectional area is equal to that of the sum of four subconductors of Figure 3.30(a). These dimensions are chosen for comparing the results obtained by the charge simulation method with the approximate method suggested by Comsa and Thanassoulis.

As seen from Figure 3.30, there is a difference of about 2 to 3 percent between the accurate results obtained by the charge simulation method and the approximate results obtained by Comsa and Thanassoulis. The main reason behind this difference is that the effect of the ground has been neglected by Comsa and Thanassoulis.

For A/d = 4 and the subbundle separation equal to 24", the values of the maximum electric field are found to be 0.073688, 0.069480, and 0.066544 volt/cm per volt for three different conductor heights of 15m, 20m, and 25m respectively. This suggests that the height of the conductor above the ground has a great effect in determining the values of the electric field. Therefore, the conductor height should not be neglected in the computation of the electric field for the split-bundle lines.

Figure 3.30 suggests that the splitting of each subbundle in four subconductors is effective in reducing the intensity of electric field for A/d ratios of 4 and 6 while A/d ratio of 2 increases the intensity of the electric field over that of an equivalent twin-bundle line of Figure 3.30(b).

Figure 3.31 illustrates the variation of the maximum electric field with the subbundle separation, 2S, for different A/d ratios for the split-twin-bundle line with two subconductors in each subbundle [Figure 3.31(a)] and the twin-bundle line [Figure 3.31(b)]. Again, the dimensions are chosen in order to compare the results obtained by the charge simulation method with those obtained by the approximate dipole method suggested by Comsa and Thanassoulis (6, 28).

Figure 3.31 shows a great difference between the two sets of results. This indicates that the approximations made in the dipole method (especially about neglecting the effect of the ground) can not be justified.

Figure 3.31 suggests that the splitting of each subbundle into two subconductors is effective in reducing the intensity of the electric field for A/d ratios of 4 and 6 and the subbundle separation greater than 24".

Although, in this section, the results are shown only for the case of a split-twin-bundle conductor with one, two, and four subconductors in each subbundle, the computer program written for this purpose can be used with few changes to include all the various cases shown in Figure 3.32. The accuracy of the results obtained for this case is as good as the one illustrated in this section.

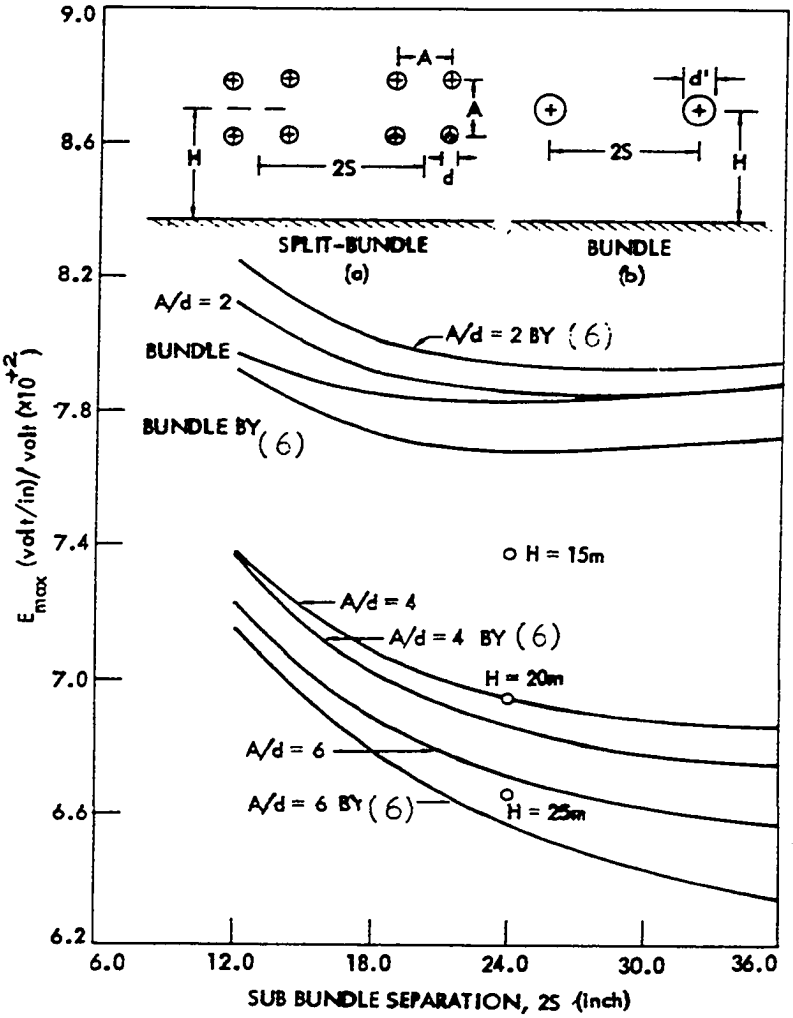

Figure 3.30. Variation of maximum electric field with subbundle separation for different ratios of A/d. d = 1.2374", d' = 2.4748", H = 2000 cm; symbol o indicates the effect of conductor height.

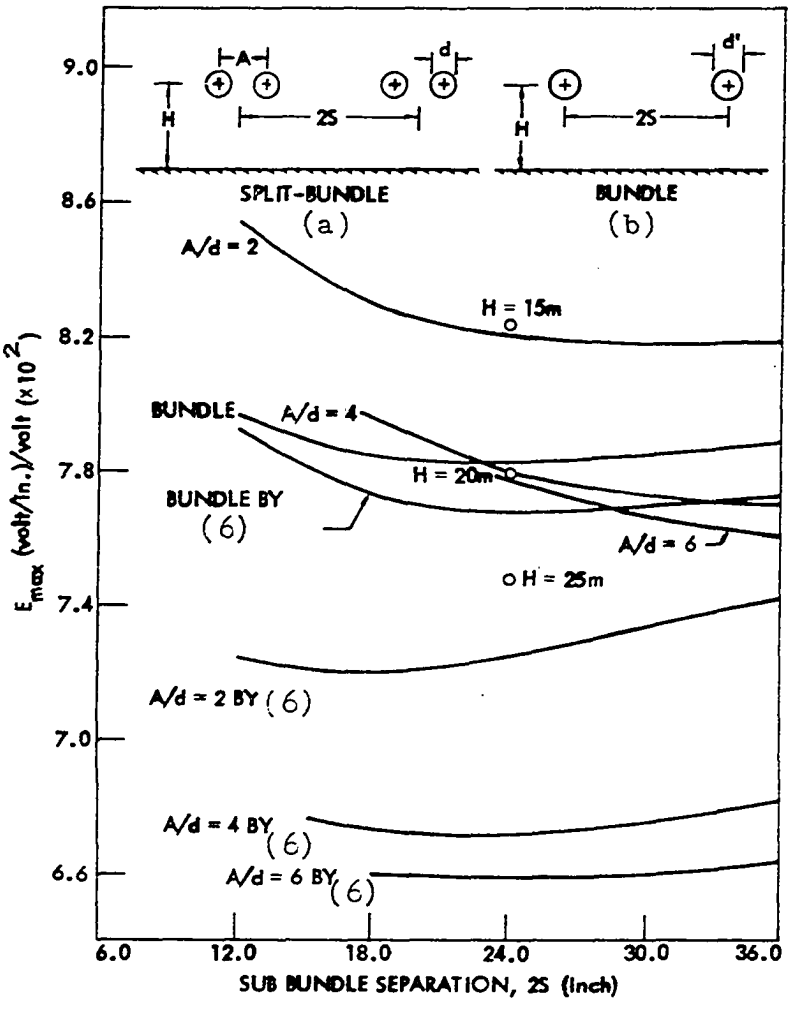

Figure 3.31. Variation of maximum electric field with subbundle separation for different ratios of A/d. d = 1.75", d' = 2.4748", H = 2000 cm; symbol o indicates the effect of conductor height.

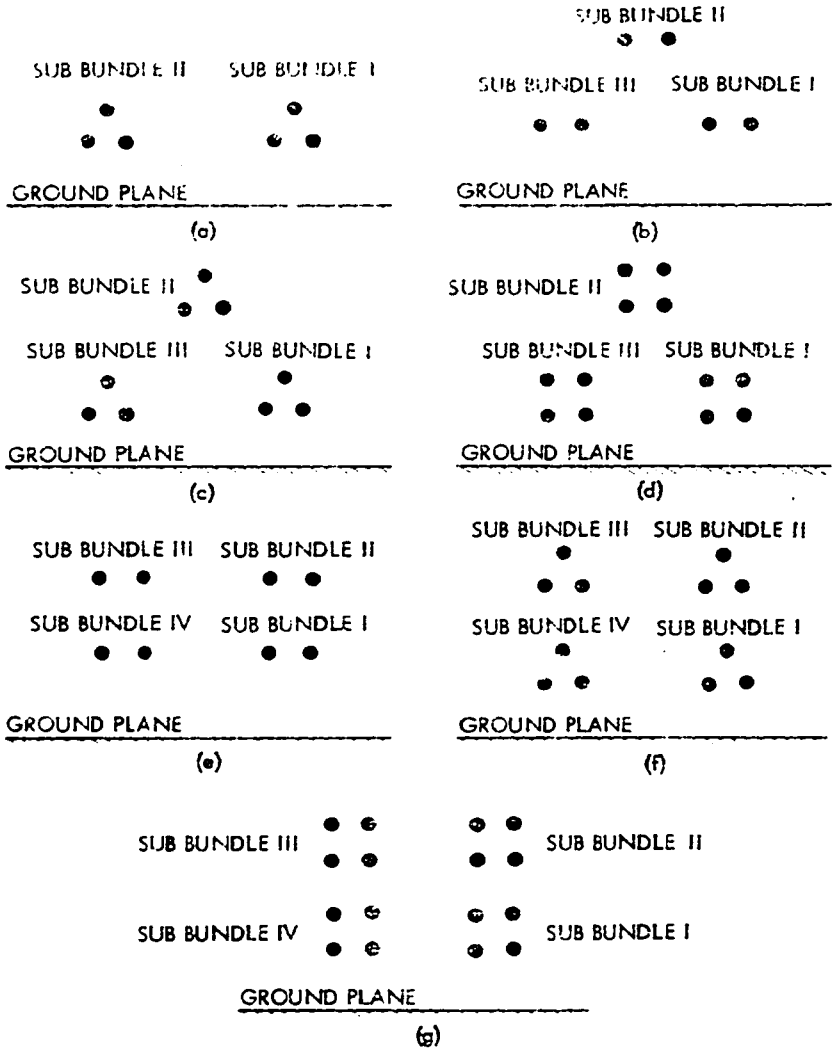

Figure 3.32. Various configurations of split-bundle transmission lines.

6. Conclusions

(1) The method described here for computing the electric field and potential is easy and gives accurate results.

(2) The accurate values of capacitance are obtained by this method by summing the values of the line charges obtained by solving the simultaneous Equations 3.41.

(3) The effect of the height of the conductor above the ground should not be neglected in the computation of the electric field for corona studies.

(4) The method described in this section can be used for any system of parallel conductors above the ground with positive polarity, negative polarity or the combination of both the polarities.

C. Computer Plotting of Equipotential and Equigradient Lines for EHV and UHV Transmission Lines

1. General

The knowledge of the exact electric field and potential distribution on the conductor surface as well as in the interelectrode space is essential for calculating and predicting the corona onset voltage, corona loss and radio interference (4). The charge simulation method described in the preceding sections is used for computing accurately the electric field and potential distribution around EHV and UHV transmission lines.

The best way to illustrate the distribution of the electric field and potential around EHV and UHV transmission lines is to plot the equipotential and equigradient lines. These plottings, which are convenient to understand, give a great deal of information regarding the distribution

of the electric field and the potential in less space. These advantages can not be achieved by tabulating the results.

The plotting of equipotential and equigradient lines by hand is difficult, inaccurate and time consuming. Therefore, a computer program is written for computing the electric field and potential distribution around EHV and UHV transmission lines and then plotting the equipotential and equigradient lines. The computer program includes one, two and four subconductors in each subbundle.

2. Programming

The plotting of equipotential and equigradient lines for only the case of a bipolar line of Figure 3.1 is explained here. Using the charge simulation method described earlier, the values of the electric field and potential at grid points around the positive conductor as shown in Figure 3.33 are computed. These values are computed in the form of a matrix of size (L x M). The size of the grid and the values of L and M depend on the geometrical parameters of the transmission lines and the levels of the equipotential and the equigradient lines we want to plot.

Since the values of the electric potential and field at the grid points which fall inside the conductor surface are not defined, the values of the potential at these points are assigned as one unit (same as the assumed conductor potential) and the values of the electric field at these points are assigned as the maximum value of the electric field on the conductor surface. This prevents the equipotential and equigradient lines from being plotted inside the conductor surface.

Once the values of the electric potential and field at grid points

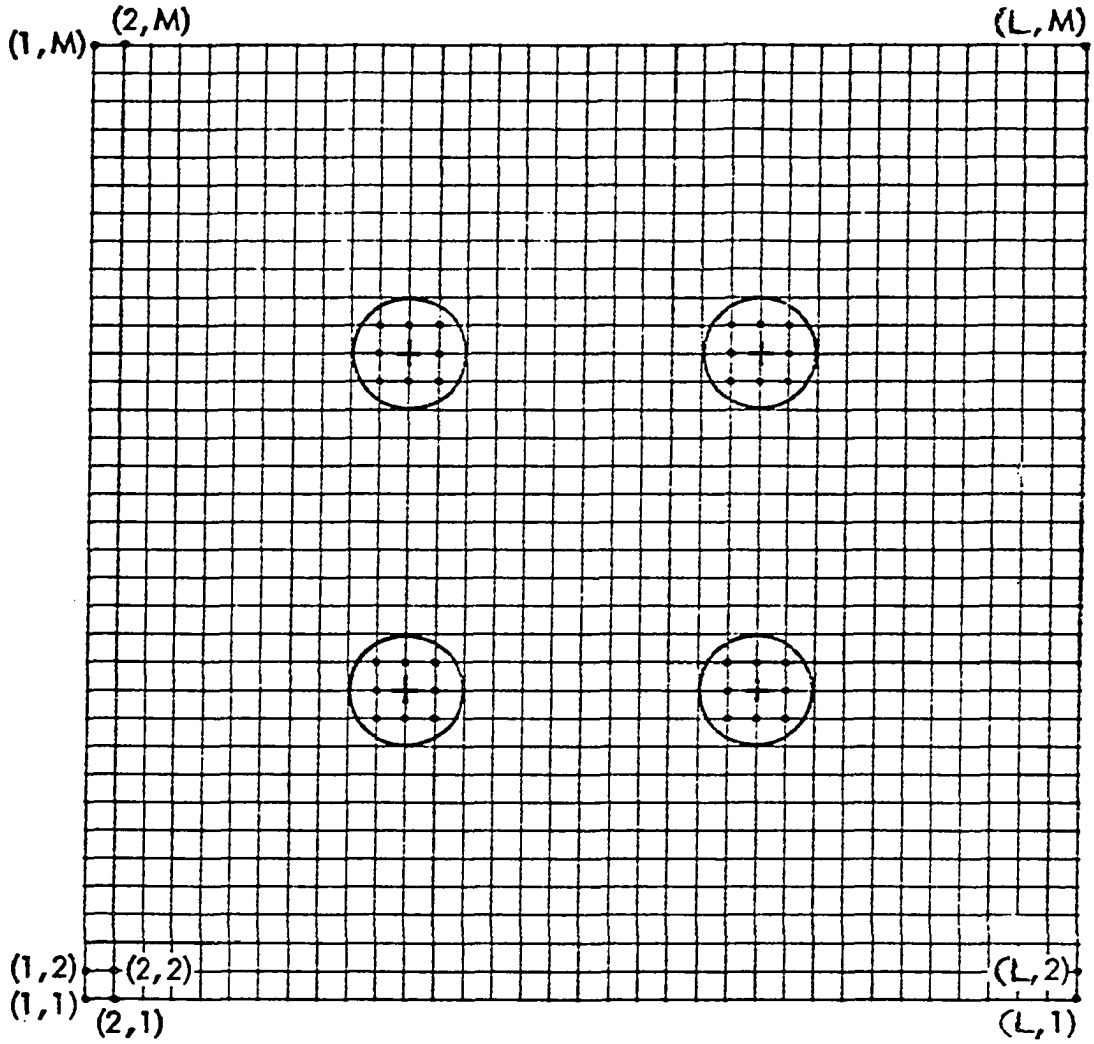

Figure 3.33. Values of electric potential and field at grid points around positive conductor of bipolar transmission line are computed in the form of a matrix.

are obtained in the form of a matrix, a subroutine CONTUR available at the Computation Center, Iowa State University is used to plot the equipotential and equigradient lines around the conductor.

The computer programs to plot the equipotential and the equigradient lines are given in Appendix C and D respectively. These programs are simple and give accurate results. These programs can also be used for plotting the equipotential and equigradient lines around conductors of Figures 3.2, 3.3, 3.14, 3.15, and 3.16 with few changes.

3. Results

Figures 3.34 and 3.35 illustrate the equipotential and equigradient lines in the vicinity of the positive conductor of the bipolar line of Figure 3.1. These results are obtained for R = 2 cm, A = B = 24 cm, H = 1500 cm, and S = 300 cm.

Figures 3.36 and 3.37 illustrate the equipotential and equigradient lines in the vicinity of the positive conductor of Figure 3.2. These results are obtained for R = 2 cm, A = 24 cm, H = 1500 cm, and S = 300 cm.

Figures 3.38 and 3.39 illustrate the equipotential and equigradient lines in the vicinity of the positive conductor of Figure 3.3. These results are obtained for R = 2 cm, H = 1500 cm and S = 300 cm.

Figures 3.40 and 3.41 illustrate the equipotential and equigradient lines in the vicinity of the subconductors of subbundle I of Figure 3.14. These results are obtained for R = 2 cm, A = B = 24 cm, H = 2000 cm, and S = 30 cm.

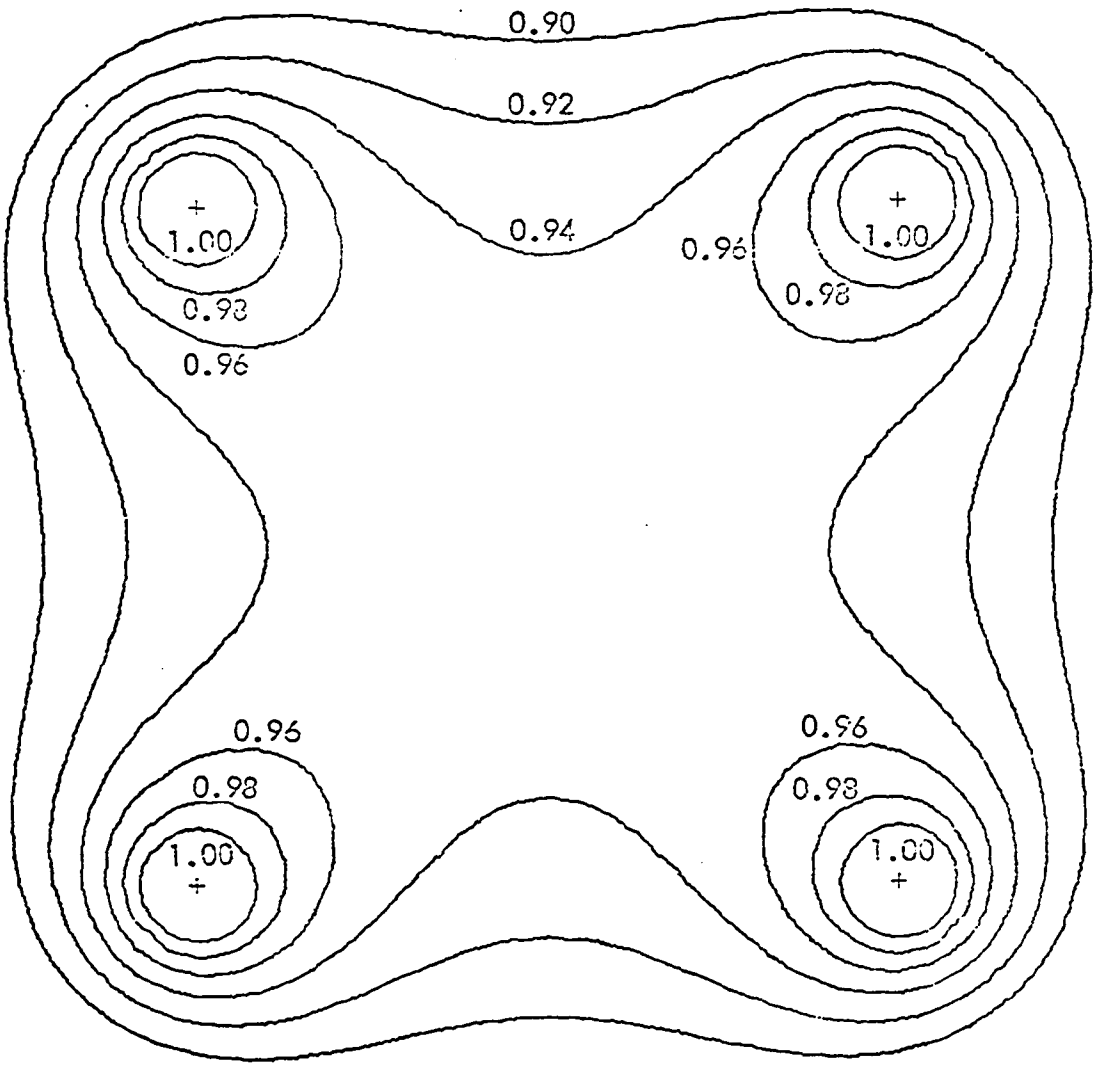

Figure 3.34. Equipotential lines in the vicinity of positive conductor of four-bundle bipolar transmission line. R = 2 cm, A = B = 24 cm, H = 1500 cm, S = 300 cm.

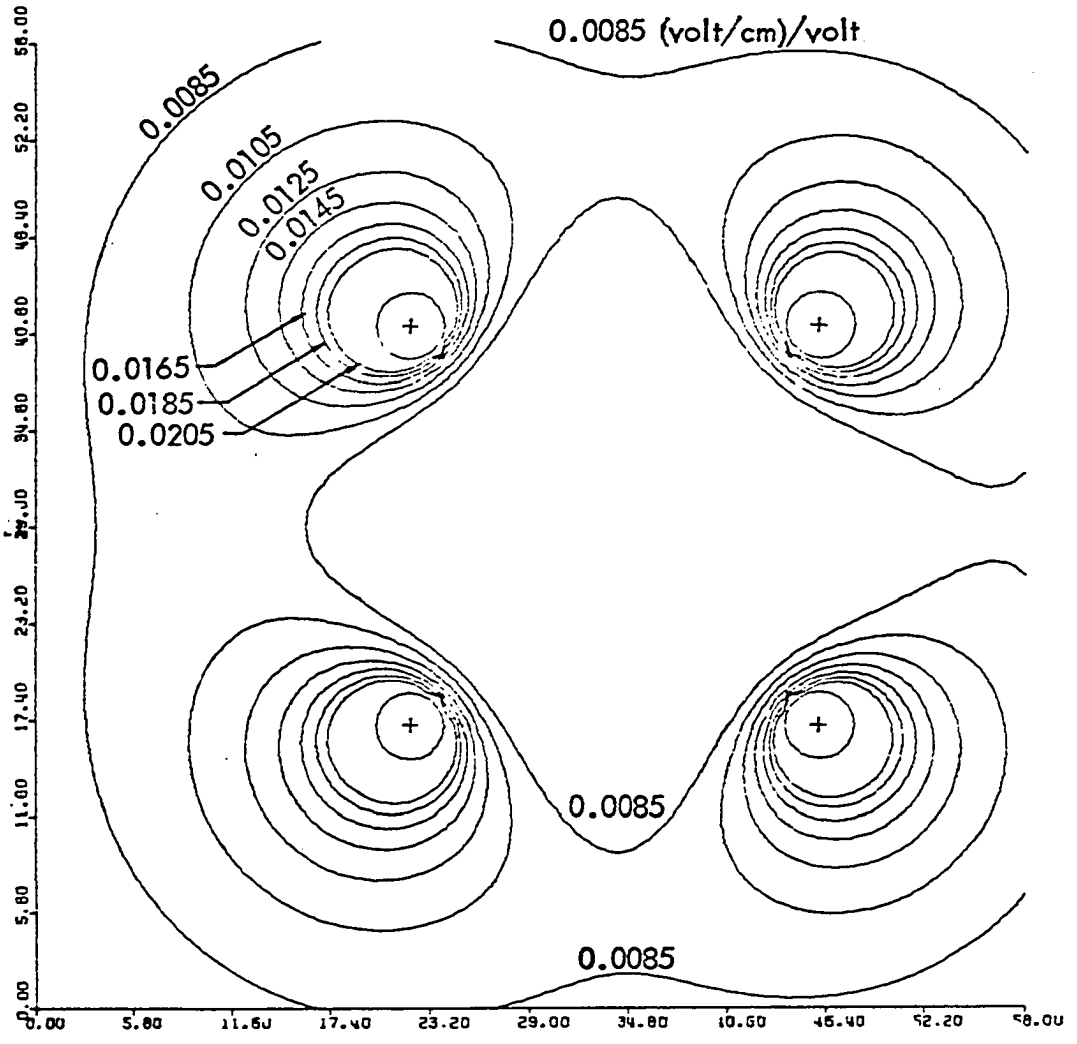

Figure 3.35. Equigradient lines in the vicinity of positive conductor of four-bundle bipolar transmission line. R = 2 cm, A = B = 24 cm, H = 1500 cm, S = 300 cm.

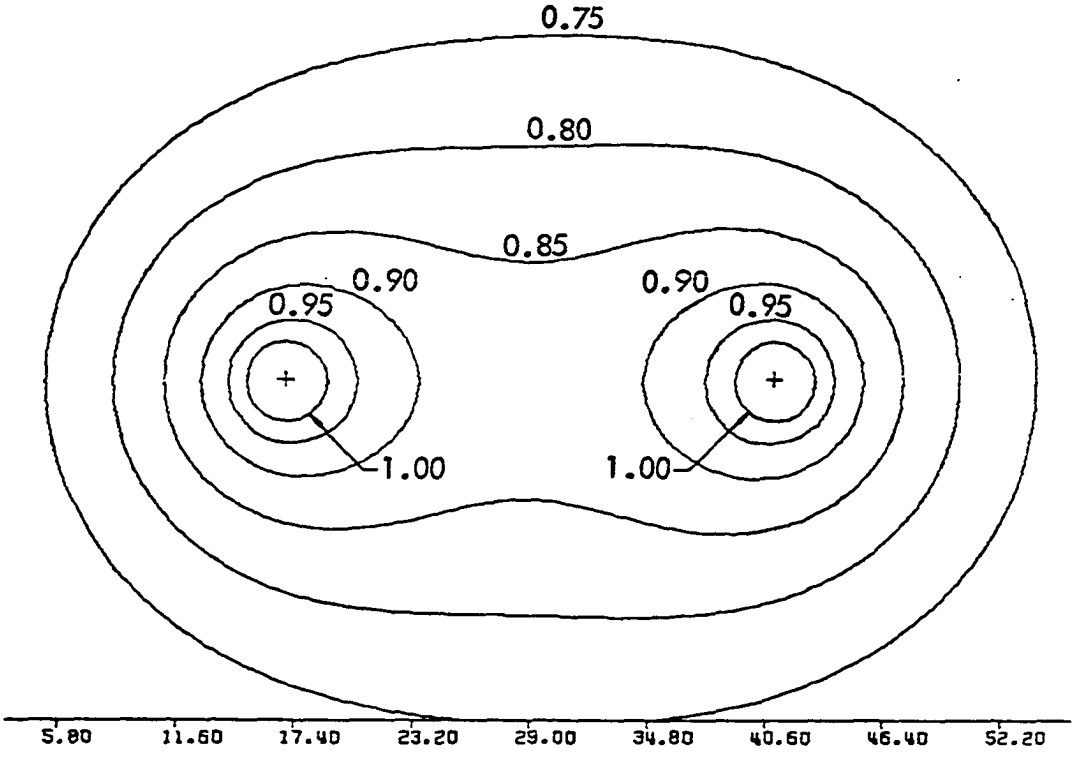

Figure 3.36. Equipotential lines in the vicinity of positive conductor of twin-bundle bipolar transmission line. R = 2 cm, A = 24 cm, H = 1500 cm, S = 300 cm.

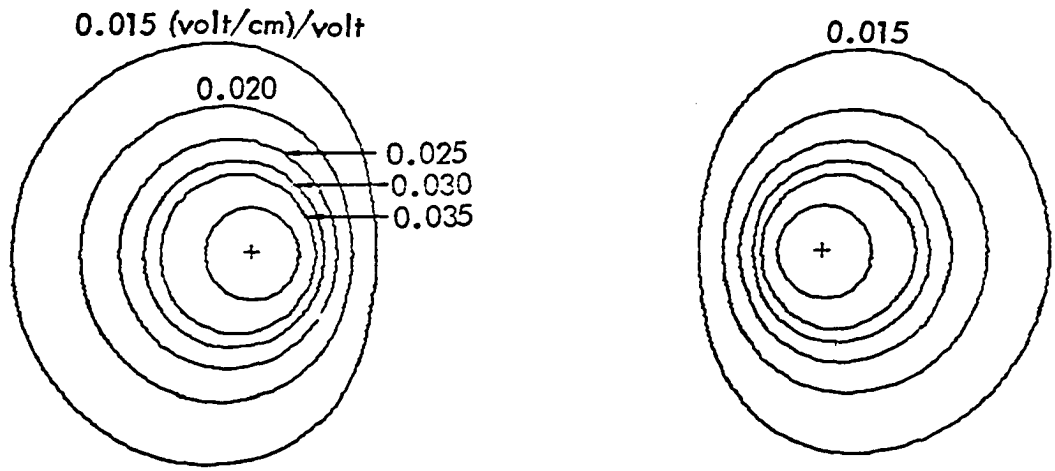

Figure 3.37. Equigradient lines in the vicinity of positive conductor of twin-bundle bipolar transmission line. R = 2 cm, A = 24 cm, H = 1500 cm, S = 300 cm.

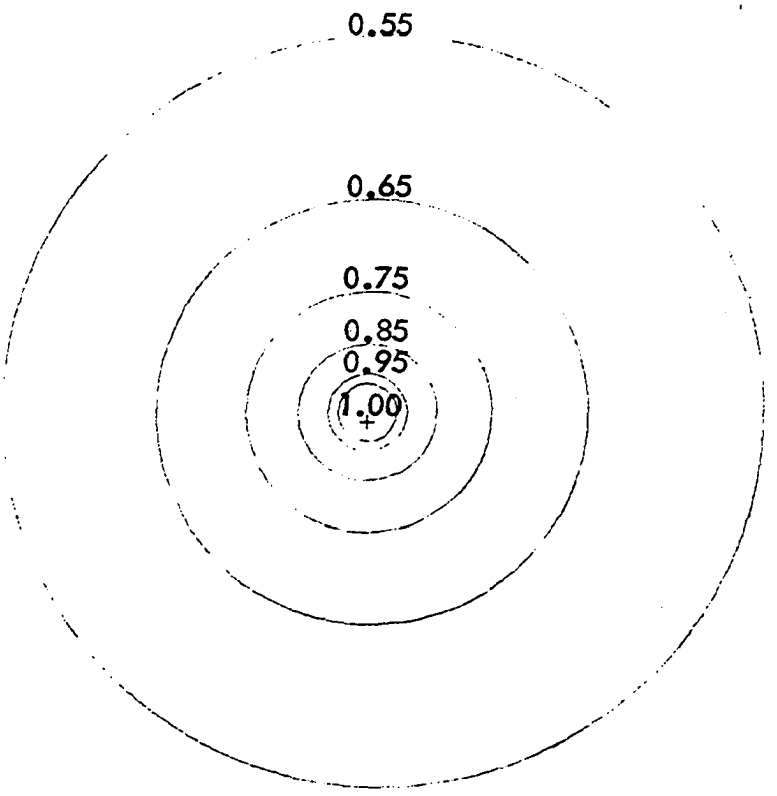

Figure 3.38. Equipotential lines in the vicinity of positive conductor of simple bipolar transmission line. R = 2 cm, H = 1500 cm, S = 300 cm.

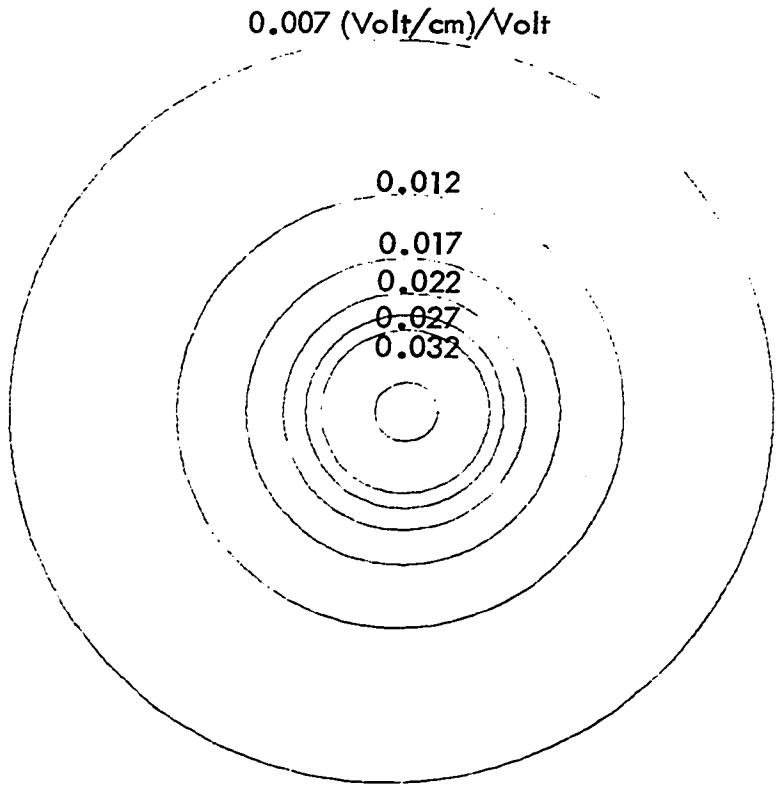

Figure 3.39. Equigradient lines in the vicinity of positive conductor of simple bipolar transmission line. R = 2 cm, H = 1500 cm, S = 300 cm.

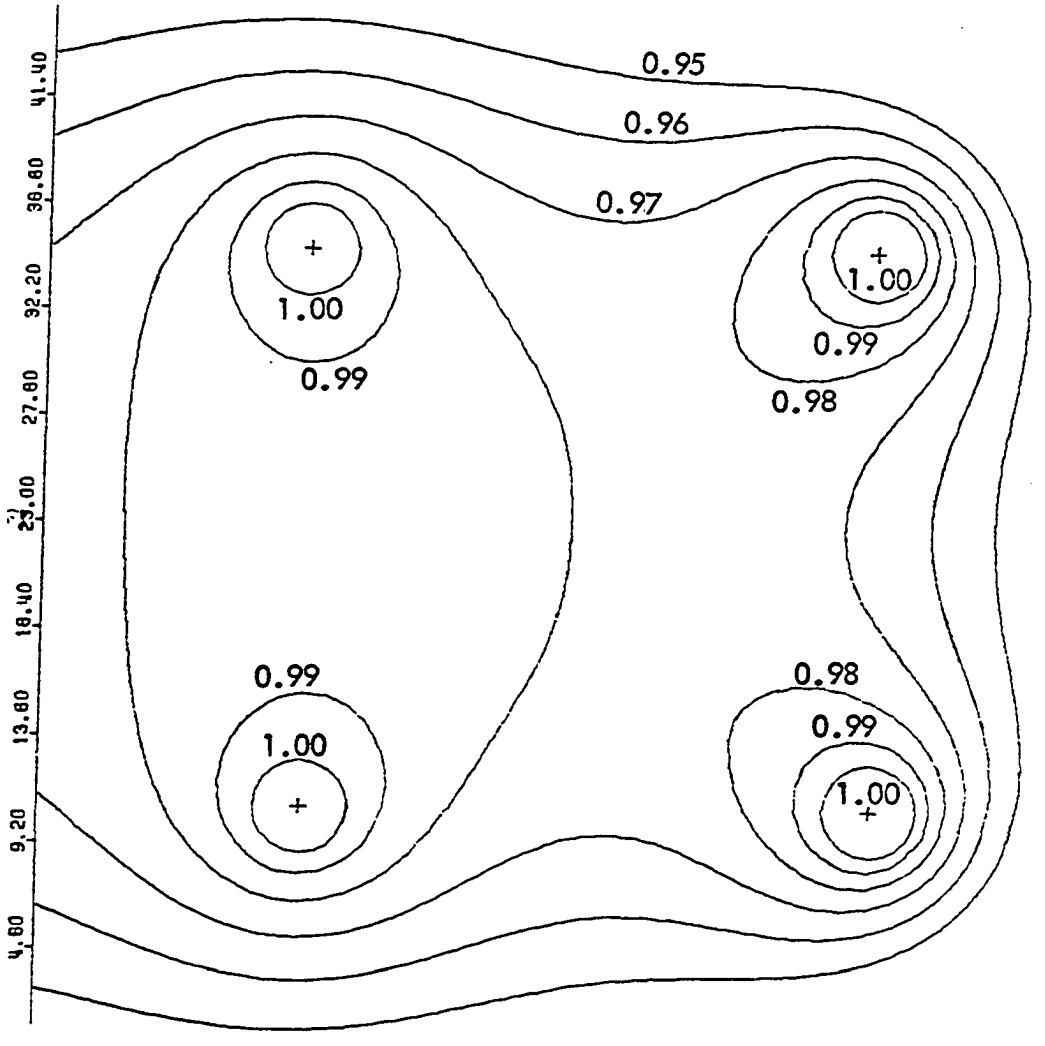

Figure 3.40. Equipotential lines in the vicinity of Bundle I subconductors of split-twin-bundle transmission line. R = 2 cm, A = B = 24 cm, H = 2000 cm, S = 30 cm.

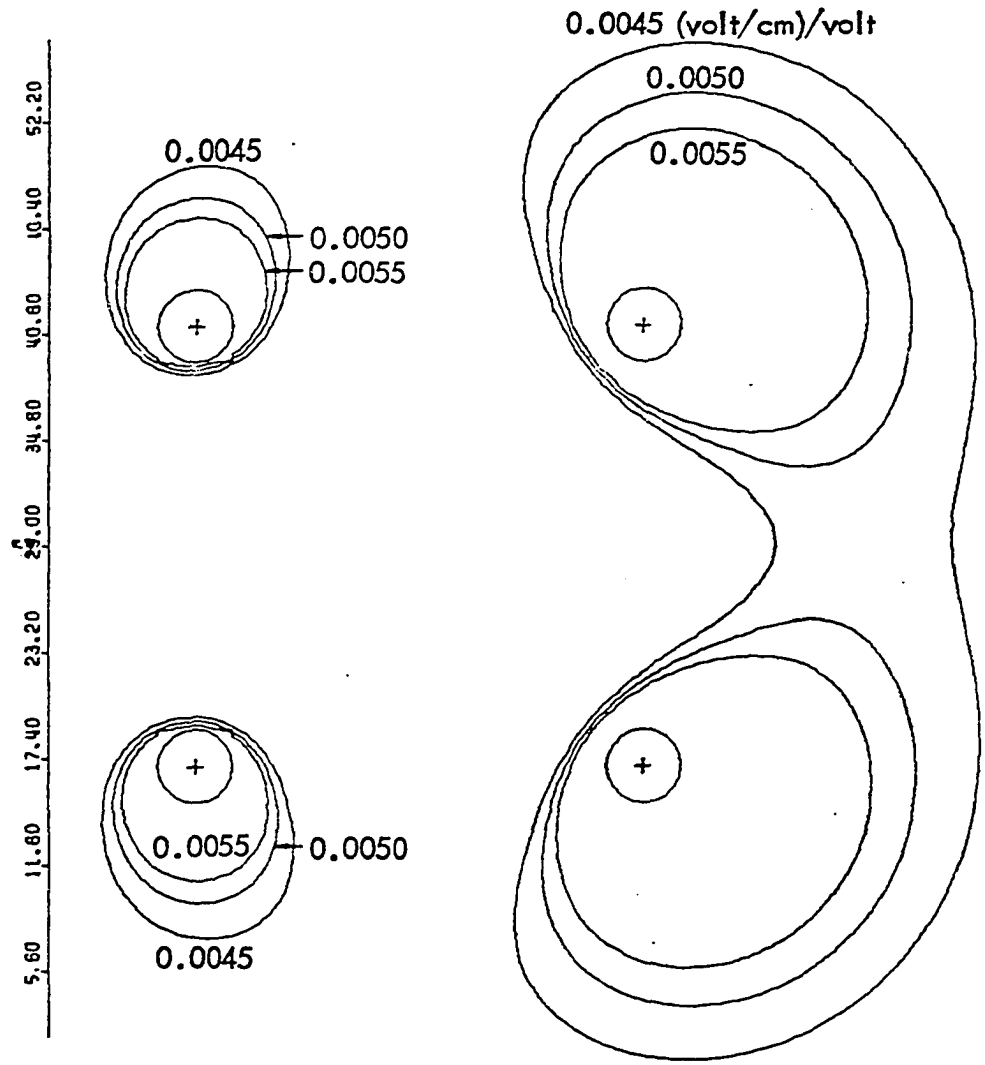

Figure 3.41. Equigradient lines in the vicinity of Bundle I subconductors of split-twin-bundle transmission line. R = 2 cm, A = B = 24 cm, H = 2000 cm, S = 30 cm.

Figures 3.42 and 3.43 illustrate the equipotential and equigradient lines in the vicinity of the subconductors of subbundle I of Figure 3.15. These results are obtained for R = 2 cm, H = 1500 cm, and S = 30 cm.

Figures 3.44 and 3.45 illustrate the equipotential and equigradient lines in the vicinity of subconductors I of Figure 3.16. These results are obtained for R = 2 cm, H = 1500 cm, and S = 30 cm.

D. Stranded Conductors Above Ground

1. General

The knowledge of the exact electric field at the conductor surface as well as in the interelectrode space is necessary to calculate corona onset voltage, corona loss and the radio interference on EHV transmission lines (4-5). A great amount of research on the problem of electric field computation has been carried out in the last several years (15-28). However, the problem of the electric field computation for the stranded and the bundled conductors as actually used in practice has not been solved. This problem has not been given enough attention by the researchers because of the complexity of the problem.

The usual procedure is to compute the electric field for smooth cylindrical conductors and then use strand factors to calculate the peripheral field on the surface of the stranded conductors. The strand factor is defined as the ratio of the electric field for a smooth cylindrical conductor to the electric field for a stranded conductor of the same radius. Since the value of the electric field on the surface

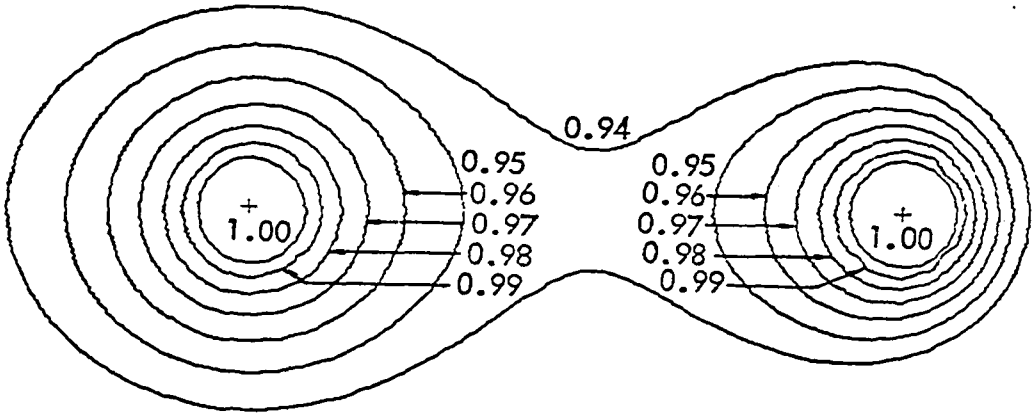

Figure 3.42. Equipotential lines in the vicinity of Bundle I sub-conductors of split-twin-bundle transmission line. R = 2 cm, A = 24 cm, H = 1500 cm, S = 30 cm.

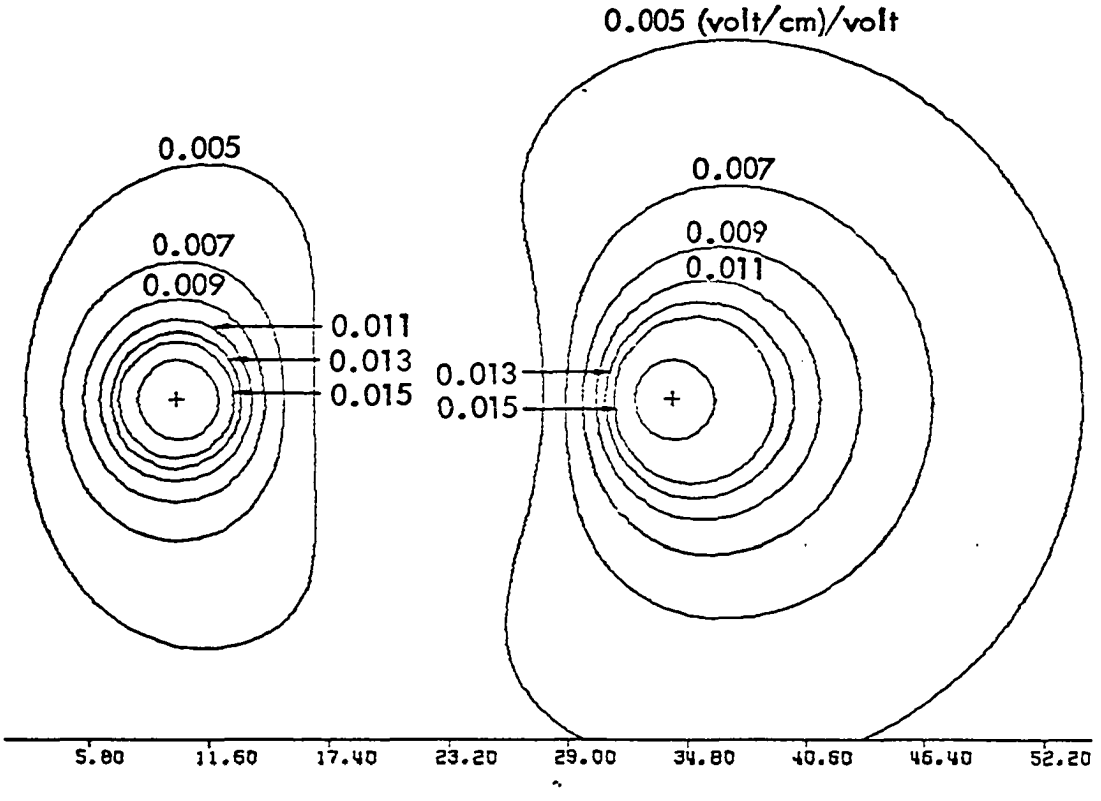

Figure 3.43. Equigradient lines in the vicinity of Bundle I subconductors of split-twin-bundle transmission line. R = 2 cm, A = 24 cm, H = 1500 cm, S = 30 cm.

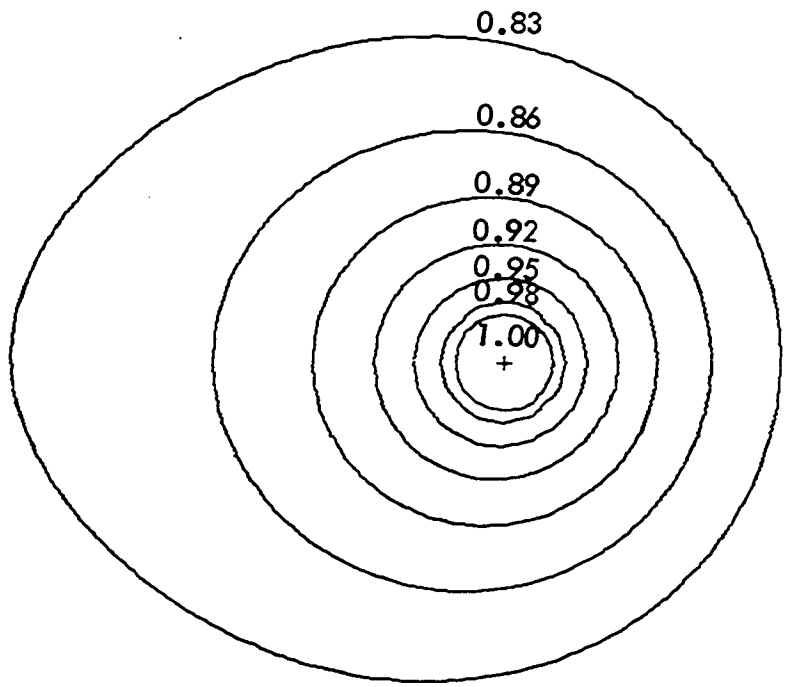

Figure 3.44. Equipotential lines in the vicinity of subconductor I of twin-bundle transmission line. R = 2 cm, H = 1500 cm, S = 30 cm.

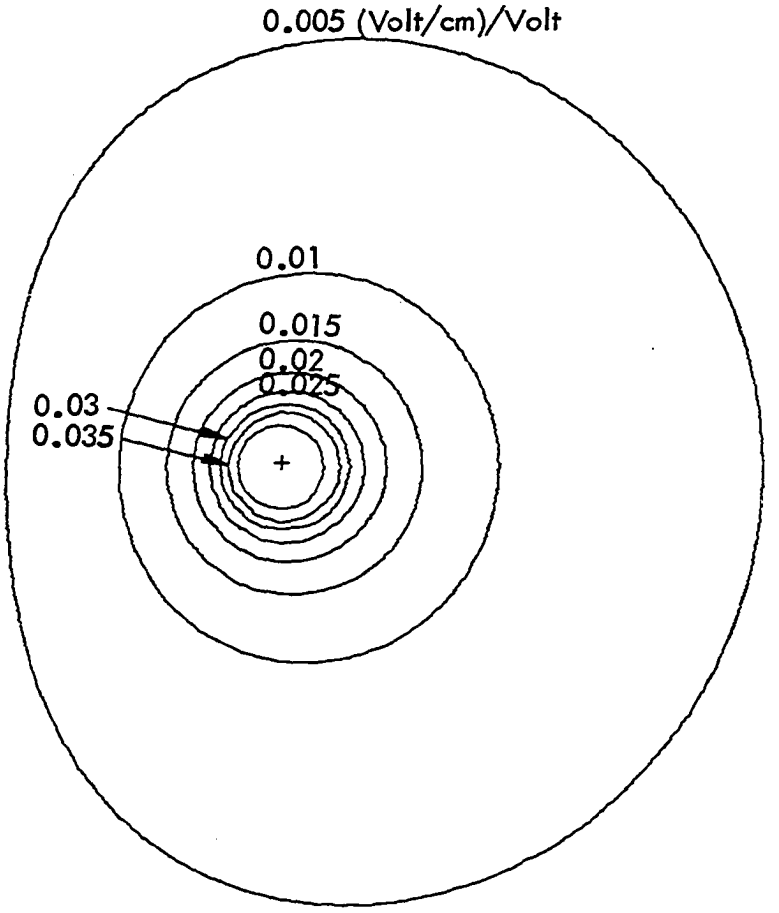

Figure 3.45. Equigradient lines in the vicinity of subconductor I of twin-bundle transmission line. R = 2 cm, H = 1500 cm, S = 30 cm.

of the stranded conductor varies from the maximum at the tip to zero at discontinuity points (where two strands touch each other), the values of the strand factor vary on the conductor surface. The strand factor is also a function of the number of strands, N, in the outermost layer of the conductor. The procedure of using the strand factors to predict the value of the electric field for stranded conductors is not sufficiently accurate for the corona calculations. Moreover, these strand factors do not remain constant everywhere in space.

Since the analytical methods for computing the field distribution for stranded conductors are not available, the numerical methods with the use of digital computers seem to be the only answer. The charge simulation method described earlier is used here to compute the electric field and capacitance of stranded conductors. Only two simple geometric configurations of the transmission line are considered in this section:

(1) A stranded conductor above ground.

(2) A twin-bundle unipolar stranded conductor above ground.

2. Mathematical formulation

The case of a single-stranded conductor above ground plane is a special case of the twin-bundle unipolar stranded conductor above the ground plane where the bundle separation is equal to zero. Therefore, only the mathematical formulation for the twin-bundle stranded conductor is given here.

The stranded bundle conductor configuration is shown in Figure 3.46.

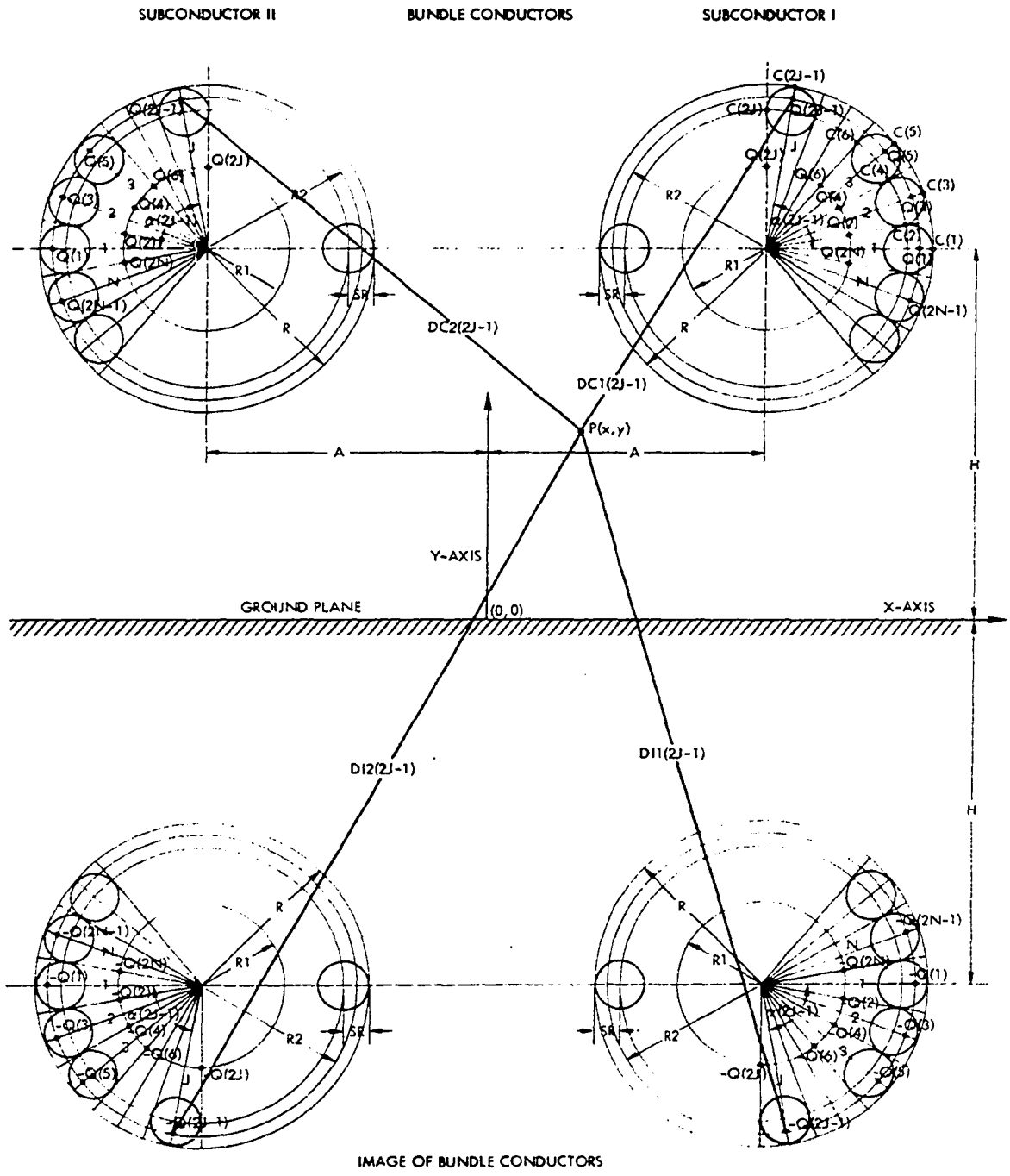

Figure 3.46. Charge representation of the unipolar twin-bundle conductor system.

The actual charge distribution on the surface of each subconductor is represented by axial line charges of unknown magnitudes Q(K), where K = 1,2,...,2N. The charges Q(2J - 1), J = 1,2,.....,N are placed symmetrically on a fictitious coaxial cylinder of radius R2, and the charges Q(2J), J = 1,2,....,N, are placed symmetrically on another coaxial cylinder of radius R1. The locations of these line charges are given by angles measured from the horizontal plane. These are designated

$$\alpha(K) = (K - 1)\cdot(360/2N),\ K = 1,2,....,2N \qquad 3.53$$

Image charges of these line charges are placed on the other side of the ground plane which is assumed at zero potential. The potential $\phi(x,y)$ at any point P(x,y) which is the algebraic sum of the potentials due to each of the line charges and their images, is given by

$$\phi(x,y) = \sum_{K=1}^{2N} -Q(K) \log_e \frac{DCi(K)\cdot DC2(K)}{DI1(K)\cdot DI2(K)} \qquad 3.54$$

where the distances DC1, DC2, DI1, and DI2 are as shown in Figure 3.46 and are given by

$$DC1(K) = (\{x[Q(K)] - x\}^2 + \{y[Q(K)] - y\}^2)^{\frac{1}{2}} \qquad 3.55$$

$$DC2(K) = (\{x[Q(K)] + x\}^2 + \{y[Q(K)] - y\}^2)^{\frac{1}{2}} \qquad 3.56$$

$$DI1(K) = (\{x[Q(K)] - x\}^2 + \{y[Q(K)] + y\}^2)^{\frac{1}{2}} \qquad 3.57$$

$$DI2(K) = (\{x[Q(K)] + x\}^2 + \{y[Q(K)] + y\}^2)^{\frac{1}{2}} \qquad 3.58$$

and x[Q(K)] and y[Q(K)] are x and y coordinates of the line charges Q(K). They can be expressed in terms of radius R1 and R2 on which the charges are placed, the height H of the conductor above the ground, and the angle $\alpha(K)$ as

$$x[Q(2J - 1)] = R2 \cdot \cos \alpha(2J - 1) + A \qquad 3.59$$

$$y[Q(2J - 1)] = R2 \cdot \sin \alpha(2J - 1) + H \qquad 3.60$$

$$x[Q(2J)] = R1 \cdot \cos \alpha(2J) + A \qquad 3.61$$

$$y[Q(2J)] = R1 \cdot \sin \alpha(2J) + H \qquad 3.62$$

where

$$J = 1,2,.....,N$$

The electric field E at point P(x,y) is given by

$$\bar{E}(x,y) = -\nabla\phi(x,y) \qquad 3.63$$

Therefore, the electric field in x and y direction are given by

$$E_X(x,y) = -\frac{\partial\phi(x,y)}{\partial x} \qquad 3.64$$

$$E_Y(x,y) = -\frac{\partial\phi(x,y)}{\partial y} \qquad 3.65$$

Using equations 3.54 to 3.58, 3.64 and 3.65, we obtain

$$E_X(x,y) = \sum_{K=1}^{2N} Q(K)\left[-\frac{X1}{Z1} + \frac{X2}{Z2} + \frac{X1}{Z3} - \frac{X2}{Z4}\right] \qquad 3.66$$

$$E_Y(x,y) = \sum_{K=1}^{2N} Q(K)\left[-\frac{Y1}{Z1} - \frac{Y1}{Z2} - \frac{Y2}{Z3} - \frac{Y2}{Z4}\right] \qquad 3.67$$

where

$$X1 = x[Q(K)] - x \qquad Z1 = X1^2 + Y1^2$$

$$Y1 = y[Q(K)] - y \qquad Z2 = X2^2 + Y1^2$$

$$X2 = x[Q(K)] + x \qquad Z3 = X1^2 + Y2^2$$

$$Y2 = y[Q(K)] + y \qquad Z4 = X2^2 + Y2^2$$

where values of x[Q(K)] and y[Q(K)] are given by Equations 3.59 to 3.62.

If we want to find E at any point located at a distance ρ from the center

of the subconductor and at an angle β from the horizontal through the center of the subconductor, then we make the following transformation of coordinates:

$$x = \rho\cos\beta + A \qquad 3.68$$

$$y = \rho\sin\beta + H \qquad 3.69$$

3. Boundary conditions

The potential at any point on the conductor surface must be equal to one unit, which is the assumed potential of the conductor with respect to the ground. To satisfy this condition, points C(K), K = 1,2,....,2N are chosen on the conductor surface and potentials at these points are equated to one unit. Potential $\phi[C(K)]$ at any point C(K) on the conductor surface is given by

$$\phi[C(K)] = -\sum_{J=1}^{2N} Q(J) \log_e \frac{DC1(J,K)\cdot DC2(J,K)}{DI1(J,K)\cdot DI2(J,K)} = 1.0 \qquad 3.70$$

where

$$DC1(J,K) = (\{x[C(K)] - x[Q(J)]\}^2 + \{y[C(K)] - y[Q(J)]\}^2)^{\frac{1}{2}} \qquad 3.71$$

$$DC2(J,K) = (\{x[C(K)] + X[Q(J)]\}^2 + \{y[C(K)] - y[Q(J)]\}^2)^{\frac{1}{2}} \qquad 3.72$$

$$DI1(J,K) = (\{x[C(K)] - x[Q(J)]\}^2 + \{y[C(K)] + y[Q(J)]\}^2)^{\frac{1}{2}} \qquad 3.73$$

$$DI2(J,K) = (\{x[C(K)] + x[Q(J)]\}^2 + \{y[C(K)] + y[Q(J)]\}^2)^{\frac{1}{2}} \qquad 3.74$$

where x[C(K)] and y[C(K)] are x and y coordinates of point C(K) and these are given by

$$x[C(2J - 1)] = R \cdot \cos \alpha(2J - 1) + A \qquad 3.75$$

$$y[C(2J - 1)] = R \cdot \sin \alpha(2J - 1) + H \qquad 3.76$$

$$x[C(2J)] = R3 \cdot \cos \alpha(2J) + A \qquad 3.77$$

$$y[C(2J)] = R3 \cdot \sin \alpha(2J) + H \qquad 3.78$$

where

$$J = 1,2,\ldots,N$$

and

$$R3 = (R^2 - 2 \cdot R \cdot SR)^{\frac{1}{2}} \qquad 3.79$$

Equations 3.77 to 3.79 give coordinates of points where the strands in the outermost layer touch one another.

The equation representing the boundary condition is 3.70. The other boundary condition is that the ground potential be zero. This condition is automatically satisfied by including image charges which are symmetrically located with respect to the ground plane.

4. Choice of parameters

To satisfy boundary conditions and to obtain solvable equations that yield a unit equipotential surface coinciding with the surface of the stranded conductor, care must be taken in choosing parameters R1 and R2. These parameters determine the position of the unknown axial line charges. After running the computer program many times, the following values of R1 and R2 were found to satisfy the boundary conditions well:

$$R1 = R/2 \qquad 3.80$$

$$R2 = R - (SR/2) \qquad 3.81$$

It was found that ±20 percent change in the value of R1 has very little effect on the accuracy of the results while a very small change in the value of R2 makes the results less accurate.

5. Programming

The computer program is written in FORTRAN IV language for IBM 360 computer available at the Computation Center, Iowa State University. Double precision arithmetic is used throughout the main program and the subroutine. The simultaneous Equations 3.70 representing the boundary conditions are solved using a subroutine which operates on the method of Gauss elimination with complete pivotting.

The main computational steps are illustrated in the flow chart of Figure 3.47. The solution of the simultaneous equations gives the values of the unknown line charges. These values are used in computing the potential and the field anywhere on the conductor surface or in the inter-electrode space. A sample computer program to compute the electric field and potential is given in Appendix E.

6. Results

Results are obtained for the case of a twin-bundle stranded conductor with 30 strands in the outermost layer (N = 30) of each subconductor with radius R = 2.235 cm, strand radius SR = 0.21146 cm, bundle spacing 2A = 45.72 cm, and the height above the ground H = 23.62 meters. This configuration of the transmission line is similar to the one considered by Abou-Seada for smooth cylindrical conductors (26).

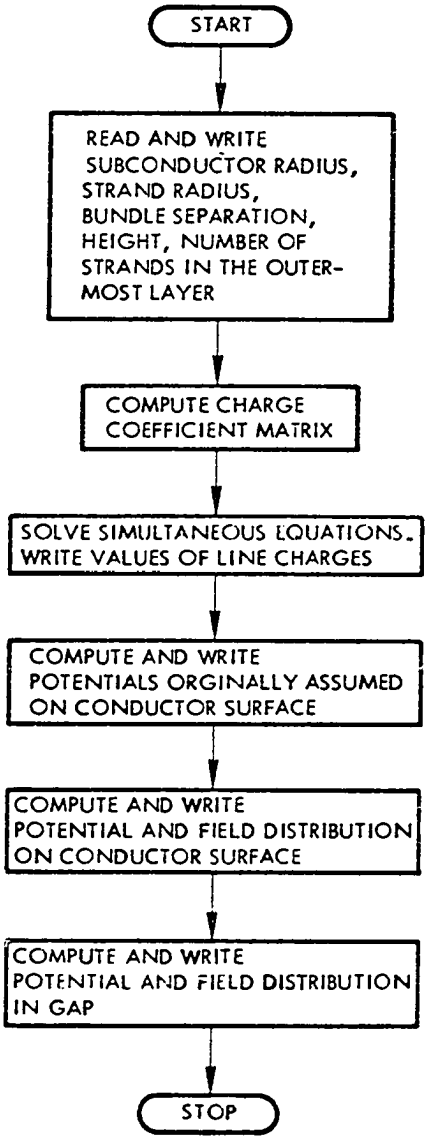

Figure 3.47. Main flow chart for the computation of electric field for stranded conductors.

The values of the line charges obtained by solving the simultaneous Equations 3.70 are shown in Table 3.11. To check the correctness of the computations, these values of the line charges are used to compute the potential along the entire subconductor surface. The values of the potential at 17 points on one of the outermost strands of subconductor I are shown in Figure 3.48. The values of the potential at symmetrically located points such as C_{11}, C_{21}, C_{31},....., C_{301}:C_{12}, C_{22}, C'_{22}, C_{32}, C'_{32}, ..., C_{302}, C_{302}:C_{13}, C'_{13}, C_{23}, C'_{23}, C_{33}, C'_{33}....., C_{303}, C'_{303}:..... etc., are very close to each other. (The difference in potential at any two symmetrically located points is less than 10^{-4} p.u. volt.)

Although the potential at any point on the subconductor surface is very close to the unit potential, considerable error exists in the region very close to the points where strands intersect each other (discontinuity points). This was revealed by computing the potentials at some points in the region close to the discontinuity points. This is shown in Figure 3.49.

The equipotential and the equigradient lines very close to the subconductor I surface are shown in Figures 3.50 and 3.51. Figures 3.52 and 3.53 show the same lines in the gap between the two subconductors.

Figure 3.54 shows the equipotential lines around subconductor I obtained by using the computer plotting program explained earlier.

The knowledge of the maximum electric field occurring on the conductor surface and the values of the capacitance are necessary in the design of EHV transmission lines. The effect of the geometric parameters of the line on the values of the maximum electric field and the

Table 3.11. Values of line charges obtained by solving simultaneous equations [(Coulomb/m/volt)/$2\pi\epsilon_o$]

Q(1) = 0.004374	Q(21) = 0.003817	Q(41) = 0.003830
Q(2) = -0.001327	Q(22) = -0.001170	Q(42) = -0.001222
Q(3) = 0.004365	Q(23) = 0.003745	Q(43) = 0.003910
Q(4) = -0.001614	Q(24) = -0.001131	Q(44) = -0.001279
Q(5) = 0.004343	Q(25) = 0.003684	Q(45) = 0.003992
Q(6) = -0.001397	Q(26) = -0.001095	Q(46) = -0.001309
Q(7) = 0.004308	Q(27) = 0.003638	Q(47) = 0.004072
Q(8) = -0.001504	Q(28) = -0.001071	Q(48) = -0.001380
Q(9) = 0.004260	Q(29) = 0.003610	Q(49) = 0.004147
Q(10) = -0.001398	Q(30) = -0.001058	Q(50) = -0.001372
Q(11) = 0.004201	Q(31) = 0.003601	Q(51) = 0.004214
Q(12) = -0.001411	Q(32) = -0.001059	Q(52) = -0.001483
Q(13) = 0.004132	Q(33) = 0.003613	Q(53) = 0.004271
Q(14) = -0.001344	Q(34) = -0.001073	Q(54) = -0.001381
Q(15) = 0.004057	Q(35) = 0.003644	Q(55) = 0.004316
Q(16) = -0.001317	Q(36) = -0.001100	Q(56) = -0.001604
Q(17) = 0.003977	Q(37) = 0.003693	Q(57) = 0.004349
Q(18) = -0.001261	Q(38) = -0.001134	Q(58) = -0.001322
Q(19) = 0.003895	Q(39) = 0.003756	Q(59) = 0.004368
Q(20) = -0.001220	Q(40) = -0.001181	Q(60) = -0.001694

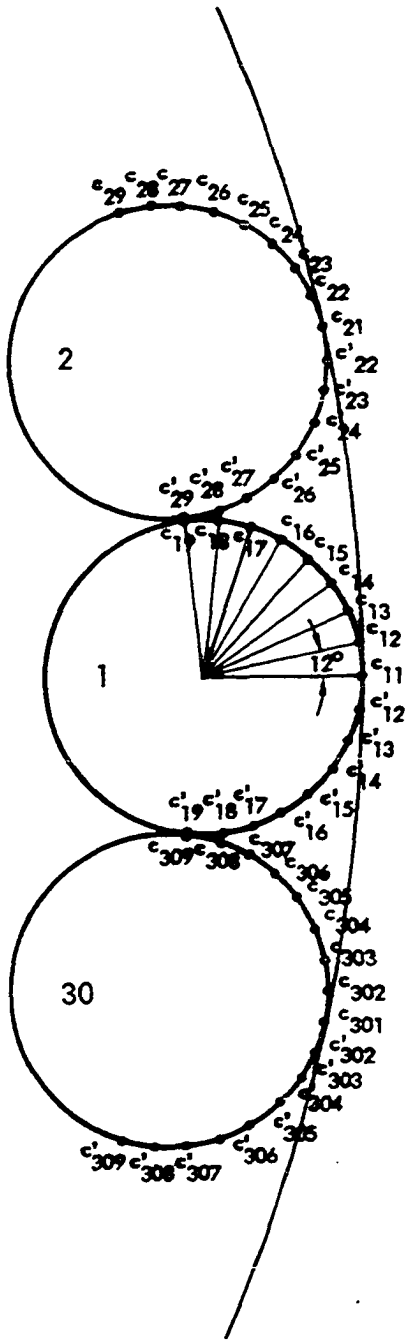

Potential at point	Potential
C_{11}	1.000000
C_{12}	0.999942
C_{13}	0.999844
C_{14}	0.999832
C_{15}	0.999964
C_{16}	1.000190
C_{17}	1.000373
C_{18}	1.000340
C_{19}	1.000000
C'_{12}	0.999943
C'_{13}	0.999844
C'_{14}	0.999833
C'_{15}	0.999964
C'_{16}	1.000191
C'_{17}	1.000373
C'_{18}	1.000340
C'_{19}	1.000000

Figure 3.48. Values of potential on the surface of strand no. 1 of subconductor I.

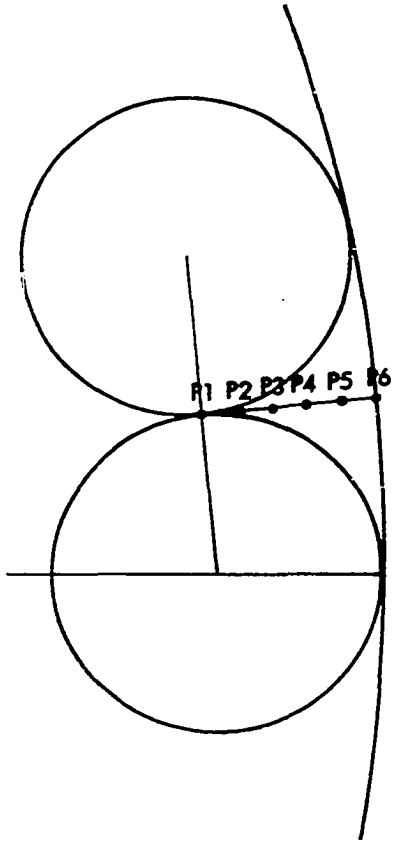

Potential at point	Potential
P1	1.000000
P2	1.000340
P3	1.000323
P4	0.999893
P5	0.999065
P6	0.997918

Figure 3.49. Values of potential in region close to the discontinuity point.

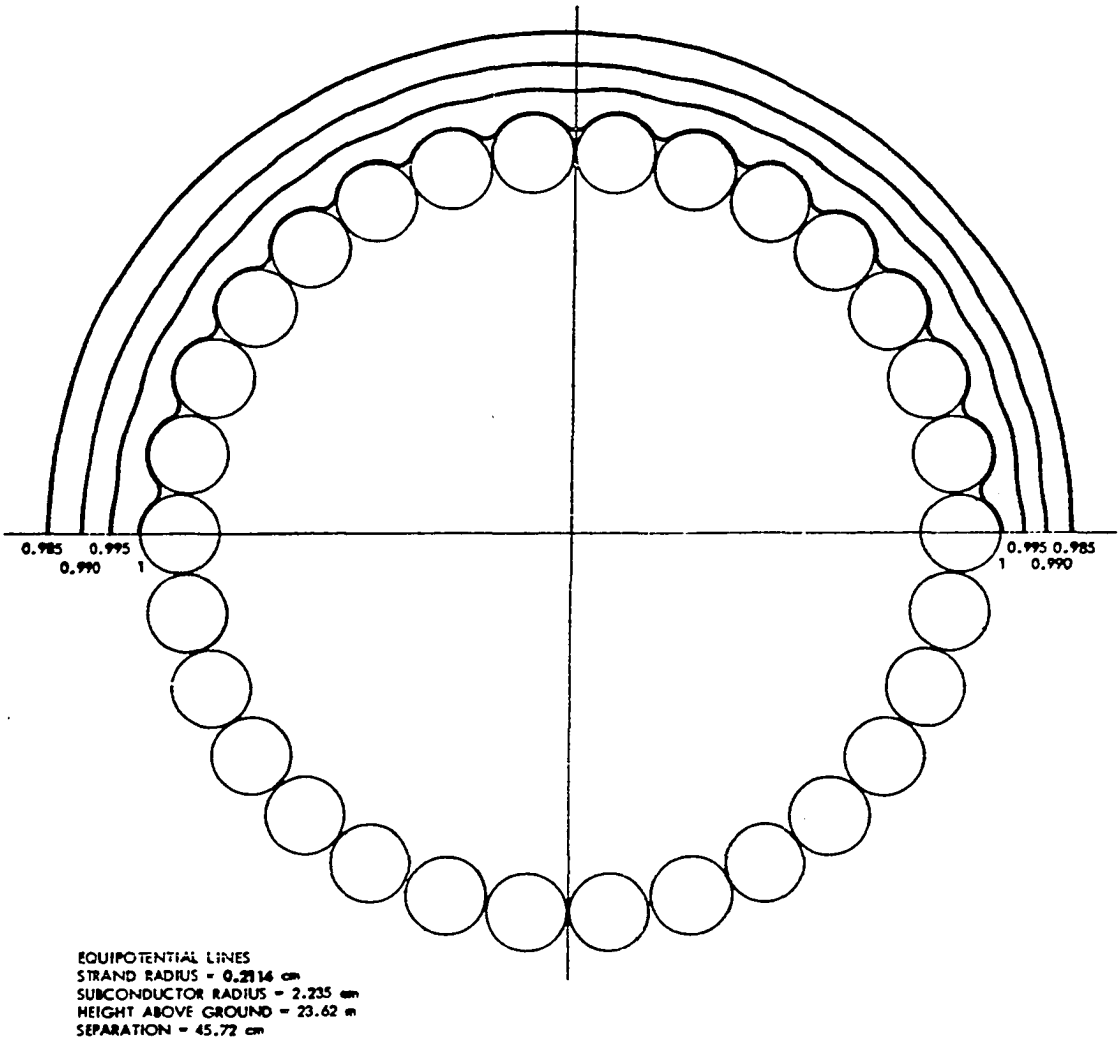

Figure 3.50. Equipotential lines very close to the surface of subconductor I.

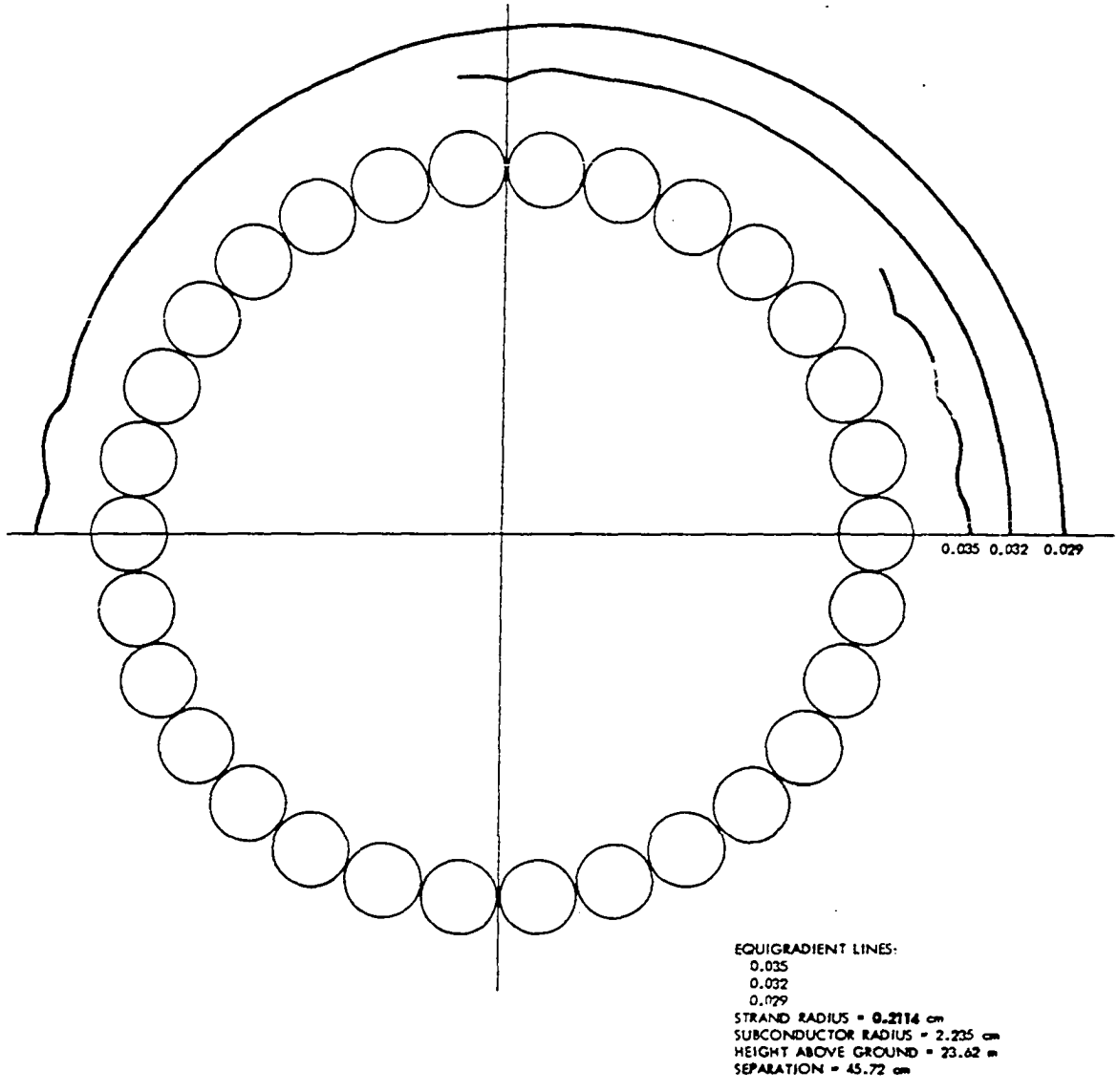

Figure 3.51. Equigradient lines very close to the surface of subconductor I.

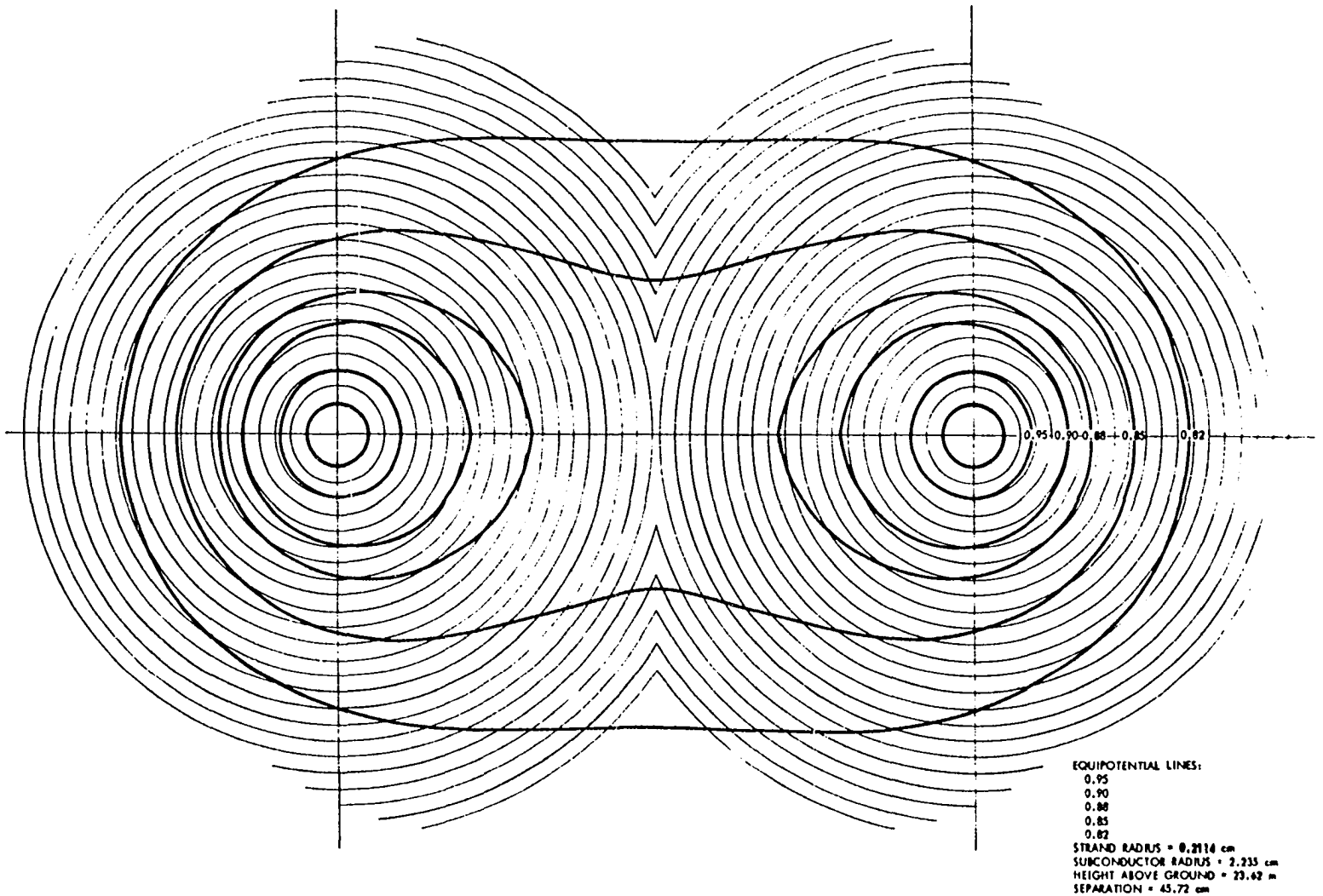

Figure 3.52. Equipotential lines in the gap between subconductors.

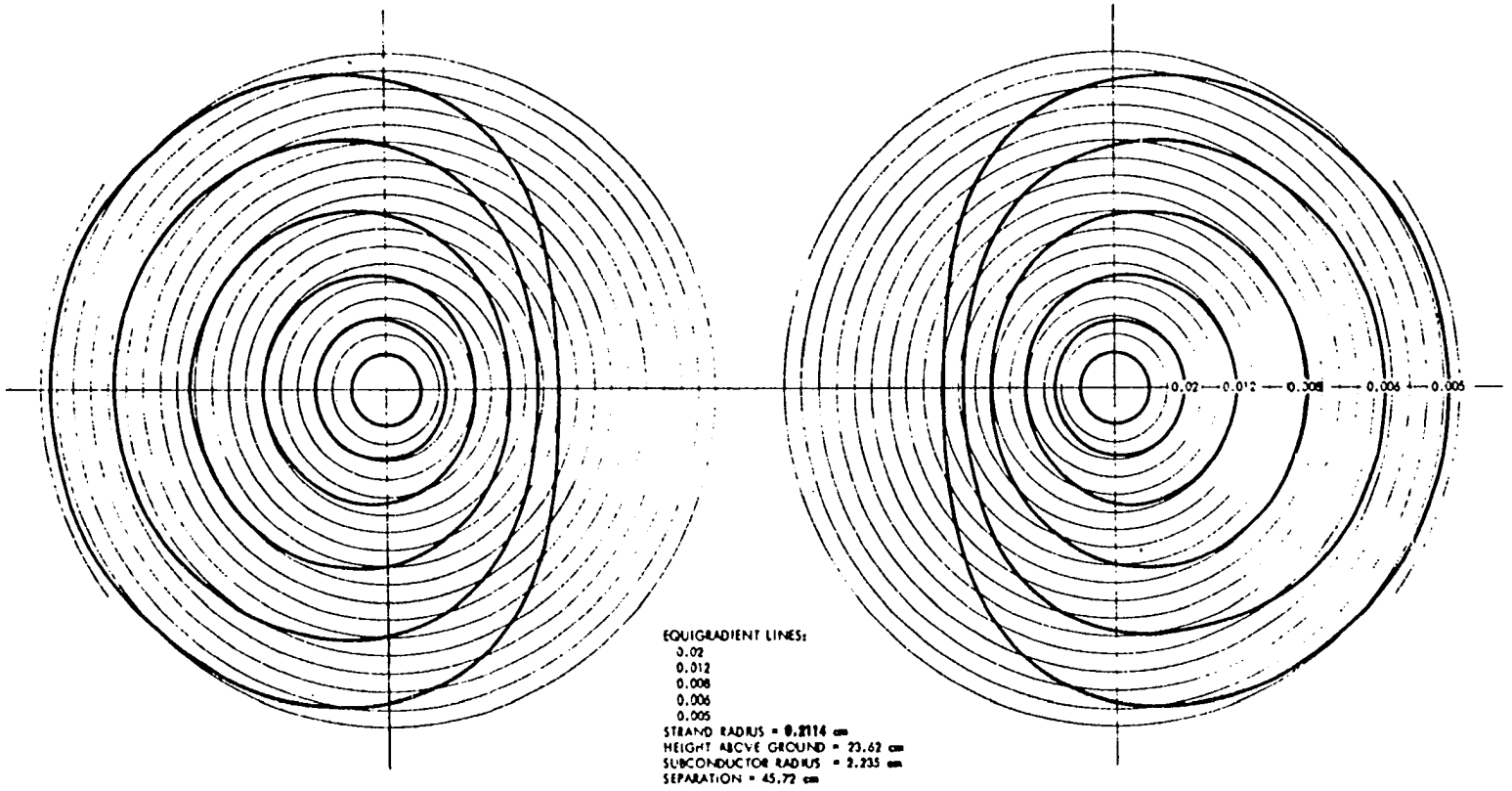

Figure 3.53. Equigradient lines in the gap between subconductors.

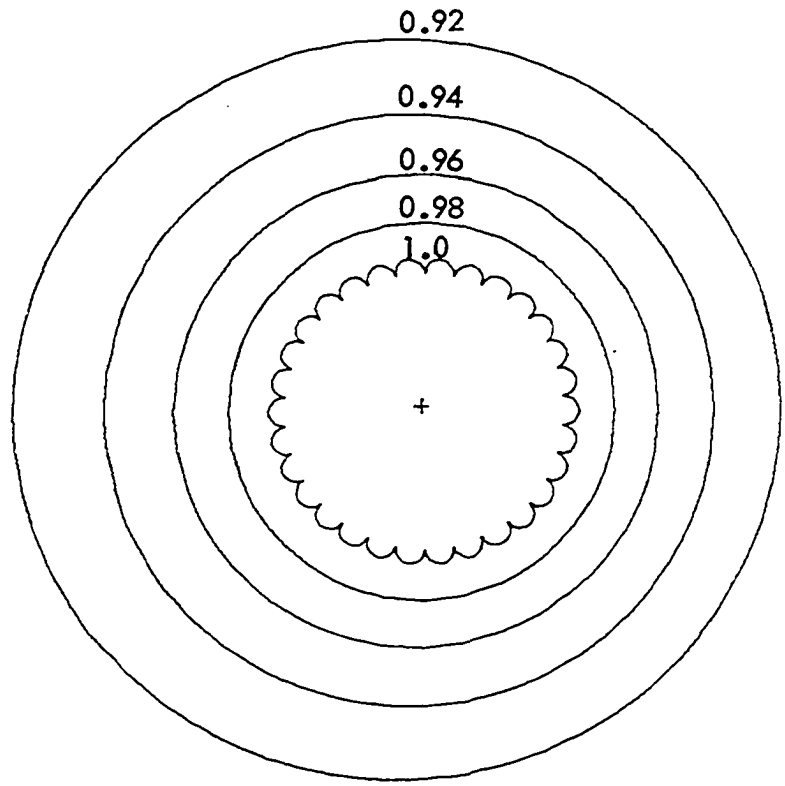

Figure 3.54. Computer plotting of equipotential lines around sub-conductor I. R = 2 cm, H = 1500 cm, A = 30 cm, N = 30, SR = 0.1893 cm.

capacitance is illustrated in Figures 3.55-3.61.

Figures 3.55-3.57 illustrate the variation of the maximum electric field and the capacitance of a single stranded conductor above the ground.

Figure 3.55 illustrates the variation of the maximum electric field and the capacitance with the conductor radius R. The height H of the conductor above the ground is kept constant at 10 m, and the number of strands N in the outermost layer is kept constant at 30. For the comparison purpose, the values of the maximum electric field of a cylindrical conductor are also shown. The values of the strand factor which is the ratio of the maximum electric field of a cylindrical conductor to the same of a stranded conductor is found to be 0.69 for all values of R. The capacitance ratio, which is the ratio of the capacitance of a stranded conductor to that of a cylindrical conductor, is found to be 0.998.

Figure 3.56 illustrates the variation of the maximum electric field and the capacitance with the conductor height. The radius of the conductor is kept constant at 2 cm, and the number of strands N is kept constant at 30. The strand factor and the capacitance ratio are found to be 0.69 and 0.998 respectively. This indicates that the strand factor and the capacitance ratio do not depend on R or H.

Figure 3.57 illustrates the variation of the maximum electric field, capacitance, strand factor and the capacitance ratio with the number of strands N in the outermost layer of the conductor. The radius of the conductor is kept constant at 2 cm, and the height above the ground is

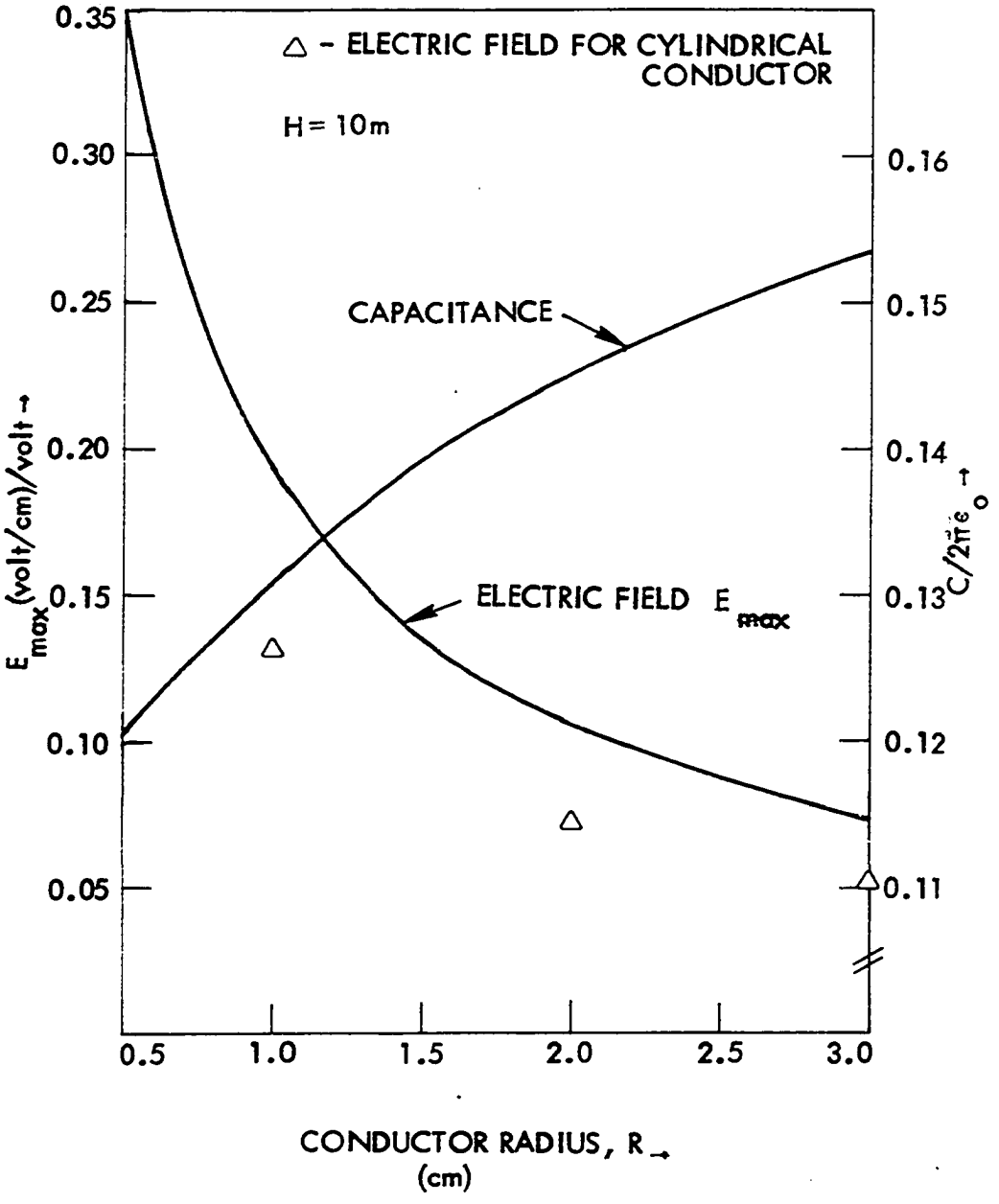

Figure 3.55. Variation of maximum electric field and capacitance with conductor radius for a single stranded conductor above ground. H = 10 m, N = 30.

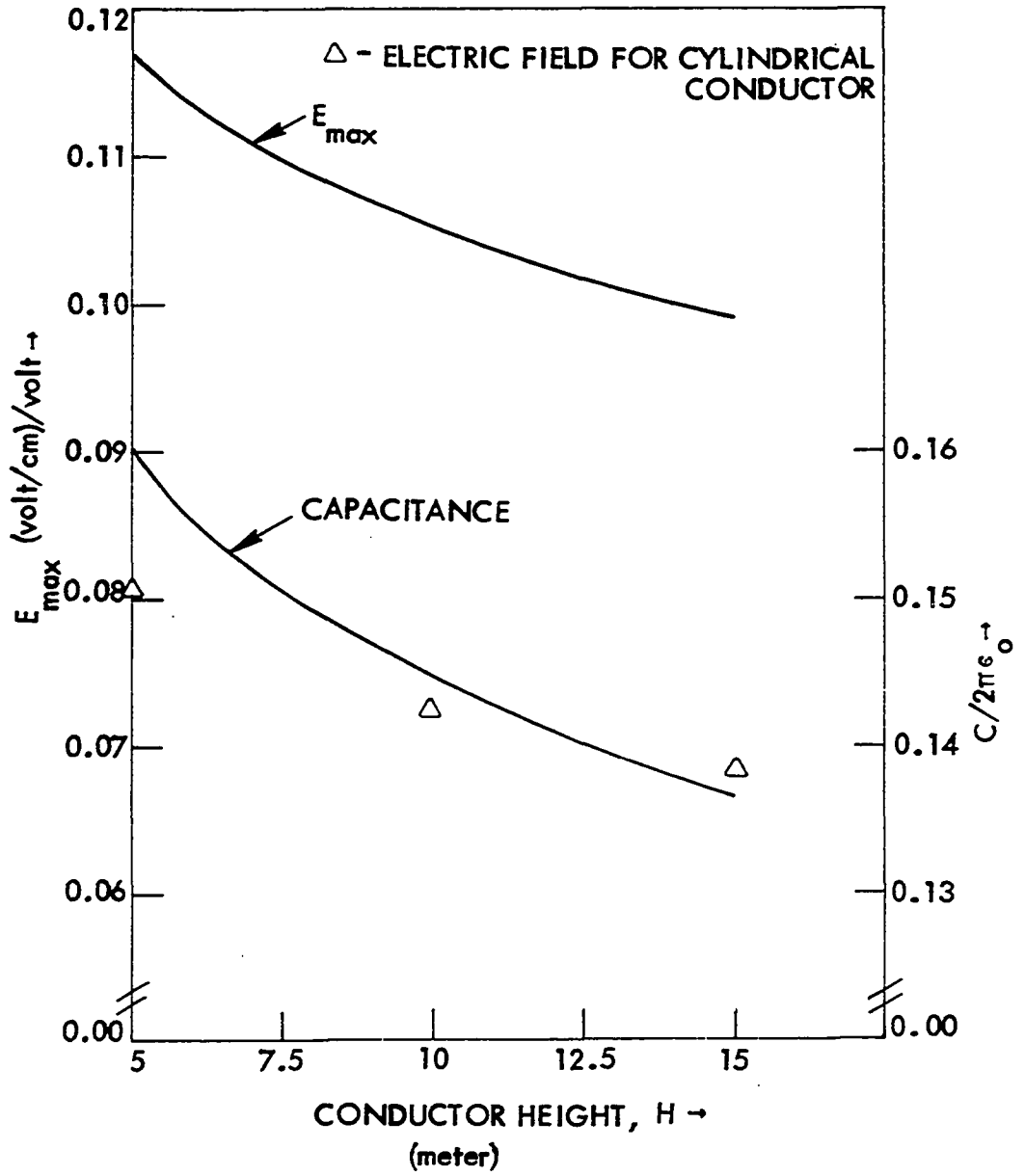

Figure 3.56. Variation of maximum electric field and capacitance with conductor height for a single stranded conductor above ground. R = 2 cm, N = 30.

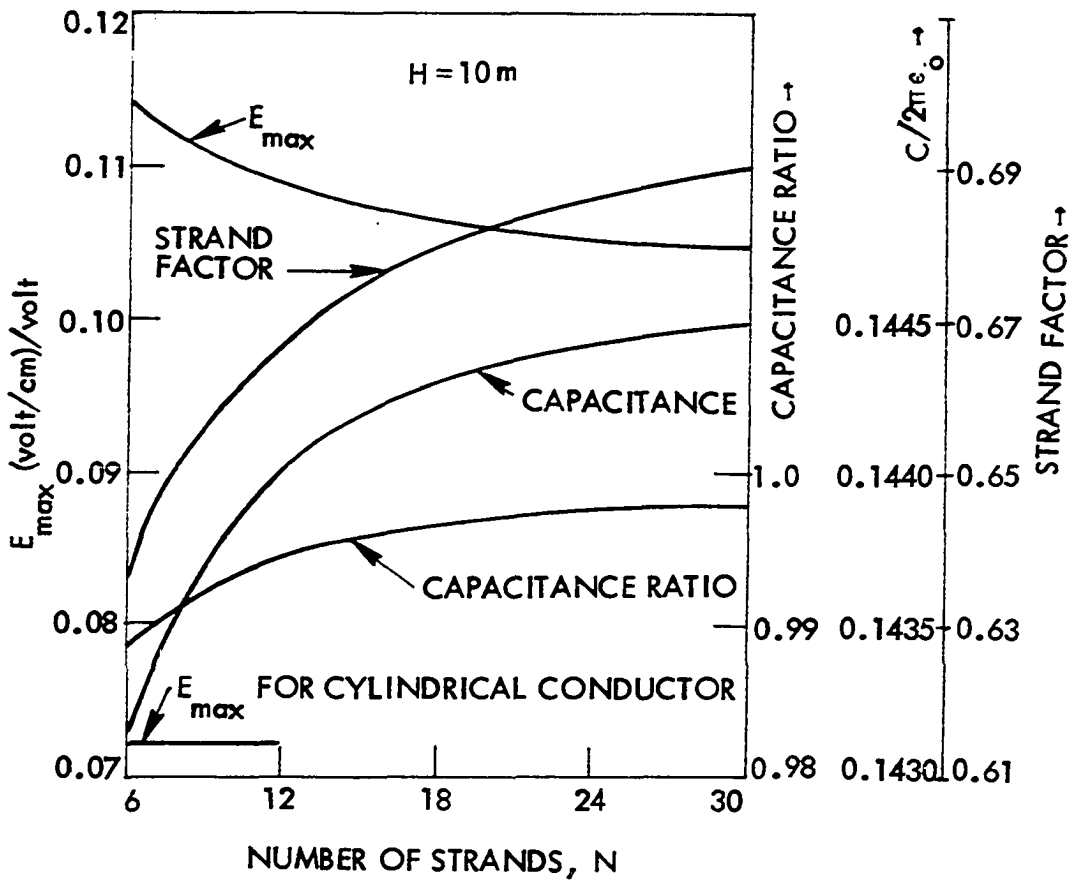

Figure 3.57. Variation of maximum electric field, capacitance, strand factor and capacitance ratio with number of strands N for a single stranded conductor above ground. R = 2 cm, H = 10 m.

kept as 10 m. Figure 3.57 indicates that the strand factor and the capacitance ratio depend only on the number of strands N.

Figures 3.58-3.61 illustrate the variation of the maximum electric field and the capacitance for a twin-bundle, unipolar stranded conductor above ground.

Figure 3.58 illustrates the variation of the maximum electric field and the capacitance with the subconductor radius R. The height of the conductor above the ground is kept at 10 m, the bundle separation is 45 cm, and the number of strands N is 30. The values of the strand factor and the capacitance ratio are found to be 0.69 and 0.999 respectively.

Figure 3.59 illustrates the variation of the maximum electric field and the capacitance with the conductor height. The radius of the conductor is kept at 2 cm, the bundle separation is 45 cm, and the number of strands is 30. The values of the strand factor and the capacitance ratio are found to be 0.69 and 0.999 respectively.

Figure 3.60 illustrates the variation of the maximum electric field and capacitance with bundle separation. The radius of the conductor is kept at 2 cm, the height of the conductor above the ground is 10 m and the number of strands N is 30. The values of the strand factor and the capacitance ratio are found to be 0.69 and 0.999 respectively.

Figures 3.58-3.60 indicate that the values of the strand factor and the capacitance ratio do not depend on the conductor radius, conductor height and the bundle separation.

Figure 3.61 illustrates the variation of the maximum electric field, the capacitance, the strand factor and the capacitance ratio with the

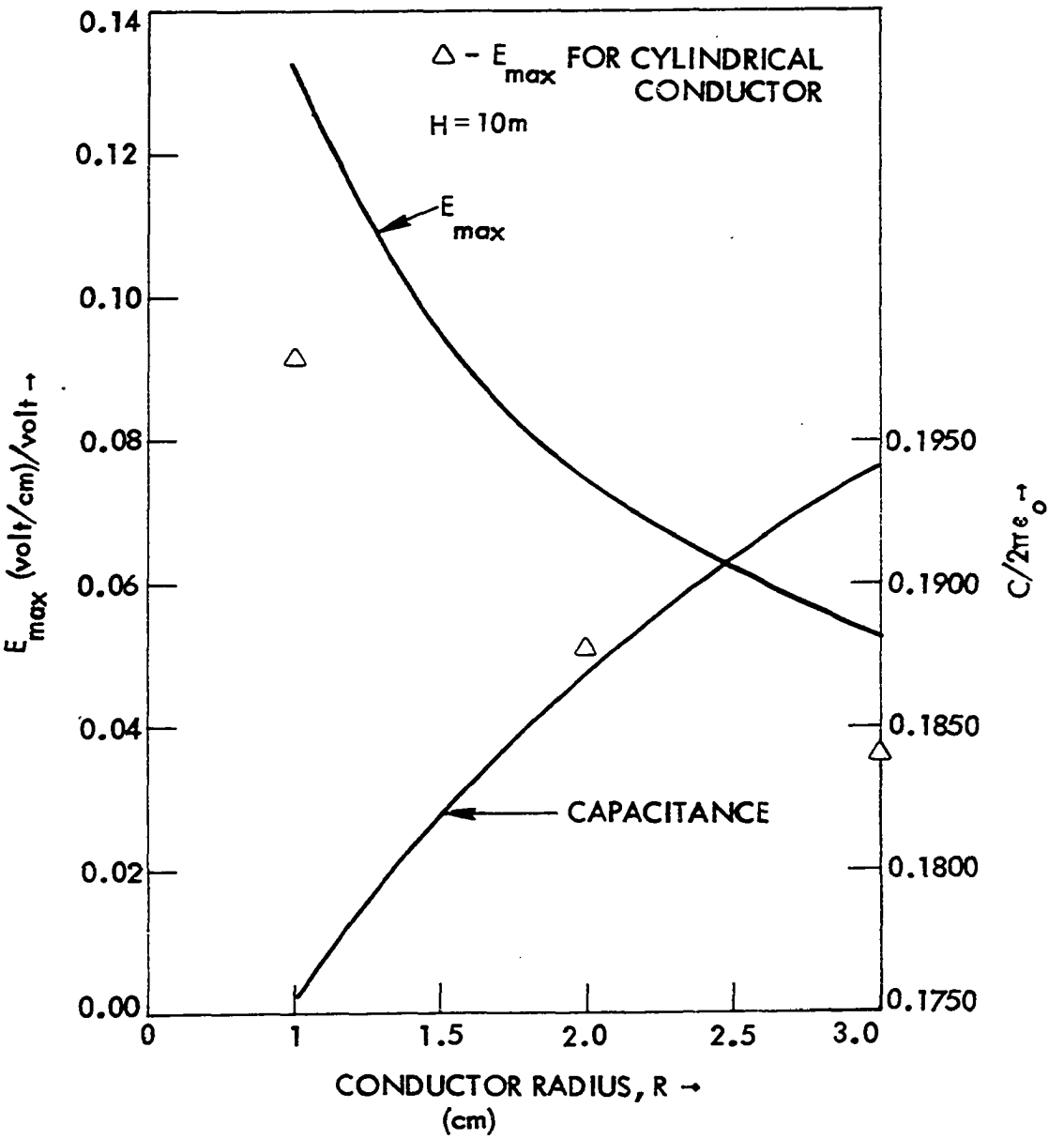

Figure 3.58. Variation of maximum electric field and capacitance with conductor radius for unipolar twin-bundle stranded conductor above ground. H = 10 m, S = 45 cm, N = 30.

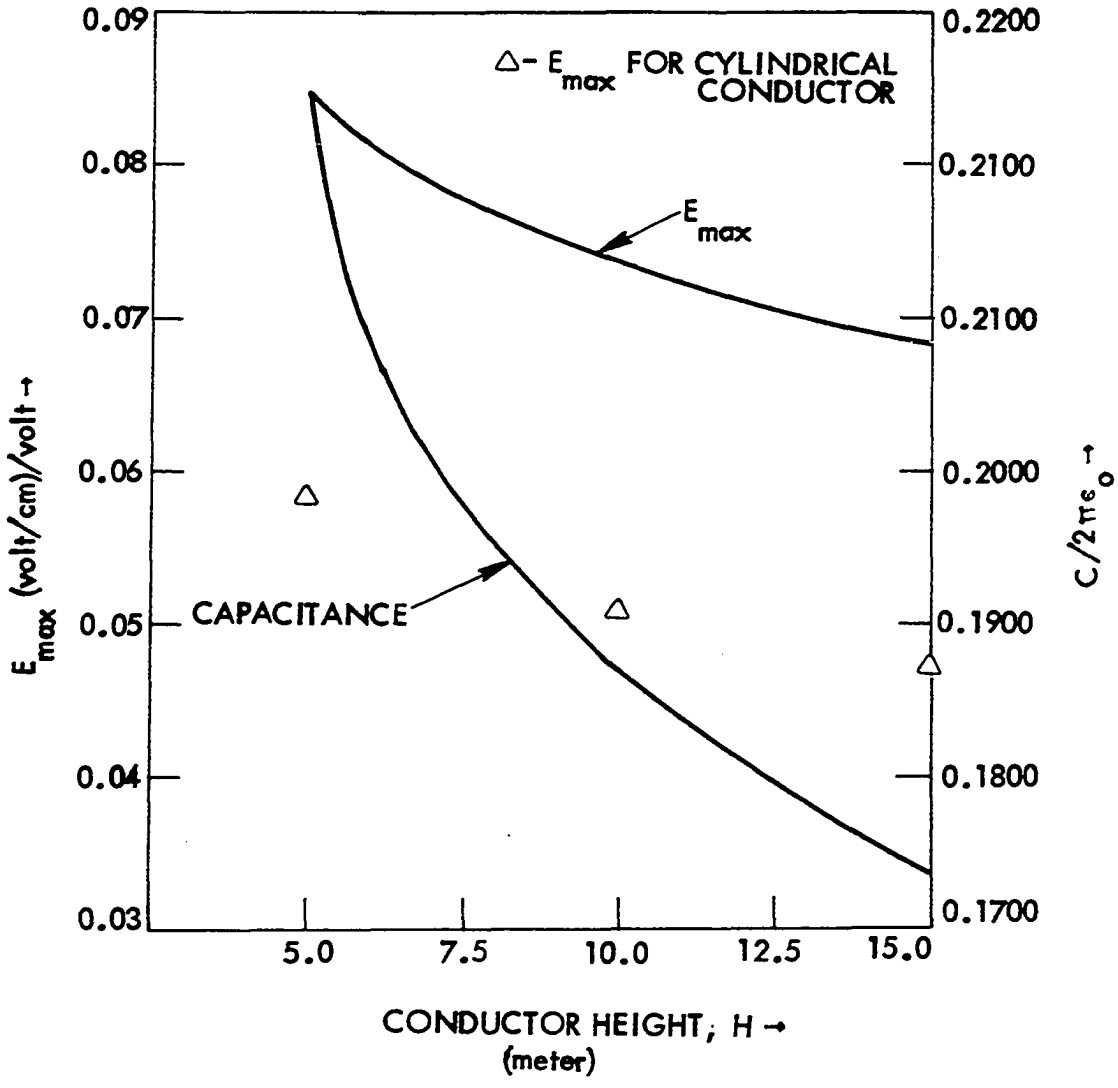

Figure 3.59. Variation of maximum electric field and capacitance with conductor height for unipolar twin-bundle stranded conductor above ground. R = 2 cm, S = 45 cm, N = 30.

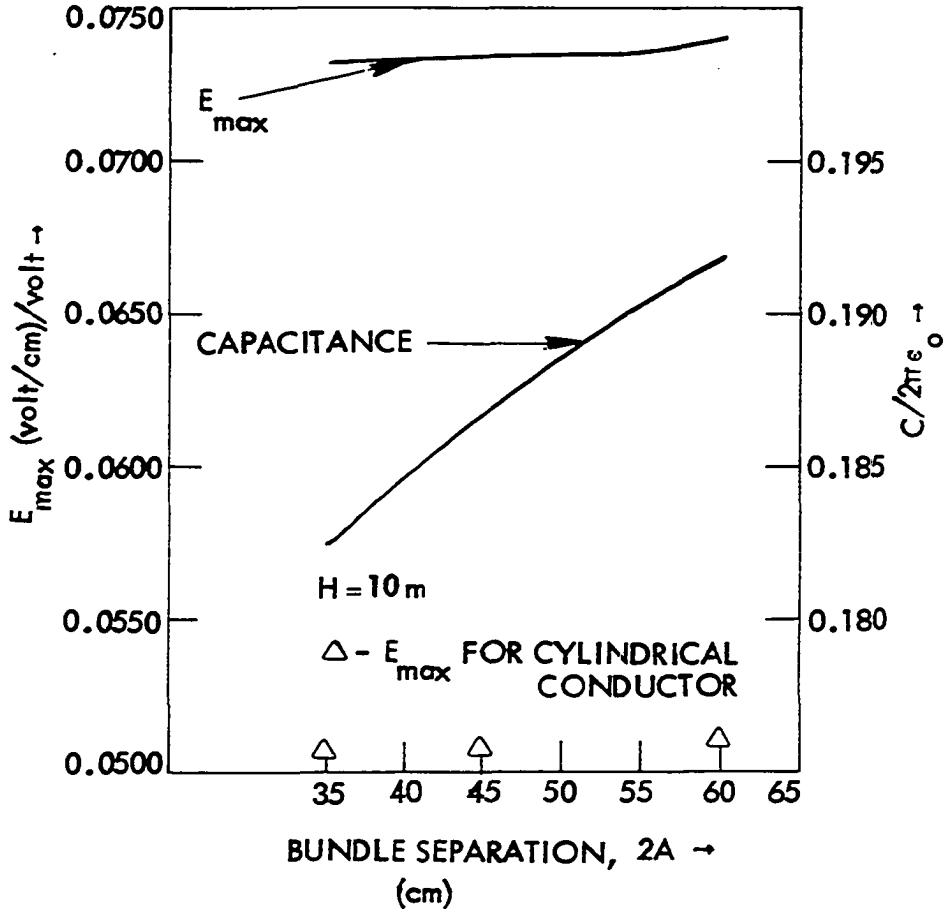

Figure 3.60. Variation of maximum electric field and capacitance with bundle separation for unipolar twin-bundle stranded conductor above ground. R = 2 cm, H = 10 m, N = 30.

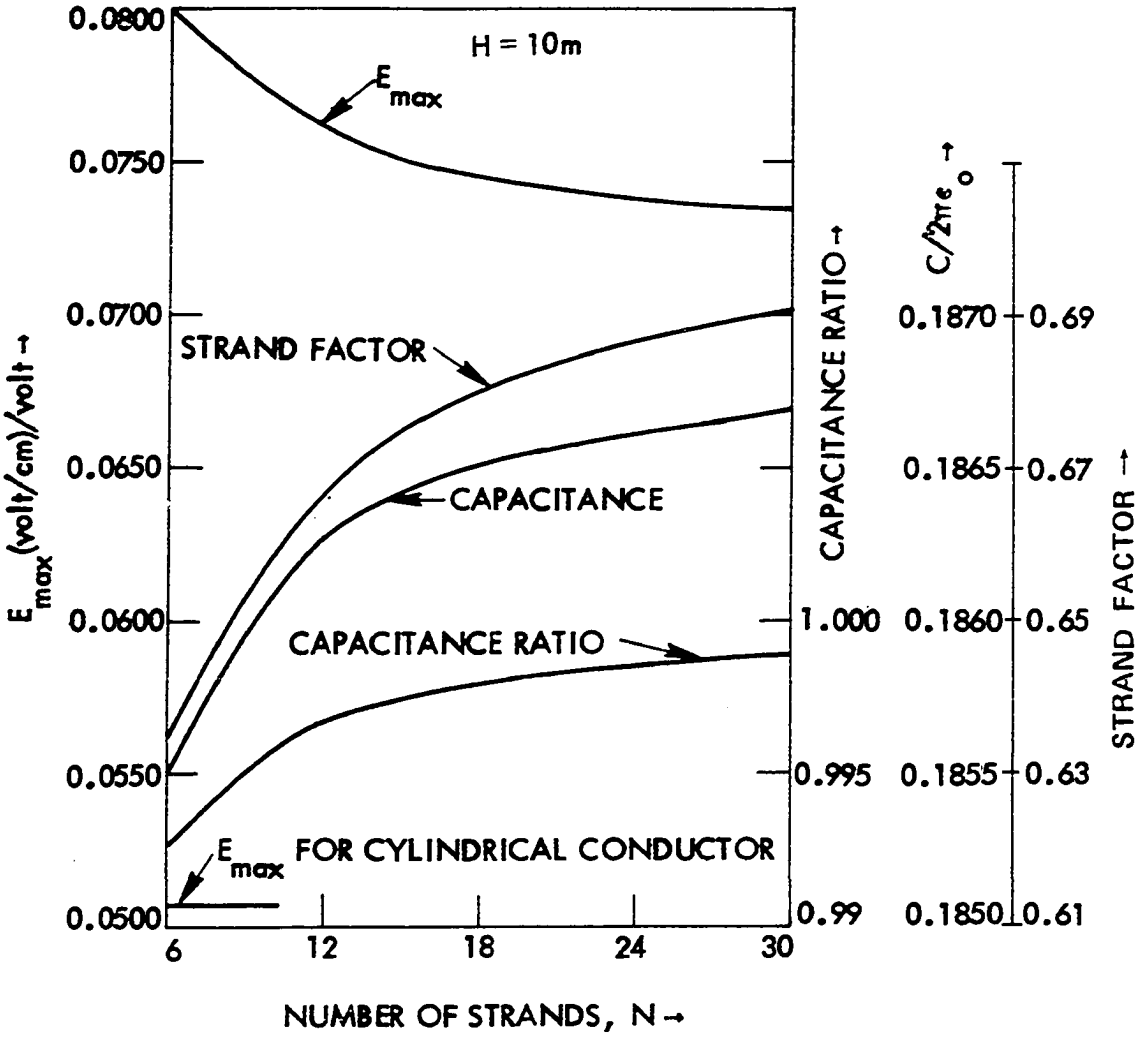

Figure 3.61. Variation of maximum electric field, capacitance, strand factor, and capacitance ratio with number of strands N for unipolar twin-bundle stranded conductor. R = 2 cm, H = 10 m, S = 45 cm.

number of strands N in the outermost layer of each subconductor. The radius of the subconductor is kept at 2 cm, the height of the conductor above the ground is 10 m and the bundle separation is 45 cm.

7. Accuracy and limitations of charge simulation method

In order to determine the accuracy of the electric field computations made by using the charge simulation method, the problem of the electric field computation of a stranded conductor inside a cylinder as shown in Figure 3.62 is solved analytically, As explained in Appendix G, the configuration of Figure 3.62B is equivalent to that of a stranded conductor above the ground (Figure 3.62A), with respect to the electric field distribution on the conductor surface. This is true only if the radius RF of the outer cylinder is equal to two times the height H of the conductor and the ratio H/R is very high.

The details of the analytical method are explained in the next section. Figure 3.63 illustrates the comparison between the charge simulation method and the analytical method regarding the electric field distribution on an outer strand surface. The radius of the conductor in both the configurations of Figure 3.62 is taken as 1 cm, and the number of strands N in the outer layer of the conductor is taken as 30. The radius RF of the outer cylinder is taken as 20 m and the height H is taken as 10 m.

Figure 3.63 indicates that the value of the maximum electric field obtained by the charge simulation method is about 3.5 percent higher than the exact value obtained by the analytical method. However, it is found that the values of the capacitance ratio obtained by both the methods are equal.

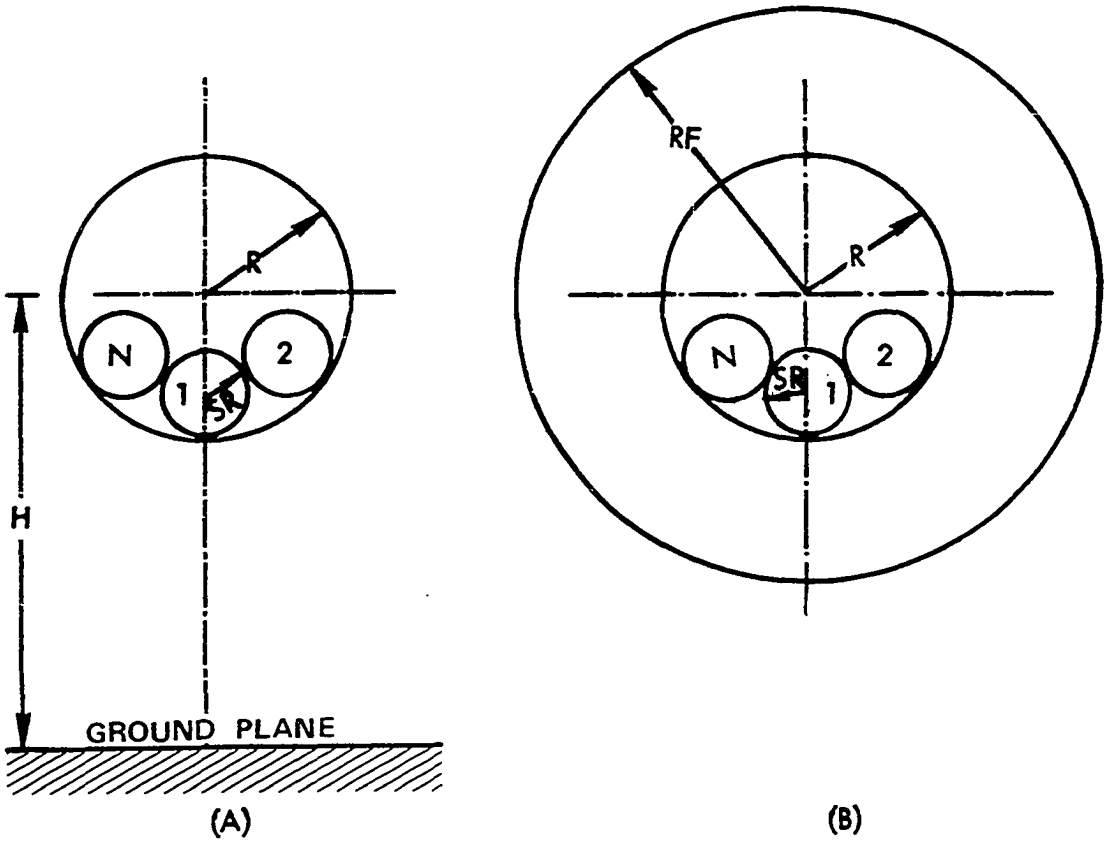

Figure 3.62. To achieve the equal electric field distribution on the conductor surface in both arrangements, RF = 2H must be satisfied, and H/R ratio must be very high.

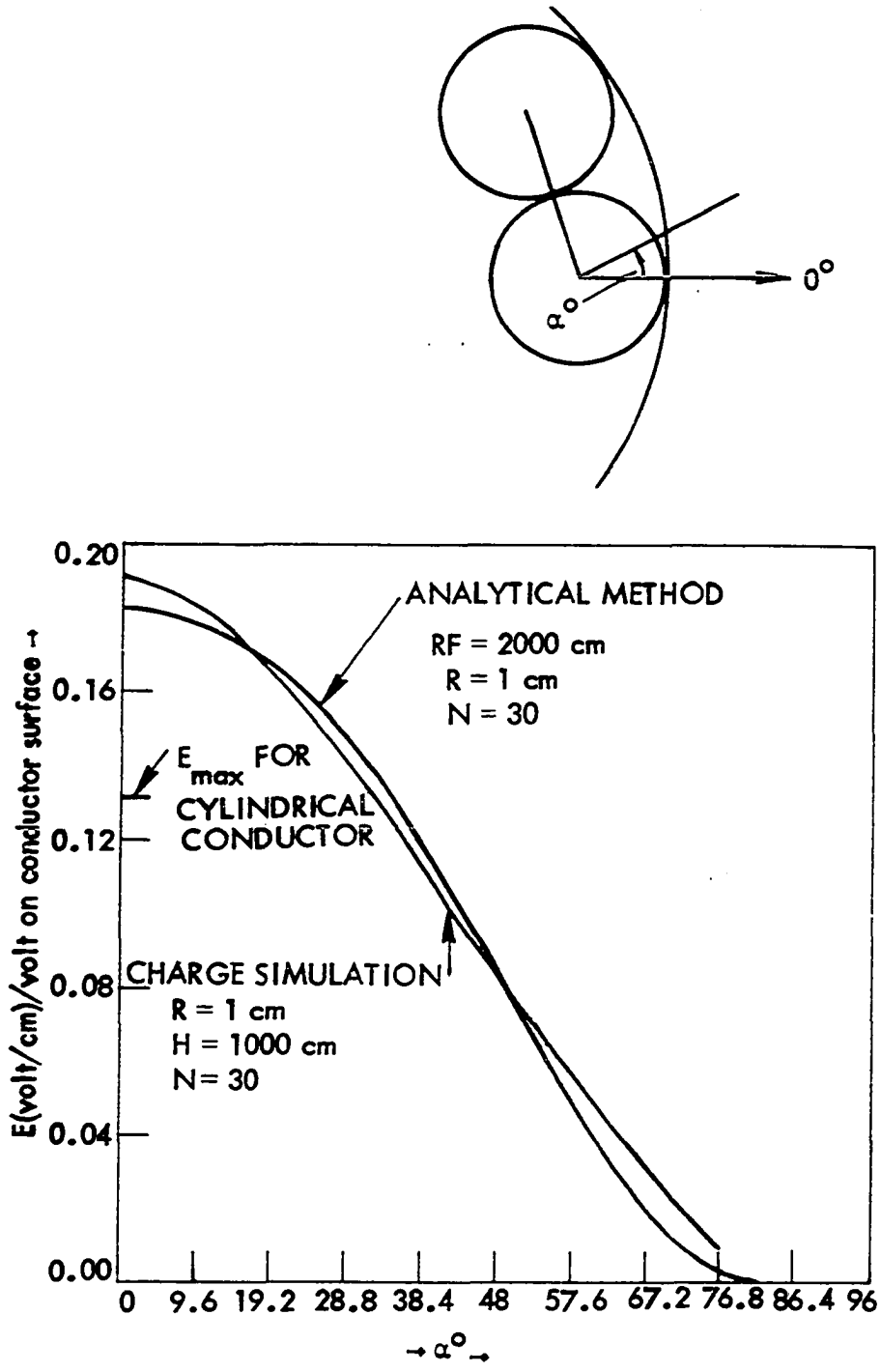

Figure 3.63. Comparison between charge simulation and analytical methods regarding electric field distribution on the outer strand surface.

The use of the charge simulation method to compute the electric field distribution for a stranded conductor with the number of subconductors greater than two is limited. This is because the number of the fictitious line charges required to simulate the conductor surface as an equipotential surface is very large. This increases the round-off error in the computation and reduces the accuracy of the results.

8. Conclusions

(1) The charge simulation method is easy to use for the computation of the electric field distribution around stranded conductors but gives only approximate results. To get the accurate values of the maximum electric field on the conductor surface, the values shown in Figures 3.55-3.61 must be reduced by 3.5 percent.

(2) The values of the capacitance of the stranded conductors obtained by the charge simulation method are accurate.

(3) The use of the charge simulation method to compute the electric field distribution around a stranded bundle conductor with the number of subconductors greater than two is limited by the accuracy of the results.

E. Stranded Conductor in a Cylinder - Analytical Method

1. General

In the design of high voltage transmission lines, the knowledge of the exact electric field at the conductor surface as well as in the interelectrode space is necessary to calculate corona onset voltage, corona loss and the radio interference (3). A considerable amount of

research on the problem of the electric field computation for EHV conductors has been carried out in the last several years (15-28). However, the problem of the electric field computation for stranded conductors as actually used in practice has not been solved.

The usual procedure is to compute the electric field for the cylindrical conductors and then use so-called strand factors to compute the peripheral field on the surface of the stranded conductors. This semi-empirical procedure is not adequate for the corona calculations since the strand factors are not applicable for computing the field distribution in the space outside the stranded conductors.

A recent paper describes a semi-analytical method for computing the electric field distribution around an isolated stranded conductor where the effect of the ground has been neglected (31). As explained earlier, for practical transmission lines, the effect of the conductor height above the ground should not be neglected since the values of the electric field vary with the conductor height over a wide range.

The previous section described the charge simulation method for computing the electric field distribution around a twin-bundle stranded conductor above the ground. However, the results obtained were only approximate.

In this section, an analytical method is described for computing the electric field distribution around a stranded conductor enclosed by an outer cylinder as shown in Figure 3.62B. Since this configuration is equivalent to a stranded conductor above the ground (as explained in Appendix G), the effect of the conductor height has been taken into account in the computation.

2. Analytical method

Figure 3.64 illustrates the geometry and the boundary conditions of the problem. The outer cylinder of radius RF is assumed to be at zero potential, and the stranded conductor of radius RC with N number of strands in the outermost layer is assumed to be at unit potential. The radius of each strand is RS.

Because of the symmetry of the problem, only the region enclosed by $\theta = 0$, $\theta = \beta = \pi/N$ and the conductors is of interest. Inside this region the Laplace equation must be satisfied. Therefore in polar form,

$$\nabla^2 V = \frac{\partial^2 V}{\partial r^2} + \frac{1}{r}\frac{\partial V}{\partial r} + \frac{1}{r^2}\frac{\partial^2 V}{\partial \theta^2} = 0 \qquad 3.82$$

where $V = V(r,\theta)$ represents the potential at any point (r,θ) in the region of interest.

By using the separation of variables technique, let

$$V(r,\theta) = R(r) \cdot T(\theta) \qquad 3.83$$

Using Equations 3.82 and 3.83, we get the following ordinary differential equations

$$\frac{d^2T}{d\theta^2} + k^2T = 0 \qquad 3.84$$

$$r^2\frac{d^2R}{dr^2} + r\frac{dR}{dr} - k^2R = 0 \qquad 3.85$$

where k^2 is the constant of separation.

For $k = 0$, the solution for the electric potential is given by

$$V(r,\theta) = R(r)\cdot T(\theta) = (A \ln r + B)\cdot(C\theta + D) \qquad 3.86$$

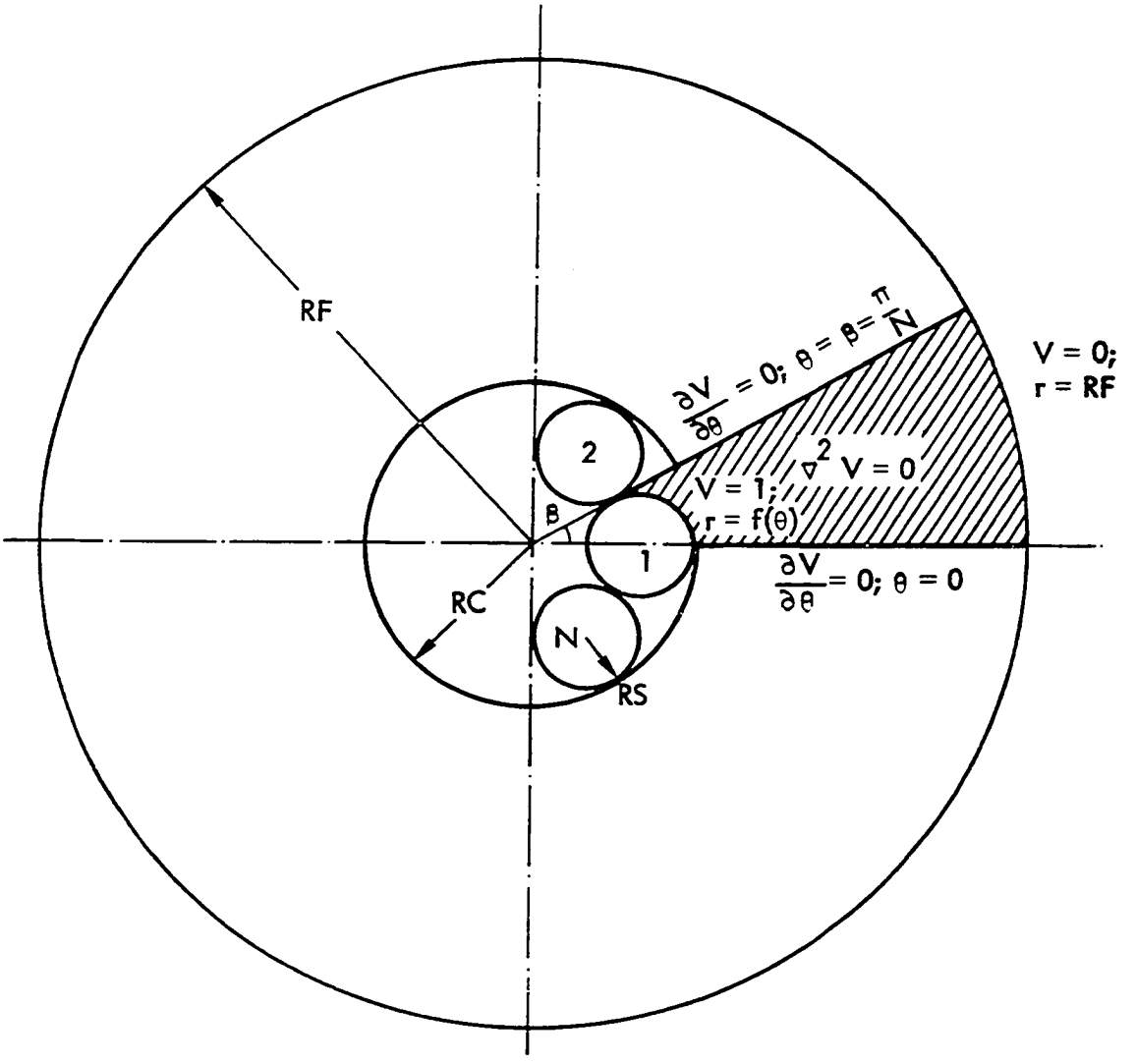

Figure 3.64. The geometry and the boundary conditions of the problem of electric field computation for a stranded conductor inside a cylinder.

where A, B, C, and D are constants.

For $k \neq 0$, the solution for the electric potential is given by

$$V(r,\theta) = R(r)\cdot T(\theta) = (Er^k + Fr^{-k})\cdot(G \cos k\theta + H \sin k\theta) \qquad 3.87$$

where E, F, G, and H are constants.

The general solution for the electric potential for all values of k is given by

$$V(r,\theta) = (A \ln r + B)\cdot(C\theta + D) + \sum_{k=1}^{\infty} (Er^k + Fr^{-k})\cdot(G \cos k\theta + H \sin k\theta) \qquad 3.88$$

Since V is single valued and periodic of period 2β,

$$C = 0 \qquad 3.89$$

$$k = \frac{m\pi}{\beta} = mN \qquad 3.90$$

Applying the boundary condition of $\partial V/\partial\theta = 0$ at $\theta = 0$,

$$H = 0 \qquad 3.91$$

Using Equations 3.89, 3.90 and 3.91, Equation 3.88 can be written as

$$V(r,\theta) = C_1 \ln r + C_2 + \sum_{m=1}^{\infty} [P_m r^{mN} + Q_m r^{-mN}]\cdot\cos(mN\theta) \qquad 3.92$$

where C_1, C_2, P_m and Q_m are constants.

Equation 3.92 satisfies the boundary conditions of $\partial V/\partial\theta = 0$ at $\theta = \beta$ automatically.

Now changing the variable r to (r/RF), Equation 3.92 can be written as

$$V(r,\theta) = C_1 \ln(r/RF) + C_2 + \sum_{m=1}^{\infty} [P_m(r/RF)^{mN} + Q_m(r/RF)^{-mN}] \cos(mN\theta) \qquad 3.93$$

Using the boundary condition of V = 0 at r = RF,

$$C_2 = 0 \tag{3.94}$$

$$P_m = -Q_m \tag{3.95}$$

Using equations 3.94 and 3.95, Equation 3.93 can be written as

$$V(r,\theta) = C_1 \ln(r/RF) + \sum_{m=1}^{\infty} P_m[(r/RF)^{mN} - (r/RF)^{-mN}]\cdot\cos(mN\theta) \tag{3.96}$$

Defining the constants C_1 and P_m in a different form, Equation 3.96 can be written as

$$V(r,\theta) = C_1 \frac{\ln(r/RF)}{\ln(RC/RF)} + \sum_{m=1}^{\infty} P_m(r/RC)^{-mN}\cdot\left[\frac{1 - (r/RF)^{2mN}}{1 - (RC/RF)^{2mN}}\right]\cdot\cos(mN\theta) \tag{3.97}$$

By simple trigonometry, the surface of the stranded conductor in the region under consideration can be described by

$$r = f(\theta) = \frac{B_1 \cos\theta + \sqrt{B_1^2\cos^2\theta - 4B_2}}{2} \tag{3.98}$$

where

$$B_1 = 2\cdot(RC - RS) \tag{3.99}$$

$$B_2 = (RC - RS)^2 - (RS)^2 \tag{3.100}$$

Applying the boundary condition at the surface of the stranded conductor, where the potential is assumed to be one unit, Equation 3.97 becomes

$$C_1 \frac{\ln[f(\theta)/RF]}{\ln[RC/RF]} + \sum_{m=1}^{\infty} P_m\cdot[f(\theta)/RC]^{-mN}\cdot\left[\frac{1-[f(\theta)/RF]^{2mN}}{1-(RC/RF)^{2mN}}\right]\cdot\cos(mN\theta) = 1 \tag{3.101}$$

Equation 3.101 can be rearranged as

$$\sum_{m=0}^{\infty} A_m U_m(\theta) = 1 = S(\theta) \qquad 3.102$$

where

$$A_0 = C_1 \qquad 3.103$$

$$U_0(\theta) = \frac{\ln[f(\theta)/RF}{\ln[RC/RF]} \qquad 3.104$$

} for m = 0

$$A_m = P_m \qquad 3.105$$

$$U_m(\theta) = [f(\theta)/RC]^{-mN} \cdot \left[\frac{1 - [f(\theta)/RF]^{2mN}}{1 - [RC/RF]^{2mN}} \right] \cdot \cos(mN\theta) \qquad 3.106$$

where $m = 1,2,.....,\infty$.

By the process of orthonormalization, Equation 3.102 results in a set of simultaneous equations (35)

$$U_{00}A_0 + U_{01}A_1 + U_{02}A_2 + \ldots\ldots\ldots + U_{0M}A_M = W_0$$

$$U_{10}A_0 + U_{11}A_1 + U_{12}A_2 + \ldots\ldots\ldots + U_{1M}A_M = W_1$$

$$U_{20}A_0 + U_{21}A_1 + U_{22}A_2 + \ldots\ldots\ldots + U_{2M}A_M = W_2 \qquad 3.107$$

$$\ldots\ldots\ldots\ldots\ldots\ldots\ldots\ldots\ldots\ldots\ldots\ldots$$

$$\ldots\ldots\ldots\ldots\ldots\ldots\ldots\ldots\ldots\ldots\ldots\ldots$$

$$U_{M0}A_0 + U_{M1}A_1 + U_{M2}A_2 + \ldots\ldots\ldots + U_{MM}A_M = W_M$$

where

$$U_{ij} = \int_0^{\beta} U_i(\theta)U_j(\theta)d\theta \qquad 3.108$$

$$W_i = \int_0^{\beta} U_i(\theta)S(\theta)d\theta \qquad 3.109$$

$i = 1,2,3,....,M$

$j = 1,2,3,....,M$

and where M indicates the value of m for which the series of Equation 3.102 converges to the desired degree of accuracy.

The solution of the simultaneous Equations 3.107 gives the values of A_m. Once these values are known, Equation 3.97 with Equation 3.103 and 3.105 can be used to compute the electric potential at any desired point on the surface of the stranded conductor or in the interelectrode space. The radial and the azimuthal electric fields at any point (r,θ) are obtained by differentiating Equation 3.97. These are given by

$$E_r(r,\theta) = -\frac{\partial V(r,\theta)}{\partial r} \qquad 3.110$$

$$E(r,\theta) = -\frac{\partial V(r,\theta)}{r\,\partial \theta} \qquad 3.111$$

3. Results

A computer program is written for computing coefficients A_m for different values of M by using Equations 3.104, 3.106 and 3.107 to 3.109. Once these coefficients are obtained, the values of the electric potential at several points on the surface of an outer strand in the interval from $\theta = 0$ to $\theta = \beta = \pi/N$ are computed by using Equations 3.97, 3.103 and 3.105 to check if the boundary condition of a unit potential on the conductor surface is satisfied. The computer program to compute the coefficients A_m is given in Appendix F1 and the computer program to calculate the electric field on the conductor surface is given in Appendix F2.

Figure 3.65 shows the computed values of the electric potential at 17 points on the surface of the outer strand in the interval from $\theta = 0$ to $\theta = \beta = \pi/N$ for different values of M. These results are obtained for RC = 2 cm, RF = 2000 cm, and N = 30. Figure 3.65 indicates that the value of M = 10 is sufficient to satisfy the boundary condition of a unit potential on the stranded conductor.

Table 3.12 shows the values of the coefficients A_m for M = 10 obtained by solving the simultaneous Equations 3.107. These coefficients, obtained for the problem described above, are used to compute the electric potential and field at any desired point on the surface of the stranded conductor or in the interelectrode space.

Table 3.13 with Figure 3.66 shows the values of the electric field and the angle of the electric field at 11 points on the surface of an outer strand in the interval from $\theta = 0$ to $\theta = \beta = \pi/N$. These values are obtained for RC = 2 cm, RF = 2000 cm, and N = 30. A slight error in the values of the electric field and the angle of the electric field very near to the discontinuity point (where two strands touch each other) is due to the round-off error in the computations.

By using the charge simulation method explained in the previous section, results are obtained for the case of a stranded conductor above the ground plane. These results are obtained for RC = 2.0 cm, H = 1000 cm, and N = 30. The results obtained by the analytical method and the charge simulation method for the equivalent geometry are compared as shown in Figure 3.67. This figure indicates a difference of about 4

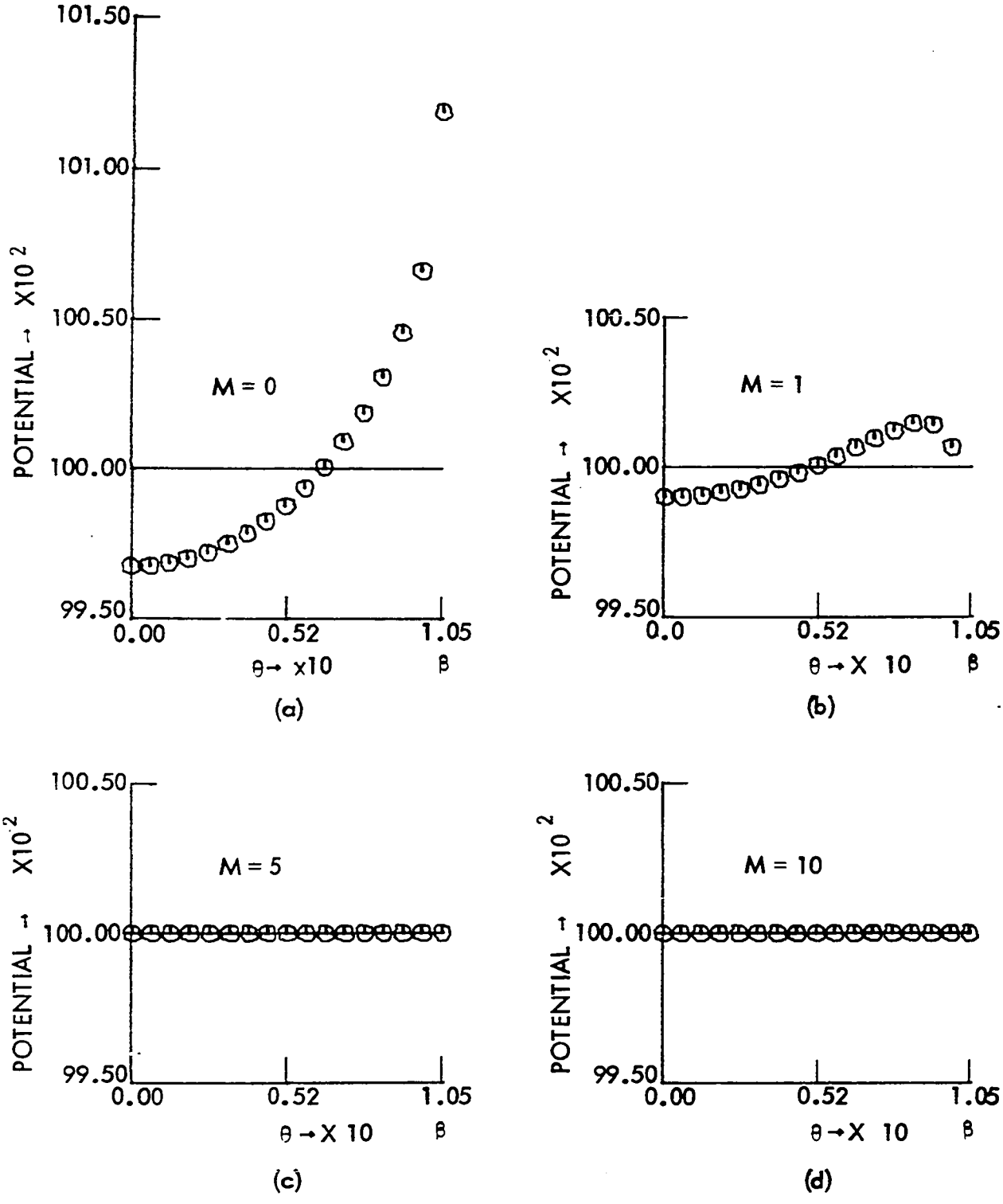

Figure 3.65. Computed values of the potential at 17 points on the surface of an outer strand in the interval from $\theta = 0$ to $\theta = \beta = \pi/N$ for different values of M.

Table 3.12. Values of coefficients A_m for M = 10, RC = 2 cm, RF = 2000 cm, N = 30

Coefficient	Value
A_0	0.9982206
A_1	0.1666446×10^{-2}
A_2	0.1085674×10^{-3}
A_3	0.4251842×10^{-5}
A_4	0.1093296×10^{-6}
A_5	0.7146589×10^{-8}
A_6	0.4319698×10^{-9}
A_7	$-0.2250174 \times 10^{-11}$
A_8	$-0.1305562 \times 10^{-11}$
A_9	$-0.05068501 \times 10^{-13}$
A_{10}	$-0.6264852 \times 10^{-15}$

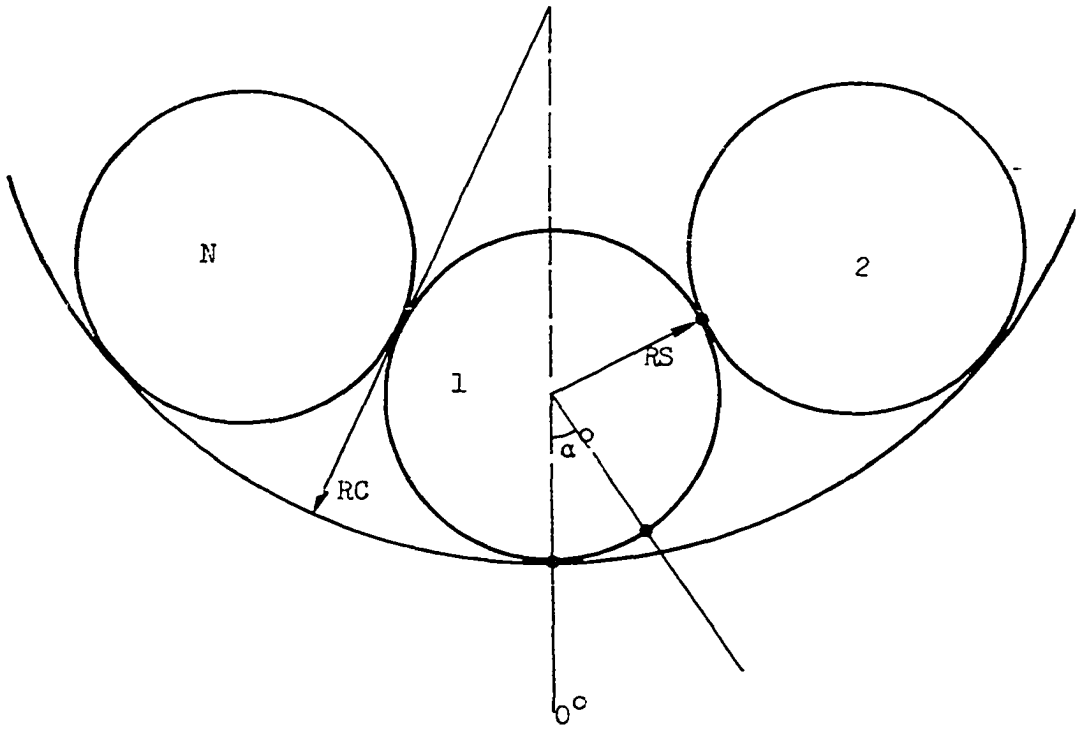

Figure 3.66. Stranded conductor with N strands in the outermost layer.

Table 3.13. Values of electric potential, field and angle of field at 11 points on the surface of the outer strand (RC = 2 cm, RF = 2000 cm, N = 30; for each entry, the potential is "1.000000")

Angle α (degrees)	Electric field (volt/cm)/volt	Angle of electric field (degrees)
0	0.100706	0.000000
9.6	0.098630	9.599936
19.2	0.092370	19.200042
28.8	0.081846	28.800055
38.4	0.067060	38.399859
48.0	0.048+52	48.000158
57.6	0.027803	57.599883
67.2	0.009750	67.200714
76.8	0.000911	76.738961
86.4	0.000007	1.997086
96.0	0.000203	6.000000

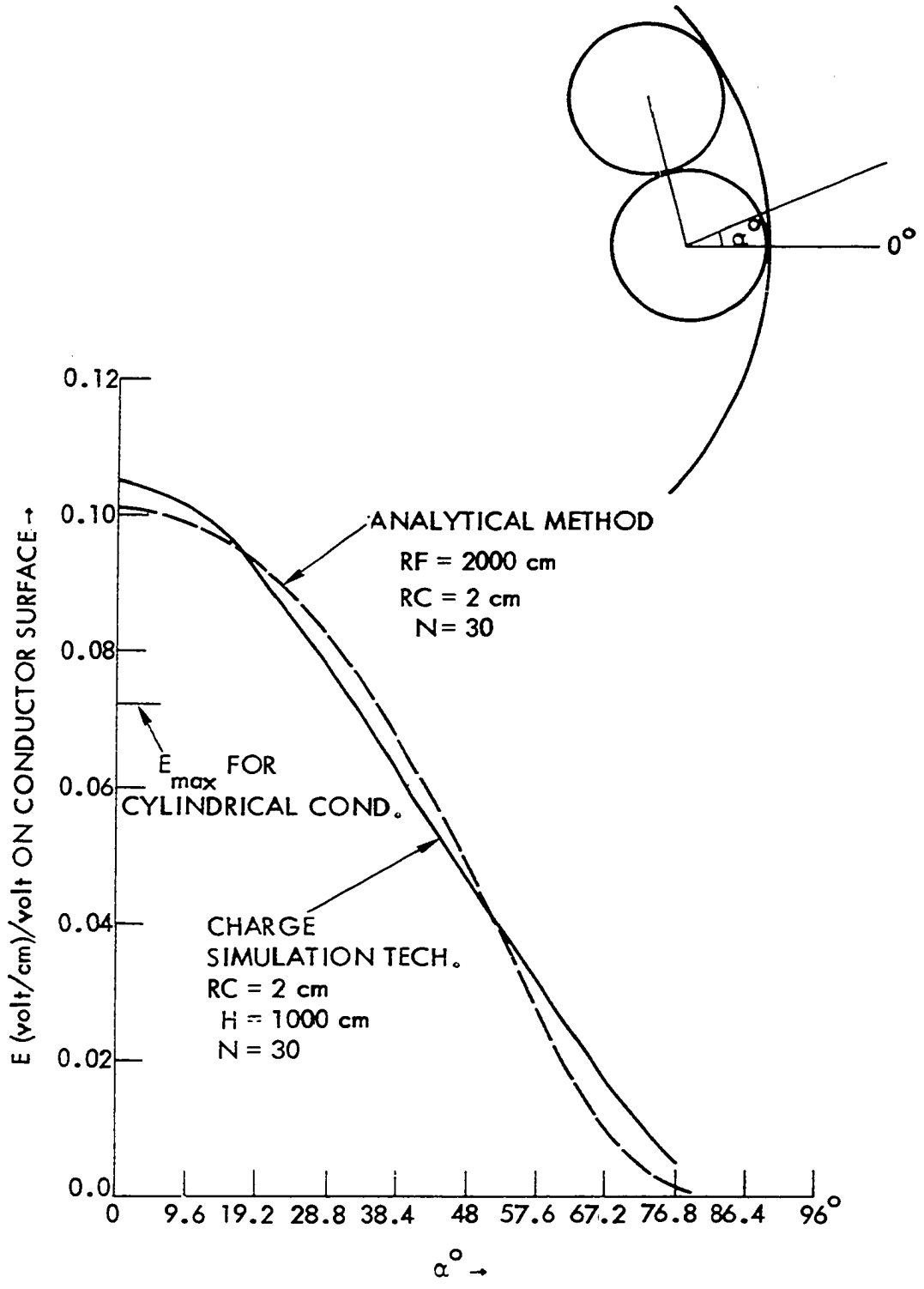

Figure 3.67. Comparison between the results obtained by the charge simulation method and the analytical method.

percent between the accurate results obtained by the analytical method and the approximate results obtained by the charge simulation method.

The effect of the ground is very important in corona calculations since the values of the electric field vary with the conductor height over a wide range. This can be explained by the following example:

The values of the maximum electric field for the stranded conductor of radius 2 cm and N = 30 are found to be 0.1169, 0.1050, and 0.0991 volt/cm per volt for three different heights of 5, 10, and 15 meters respectively. This indicates that by decreasing the conductor height from 15 meters to 5 meters, the maximum electric field increases by 18 percent. Since all corona calculations are very sensitive to the values of the electric field, a very small error in the values of the electric field might result in a very large error in the values of the corona onset voltage, corona loss and the radio interference. Therefore, the effect of the ground should not be neglected.

In the analytical method as explained in this section, the effect of the ground has been considered by assuming the outer cylinder as an equivalent ground of zero potential.

4. Conclusions

(1) The analytical method gives accurate values of the electric potential and field on the surface of the stranded conductor but this method is difficult to use. Moreover, the application of this method for the electric field computation for the practical transmission lines seems extremely difficult.

(2) The results obtained by the charge simulation method are approximate, but this method is easy to use and it is possible to apply this method for the electric field computation for the practical transmission lines.

(3) The effect of the ground has been taken into consideration in both the methods.

IV. BIBLIOGRAPHY

1. M. McHone. "Ultra high voltage transmission." Energy International, 9, No. 5 (May 1972), 13-16.

2. A. Fischer. "Research objectives for ultra high voltage transmission systems." Transactions of the South African Institute of Electrical Engineers, (May 1973), 78-88.

3. J. Tranen and G. Wilson. "Electrostatically induced voltages and currents on conducting objects under EHV transmission lines." IEEE Trans. Power Apparatus and Systems, PAS-90, No. 2 (March-April 1971), 768-776.

4. EHV Transmission Line Reference Book. New York: Edison Electric Institute, 1968.

5. E. Nasser. Fundamentals of Gaseous Ionization and Plasma Electronics. New York: Wiley Interscience, 1971.

6. R. Comsa and P. Thanassoulis. "Calculation of maximum voltage gradients. Part II: Split-bundle conductors." 90, No. 1 (January-February 1971), 150-157.

7. J. Anderson and L. Barthold. "Design challenges of transmission lines above 765 kv." IEEE EHV Transmission Conference, Montreal, Canada, September 1968.

8. G. Juette and L. Zaffanella. "Radio noise currents and audible noise on short sections of UHV bundle conductors." IEEE Trans. Power Apparatus and Systems, PAS-89, No. 5 (May-June 1970), 902-913.

9. Y. Sawada. "Calculating method of radio noise level and its application to design of ac power transmission lines." IEEE Trans. Power Apparatus and Systems, PAS-89, No. 5 (May-June 1970), 844-853.

10. M. Sarma and W. Janischewskyj. "Corona loss characteristics of practical HVDC transmission lines, Part I: Unipolar lines." IEEE Trans. Power Apparatus and Systems, PAS-89, No. 5 (May-June 1970), 860-867.

11. M. Abou-Seada. Digital Computer Calculation of Corona Thresholds in Non-uniform Fields. Ph.D. Thesis, Iowa State University, 1970.

12. P. Thomas. "Output and regulation in long distance lines." AIEE Trans. Power Apparatus and Systems, PAS-28, Part I (1909), 615-640.

13. P. Thomas. "Calculation of high tension lines." AIEE Trans. Power Apparatus and Systems, PAS-28, Part I (1909), 641-686.

14. E. Clarke. "Three phase multiple conductor circuits." AIEE Trans. Power Apparatus and Systems, 51 (1932), 820-821.

15. G. Adams. "Voltage gradients on high voltage transmission lines." AIEE Trans. Power Apparatus and Systems, 74, Part III (April 1955), 5-11.

16. C. Miller. "Mathematical prediction of radio and corona characteristics of smooth bundled conductors." AIEE Trans. Power Apparatus and Systems, PAS-75, Part III (October 1956), 1029-1037.

17. J. Reichman. "Bundled conductor voltage gradient calculations." AIEE Trans. Power Apparatus and Systems, PAS-78, Part III-A (August 1959), 598-607.

18. S. King. "The electric field near bundle conductors." IEE Proc., 106, Part C (June 1959), 200-206.

19. T. Sreenivasan. "Potential, potential gradient and evaluation of corona loss in dual conductor transmission lines." Institution of Engineers (India), 40, Part II, No. 12 (August 1960), 419-428.

20. A. Timascheff. "Field patterns of bundle conductors and their electrostatic properties." AIEE Trans. Power Apparatus and Systems, PAS-80, Part III, (October 1961), 590-597.

21. A. Timascheff. "Equigradient lines in the vicinity of bundle conductors." AIEE Trans. Power Apparatus and Systems, PAS-82, Part III (April 1963), 104-110.

22. N. Tikhodeev. "Some peculiarities of corona discharge on bundle conductors at a constant voltage." Journal of Technical Physics, 23, No. 10 (October 1953), 1773-1778.

23. N. Tikhodeev. "On the calculation of initial voltages of the total corona on dc transmission lines." Electrichestvo, No. 10 (1957), 12-19.

24. G. Aleksandrov. "Converted method of images in a circle and its application to the solution of plane electrostatic problems." Electrichestvo, No. 9 (1958), 20-23.

25. M. Sarma and W. Janischewskyj. "Electric field of a system of parallel cylindrical conductors." IEEE Trans. Power Apparatus and Systems, PAS-88, No. 7 (July 1969), 1069-1079.

26. M. Abou-Seada and E. Nasser. "Digital computer calculation of the potential and its gradient of a twin cylindrical conductor." IEEE Trans. Power Apparatus and Systems, PAS-88, No. 12 (December 1969), 1802-1814.

27. M. Abou-Seada and E. Nasser. "Calculation of the potential gradient of twin-cylindrical bipolar conductors with various geometrical parameters." IEEE Trans. Power Apparatus and Systems, PAS-90, No. 4 (July-August 1971), 1822-1829.

28. P. Thanassoulis and R. Comsa. "Calculation of the maximum voltage gradients, Part I: bundle conductors." IEEE Trans. Power Apparatus and Systems, PAS-90, No. 1 (January-February 1971), 145-150.

29. M. Sarma and W. Janischewskyj. "Analysis of corona losses on dc transmission lines." IEEE Trans. Power Apparatus and Systems, PAS-88, No. 5 (May 1969), 718-731.

30. M. Sarma and W. Janischewskyj. "Analysis of corona losses on dc transmission line, Part II: Bipolar corona." IEEE Trans. Power Apparatus and Systems, PAS-88, No. 10 (October 1969), 1476-1491.

31. J. Andrews and A. Shrapnel. "Electric field distribution around an isolated stranded conductor." Proc. IEE, 119, No. 8 (August 1972), 1162-1166.

32. E. Kimbark. Direct Current Transmission. New York: Wiley Interscience, 1971.

33. C. Adamson and N. Hingorani. High Voltage Direct Current Power Transmission. London: Garraway Limited, 1960.

34. P. Danfoss and B. Hammarkund. "Must HVDC go to UHV levels?" Electrical World (USA), 179, No. 7 (April 1973), 60-61.

35. L. Kantrovich and V. Krylov. Approximate Methods of Higher Analysis. New York: Interscience Publishers, Inc., 1958.

36. W. Hayt. Engineering Electromagnetics. New York: McGraw-Hill, Inc., 1967.

V. ACKNOWLEDGMENTS

I wish to express my sincere appreciation to my major professor Dr. Essam Nasser for suggesting the problem and his encouragement throughout the development of this thesis.

I wish to thank Dr. Paul Anderson, the director of the Power Affiliate Program, for the financial support to carry out this project.

Special thanks should go to Dr. Selim for writing a computer program for the last part of the dissertation.

VI. APPENDIX A

```
C     ..................................................
C
C      COMPUTATION OF CAPACITANCE AND DISTRIBUTION OF POTENCIAL
C     AND ELECTROSTATIC FIELD ON CONDUCTOR SURFACE
C      FOR THE BIPOLAR LINE OF FOUR SUBCONDUCTORS
C      ABOVE GROUND
C
C     ..................................................
      IMPLICIT REAL*8(A-H,O-Z)
      DIMENSION ALPHA(15),XC1(60),YC1(60),XQ1(60),YQ1(60)
      DIMENSION COEFF(60,60),COEFC(60,60),Q(60),V(60)
      DIMENSION COEFD(60,60),EX(60),EY(60),E(60),GAMA(60)
      DIMENSION BETA(8)
C
      DIMENSION L(60),M(60)
C
      READ(5,6) PER
    6 FORMAT(D15.4)
      READ(5,5) H,R,A,B,S
    5 FORMAT(5F10.2)
C
C     ..........................................
C
      PI=3.141592653589793
      SS=2.0D0*S
      P2=R/2.0D0
C
C     ................................
C
      WRITE(6,10) H,R,A,B,SS
      WRITE(6,11) PER
      WRITE(6,12) P2
   10 FORMAT('1',//,10X,'CONDUCTOR HEIGHT=',F10.2,//,10X,'CONDUCTOR RADI
     1US=',F10.2,//,10X,'SUBCONDUCTOR HORIZONTAL SEPERATION=',F10.2,//,1
     20X,'SUBCONDUCTOR VERTICAL SEPERATION=',F10.2,//,10X,'BUNDLE SEPERA
     3TION=',F10.2,//)
   11 FORMAT(' ',10X,'PERMITIVITTY=',E12.4,//)
   12 FORMAT(' ',10X,'CHARGE RADIUS=',F6.3,//)
```

```
C
C     ..............................
C
      N=60
      NN=N/4
      DO 15 K=1,NN
   15 ALPHA(K)=((K-1)*2.0D0*PI)/NN
C     ..................................
C
C     COMPUTE COORDINATES OF POINTS ON CONDUCTOR SURFACE
C
C     ..................................
      DO 20 J1=1,NN
      XC1(J1)=S+(A/2.0D0)+(R*DCOS(ALPHA(J1)))
   20 YC1(J1)=H+(B/2.0D0)+(R*DSIN(ALPHA(J1)))

      DO 30 J1=1,NN
      J2=J1+NN
      XC1(J2)=S-(A/2.0D0)+(R*DCOS(ALPHA(J1)))
   30 YC1(J2)=YC1(J1)
      DO 40 J1=1,NN
      J2=J1+NN
      J3=J1+(2*NN)
      XC1(J3)=XC1(J2)
   40 YC1(J3)=H-(B/2.0D0)+(R*DSIN(ALPHA(J1)))
      DO 50 J1=1,NN
      J2=J1+NN
      J3=J1+(2*NN)
      J4=J1+(3*NN)
      XC1(J4)=XC1(J1)
   50 YC1(J4)=YC1(J3)
C     ..............................................
C
C      COMPUTE COOPDINATES OF CHARGES INSIDE CONDUCTOR
C
C     ..............................................
      DO 60 K1=1,NN
      XQ1(K1)=S+(A/2.0D0)+(P2*DCOS(ALPHA(K1)))
   60 YQ1(K1)=H+(B/2.0D0)+(P2*DSIN(ALPHA(K1)))
```

```
      DO 7C K1=1,NN
      K2=K1+NN
      XQ1(K2)=S-(A/2.0D0)+(P2*DCOS(ALPHA(K1)))
   70 YQ1(K2)=YQ1(K1)
      DO 80 K1=1,NN
      K2=K1+NN
      K3=K1+(2*NN)
      XQ1(K3)=XQ1(K2)
   80 YQ1(K3)=H-(B/2.0D0)+(P2*DSIN(ALPHA(K1)))
      DO 90 K1=1,NN
      K2=K1+NN
      K3=K1+(2*NN)
      K4=K1+(3*NN)
      XQ1(K4)=XQ1(K1)
   90 YQ1(K4)=YQ1(K3)
C     ..........................................
C
C     COMPUTE CHARGE COEFFICIENT MATRIX
C
C     ..........................................
      DO 100 J=1,N
      DO 100 K=1,N
      X1=XC1(J)-XQ1(K)
      Y1=YC1(J)-YQ1(K)
      X2=XC1(J)+XQ1(K)
      Y2=YC1(J)+YQ1(K)
      Z1=X1*X1+Y1*Y1
      Z2=X1*X1+Y2*Y2
      Z3=X2*X2+Y1*Y1
      Z4=X2*X2+Y2*Y2

  100 COEFF(J,K)=DLOG((Z2*Z3)/(Z1*Z4))/2.0D0
C     ..........................................
C
C     SOLVE FOR CHARGES AND CHECK ACCURACY OF RESULTS
C
C     ..........................................
```

```
      DO 110 J=1,N
      DO 110 K=1,N
  110 COEFC(J,K)=COEFF(J,K)
      DO 120 J=1,N
  120 Q(J)=1.0D0
      CALL DGELG(Q,COEFF,N,1,1.E-11,IER)
      DO 130 J=1,N
      V(J)=0.0D0
      DO 130 K=1,N
  130 V(J)=V(J)+COEFC(J,K)*Q(K)
      WRITE(6,140)
      DO 150 J=1,N
      WRITE(6,160) J,Q(J),V(J)
  150 CONTINUE
  140 FORMAT('1',15X,'CHARGES',20X,'POTENCIAL',//)
  160 FORMAT(' ',2X,I2,10X,F15.6,20X,F15.6)
C
C     COMPUTE CAPACITANCE OF CONDUCTOR
C
      QT=0.0D0
      DO 170 J=1,N
  170 QT=QT+Q(J)
      QTC=QT*2.0D0*PI*PER
      WRITE(6,180) QT,QTC
  180 FORMAT(///,' ',10X,'TOTAL CHARGE ON FOUR CONDUCTORS=',F15.8,/,10X,
     1'CAPACITANCE=',D15.8)
C     ..................................
C
C     COMPUTE POTENCIAL AND FIELD DISTRIBUTION ON CONDUCTOR SURFACE
C
C     ..................................
C
C
C     COMPUTE COORDINATES OF POINTS ON CONDUCTOR SURFACE
C
      NP=8
      DO 190 K=1,NP
  190 BETA(K)=((K-1)*2.0D0*PI)/NP
```

```
      DO 200 J1=1,NP
      XC1(J1)=S+(A/2.0D0)+(R*DCOS(BETA(J1)))
  200 YC1(J1)=H+(B/2.0D0)+(R*DSIN(BETA(J1)))
      DO 210 J1=1,NP
      J2=J1+NP
      XC1(J2)=S-(A/2.0D0)+(R*DCOS(BETA(J1)))
  210 YC1(J2)=YC1(J1)
      DO 220 J1=1,NP
      J2=J1+NP

      J3=J1+(2*NP)
      XC1(J3)=XC1(J2)
  220 YC1(J3)=H-(B/2.0D0)+(R*DSIN(BETA(J1)))
      DO 230 J1=1,NP
      J2=J1+NP
      J3=J1+(2*NP)
      J4=J1+(3*NP)
      XC1(J4)=XC1(J1)
  230 YC1(J4)=YC1(J3)
C
C
C

      NQ=4*NP
      DO 240 J=1,NQ
      DO 240 K=1,N
      X1=XC1(J)-XQ1(K)
      X2=XC1(J)+XQ1(K)
      Y1=YC1(J)-YQ1(K)
      Y2=YC1(J)+YQ1(K)
      Z1=X1*X1+Y1*Y1
      Z2=X1*X1+Y2*Y2
      Z3=X2*X2+Y1*Y1
      Z4=X2*X2+Y2*Y2
      COEFF(J,K)=DLOG((Z2*Z3)/(Z1*Z4))/2.0D0
      COEFC(J,K)=(X1/Z1)+(X2/Z4)-(X1/Z2)-(X2/Z3)
  240 COEFD(J,K)=(Y1/Z1)+(Y2/Z4)-(Y2/Z2)-(Y1/Z3)
C
C
```

```
C
      DO 250 J=1,NQ
      V(J)=0.0D0
      DO 250 K=1,N
  250 V(J)=V(J)+COEFF(J,K)*Q(K)
C
C
      DO 260 J=1,NQ
      EX(J)=0.0D0
      DO 260 K=1,N
  260 EX(J)=EX(J)+COEFC(J,K)*Q(K)
C
C
      DO 270 J=1,NQ
      EY(J)=0.0D0
      DO 270 K=1,N
  270 EY(J)=EY(J)+COEFC(J,K)*Q(K)
C
C
      DO 280 J=1,NQ
      E(J)=DSQRT(EX(J)*EX(J)+EY(J)*EY(J))
      GAMA(J)=DATAN2(EY(J),EX(J))
  280 GAMA(J)=(180.0D0/PI)*GAMA(J)
C
C


C
      WRITE(6,300)
      WRITE(6,310)(V(J),EX(J),EY(J),E(J),GAMA(J),J=1,NQ)
  300 FORMAT(' ',4X,'POTENCIAL',13X,'EX',18X,'EY',18X,'E',18X,'GAMA',//)
  310 FORMAT(' ',2X,F10.6,10X,F10.6,10X,F10.6,10X,F10.6,10X,F12.6)
C
C
C
      STOP
      END
```

VII. APPENDIX B

```
C     ..................................................
C
C     COMPUTATION OF CAPACITANCE AND DISTRIBUTION OF POTENCIAL
C    AND ELECTROSTATIC FIELD ON CONDUCTOR SURFACE
C     FOR SPLIT BUNDLE TRANSMISSION LINE- FOUR SUBCONUCTORS IN EACH
C     SUBBUNDLE -ABOVE GROUND
C
C     ..................................................
      IMPLICIT REAL*8(A-H,O-Z)
      DIMENSION ALPHA(15),XC1(60),YC1(60),XQ1(60),YQ1(60)
      DIMENSION COEFF(60,60),COEFC(60,60),Q(60),V(60)
      DIMENSION COEFD(60,60),EX(60),EY(60),E(60),GAMA(60)
      DIMENSION BETA(8)
C
      DIMENSION L(60),M(60)
C
      READ(5,6) PER
    6 FORMAT(D15.4)
      READ(5,5) H,R,A,B,S
    5 FORMAT(5F10.2)
C
C     ..........................................
C
      PI=3.141592653589793
      SS=2.0D0*S
      P2=R/2.0D0
C
C     ..................................
C
      WRITE(6,10) H,R,A,B,SS
      WRITE(6,11) PER
      WRITE(6,12) P2
   10 FORMAT('1',//,10X,'CONDUCTOR HEIGHT=',F10.2,//,10X,'CONDUCTOR RADI
     1US=',F10.2,//,10X,'SUBCONDUCTOR HORIZONTAL SEPERATION=',F10.2,//,1
     20X,'SUBCONDUCTOR VERTICAL SEPERATION=',F10.2,//,10X,'BUNDLE SEPERA
     3TION=',F10.2,//)
   11 FORMAT(' ',10X,'PERMITIVITTY=',E12.4,//)
   12 FORMAT(' ',10X,'CHARGE RADIUS=',F6.3,//)
```

```
C
C     ..............................
C
      N=60
      NN=N/4
      DO 15 K=1,NN
   15 ALPHA(K)=((K-1)*2.0D0*PI)/NN
C     ..................................
C
C     COMPUTE COORDINATES OF POINTS ON CONDUCTOR SURFACE
C
C     ..................................
      DO 20 J1=1,NN
      XC1(J1)=S+(A/2.0D0)+(R*DCOS(ALPHA(J1)))
   20 YC1(J1)=H+(B/2.0D0)+(R*DSIN(ALPHA(J1)))


      DO 30 J1=1,NN
      J2=J1+NN
      XC1(J2)=S-(A/2.0D0)+(R*DCOS(ALPHA(J1)))
   30 YC1(J2)=YC1(J1)
      DO 40 J1=1,NN
      J2=J1+NN
      J3=J1+(2*NN)
      XC1(J3)=XC1(J2)
   40 YC1(J3)=H-(B/2.0D0)+(R*DSIN(ALPHA(J1)))
      DO 50 J1=1,NN
      J2=J1+NN
      J3=J1+(2*NN)
      J4=J1+(3*NN)
      XC1(J4)=XC1(J1)
   50 YC1(J4)=YC1(J3)
C     ..............................................
C
C      COMPUTE COORDINATES OF CHARGES INSIDE CONDUCTOR
C
```

```
C     ..........................................
      DO 60 K1=1,NN
      XQ1(K1)=S+(A/2.0D0)+(P2*DCOS(ALPHA(K1)))
   60 YQ1(K1)=H+(B/2.0D0)+(P2*DSIN(ALPHA(K1)))
      DO 70 K1=1,NN
      K2=K1+NN
      XQ1(K2)=S-(A/2.0D0)+(P2*DCOS(ALPHA(K1)))
   70 YQ1(K2)=YQ1(K1)
      DO 80 K1=1,NN
      K2=K1+NN
      K3=K1+(2*NN)
      XQ1(K3)=XQ1(K2)
   80 YQ1(K3)=H-(B/2.0D0)+(P2*DSIN(ALPHA(K1)))
      DO 90 K1=1,NN
      K2=K1+NN
      K3=K1+(2*NN)
      K4=K1+(3*NN)
      XQ1(K4)=XQ1(K1)
   90 YQ1(K4)=YQ1(K3)
C     ..........................................
C
C     COMPUTE CHARGE COEFFICIENT MATRIX
C
C     ..........................................
      DO 100 J=1,N
      DO 100 K=1,N
      X1=XC1(J)-XQ1(K)
      Y1=YC1(J)-YQ1(K)
      X2=XC1(J)+XQ1(K)
      Y2=YC1(J)+YQ1(K)
      Z1=X1*X1+Y1*Y1
      Z2=X1*X1+Y2*Y2
      Z3=X2*X2+Y1*Y1
      Z4=X2*X2+Y2*Y2
```

```
  100 COEFF(J,K)=DLOG((Z2*Z4)/(Z1*Z3))/2.0D0
C     ..........................................
C
C     SOLVE FOR CHARGES AND CHECK ACCURACY OF RESULTS
C
C     ..........................................
      DO 110 J=1,N
      DO 110 K=1,N
  110 COEFC(J,K)=COEFF(J,K)
      DO 120 J=1,N
  120 Q(J)=1.0D0
      CALL DGELG(Q,COEFF,N,1,1.E-11,IER)
      DO 130 J=1,N
      V(J)=0.0D0
      DO 130 K=1,N
  130 V(J)=V(J)+COEFC(J,K)*Q(K)
      WRITE(6,140)
      DO 150 J=1,N
      WRITE(6,160) J,Q(J),V(J)
  150 CONTINUE
  140 FORMAT('1',15X,'CHARGES',20X,'POTENCIAL',//)
  160 FORMAT(' ',2X,I2,10X,F15.6,20X,F15.6)
C
C     COMPUTE CAPACITANCE OF CONDUCTOR
C
      QT=0.0D0
      DO 170 J=1,N
  170 QT=QT+Q(J)
      QTC=QT*2.0D0*PI*PER
      WRITE(6,180) QT,QTC
  180 FORMAT(///,' ',10X,'TOTAL CHARGE ON FOUR CONDUCTORS=',F15.8,/,10X,
     1'CAPACITANCE=',D15.8)
C     ..................................
C
C     COMPUTE POTENCIAL AND FIELD DISTRIBUTION ON CONDUCTOR SURFACE
C
C     ..................................
```

```
C
C
C     COMPUTE COORDINATES OF POINTS ON CONDUCTOR SURFACE
C
      NP=8
      DO 190 K=1,NP
  190 BETA(K)=((K-1)*2.0D0*PI)/NP
      DO 200 J1=1,NP
      XC1(J1)=S+(A/2.0D0)+(R*DCOS(BETA(J1)))
  200 YC1(J1)=H+(B/2.0D0)+(R*DSIN(BETA(J1)))
      DO 210 J1=1,NP
      J2=J1+NP
      XC1(J2)=S-(A/2.0D0)+(R*DCOS(BETA(J1)))
  210 YC1(J2)=YC1(J1)
      DO 220 J1=1,NP
      J2=J1+NP

      J3=J1+(2*NP)
      XC1(J3)=XC1(J2)
  220 YC1(J3)=H-(B/2.0D0)+(R*DSIN(BETA(J1)))
      DO 230 J1=1,NP
      J2=J1+NP
      J3=J1+(2*NP)
      J4=J1+(3*NP)
      XC1(J4)=XC1(J1)
  230 YC1(J4)=YC1(J3)
C
C
C
      NQ=4*NP
      DO 240 J=1,NQ
      DO 240 K=1,N
      X1=XC1(J)-XQ1(K)
      X2=XC1(J)+XQ1(K)
      Y1=YC1(J)-YQ1(K)
      Y2=YC1(J)+YQ1(K)
      Z1=X1*X1+Y1*Y1
      Z2=X1*X1+Y2*Y2
```

```
      Z3=X2*X2+Y1*Y1
      Z4=X2*X2+Y2*Y2
      COEFF(J,K)=DLOG((Z2*Z4)/(Z1*Z3))/2.0D0
      COEFC(J,K)=(X1/Z1)+(X2/Z3)-(X1/Z2)-(X2/Z4)
  240 COEFD(J,K)=(Y1/Z1)+(Y1/Z3)-(Y2/Z2)-(Y2/Z4)
C
C
C
      DO 250 J=1,NQ
      V(J)=0.0D0
      DO 250 K=1,N
  250 V(J)=V(J)+COEFF(J,K)*Q(K)
C
C
      DO 260 J=1,NQ
      EX(J)=0.0D0
      DO 260 K=1,N
  260 EX(J)=EX(J)+COEFC(J,K)*Q(K)
C
C
      DO 270 J=1,NQ
      EY(J)=0.0D0
      DO 270 K=1,N
  270 EY(J)=EY(J)+COEFC(J,K)*Q(K)
C
C
      DO 280 J=1,NQ
      E(J)=DSQRT(EX(J)*EX(J)+EY(J)*EY(J))
      GAMA(J)=DATAN2(EY(J),EX(J))
  280 GAMA(J)=(180.0D0/PI)*GAMA(J)
C
C
```

```
C
      WRITE(6,300)
      WRITE(6,310)(V(J),EX(J),EY(J),E(J),GAMA(J),J=1,NQ)
  300 FORMAT(' ',4X,'POTENCIAL',13X,'EX',18X,'EY',18X,'E',18X,'GAMA',//)
  310 FORMAT(' ',2X,F10.6,10X,F10.6,10X,F10.6,10X,F10.6,10X,F12.6)
C
C
C
      STOP
      END
```

VIII. APPENDIX C

```
C     ..................................................
C
C     COMPUTER PLOTTING OF EQUIPOTENCIAL LINES FOR FOUR-BUNDLE
C     BIPOLAR LINE
C     ..................................................
      IMPLICIT REAL*8(A-H,O-Z)
      REAL*4 X(23),Y(23),BETA
      REAL*4 XX(4)/17.,17.,41.,41./,YY(4)/17.,41.,41.,17./
      REAL*4 DATE(7),PARM(11),VMS(81,81)
      CALL LABEL(DATE,PARM,NPARM)
      DIMENSION ALPHA(15),XC1(60),YC1(60),XQ1(60),YQ1(60)
      DIMENSION COEFF(60,60),COEFC(60,60),Q(60),V(60)
      DIMENSION VM(59,59)
      EQUIVALENCE (VMS(1,1),COEFF(1,1))
C
      DIMENSION L(60),M(60)
C
      READ(5,6) PER
    6 FORMAT(D15.4)
      READ(5,5) H,R,A,B,S
    5 FORMAT(5F10.2)
C
C     ..........................................
C
      PI=3.141592653589793
      SS=2.0D0*S
      P2=R/2.0D0
C
C     ................................
C
      WRITE(6,10) H,R,A,B,SS
      WRITE(6,11) PER
      WRITE(6,12) P2
   10 FORMAT('1',//,10X,'CONDUCTOR HEIGHT=',F10.2,//,10X,'CONDUCTOR RADI
     1US=',F10.2,//,10X,'SUBCONDUCTOR HORIZONTAL SEPERATION=',F10.2,//,1
     20X,'SUBCONDUCTOR VERTICAL SEPERATION=',F10.2,//,10X,'BUNDLE SEPERA
     3TION=',F10.2,//)
   11 FORMAT(' ',10X,'PERMITIVITTY=',E12.4,//)
   12 FORMAT(' ',10X,'CHARGE RADIUS=',F6.3,//)
```

```
C
C     ..............................
C
      N=60
      NN=N/4
      DO 15 K=1,NN
   15 ALPHA(K)=((K-1)*2.0D0*PI)/NN
C     ....................................
C
C     COMPUTE COORDINATES OF POINTS ON CONDUCTOR SURFACE
C
C     ....................................
      DO 20 J1=1,NN
      XC1(J1)=S+(A/2.0D0)+(R*DCOS(ALPHA(J1)))

   20 YC1(J1)=H+(B/2.0D0)+(R*DSIN(ALPHA(J1)))
      DO 30 J1=1,NN
      J2=J1+NN
      XC1(J2)=S-(A/2.0D0)+(R*DCOS(ALPHA(J1)))
   30 YC1(J2)=YC1(J1)
      DO 40 J1=1,NN
      J2=J1+NN
      J3=J1+(2*NN)
      XC1(J3)=XC1(J2)
   40 YC1(J3)=H-(B/2.0D0)+(R*DSIN(ALPHA(J1)))
      DO 50 J1=1,NN
      J2=J1+NN
      J3=J1+(2*NN)
      J4=J1+(3*NN)
      XC1(J4)=XC1(J1)
   50 YC1(J4)=YC1(J3)
C     ..............................................
C
C      COMPUTE COORDINATES OF CHARGES INSIDE CONDUCTOR
C
C     ..............................................
      DO 60 K1=1,NN
      XQ1(K1)=S+(A/2.0D0)+(P2*DCOS(ALPHA(K1)))
   60 YQ1(K1)=H+(B/2.0D0)+(P2*DSIN(ALPHA(K1)))
```

```
      DO 70 K1=1,NN
      K2=K1+NN
      XQ1(K2)=S-(A/2.0D0)+(P2*DCOS(ALPHA(K1)))
   70 YQ1(K2)=YQ1(K1)
      DO 80 K1=1,NN
      K2=K1+NN
      K3=K1+(2*NN)
      XQ1(K3)=XQ1(K2)
   80 YQ1(K3)=H-(B/2.0D0)+(P2*DSIN(ALPHA(K1)))
      DO 90 K1=1,NN
      K2=K1+NN
      K3=K1+(2*NN)
      K4=K1+(3*NN)
      XQ1(K4)=XQ1(K1)
   90 YQ1(K4)=YQ1(K3)
C     ..........................................
C
C     COMPUTE CHARGE COEFFICIENT MATRIX
C
C     ..........................................
      DO 100 J=1,N
      DO 100 K=1,N
      X1=XC1(J)-XQ1(K)
      Y1=YC1(J)-YQ1(K)
      X2=XC1(J)+XQ1(K)
      Y2=YC1(J)+YQ1(K)
      Z1=X1*X1+Y1*Y1
      Z2=X1*X1+Y2*Y2
      Z3=X2*X2+Y1*Y1
      Z4=X2*X2+Y2*Y2
  100 COEFF(J,K)=DLOG((Z2*Z3)/(Z1*Z4))/2.0D0
C     ..........................................
C
C     SOLVE FOR CHARGES AND CHECK ACCURACY OF RESULTS
C
C     ..........................................
```

```
      DO 110 J=1,N
      DO 110 K=1,N
  110 COEFC(J,K)=COEFF(J,K)
      DO 120 J=1,N
  120 Q(J)=1.0D0
      CALL DGELG(Q,COEFF,N,1,1.E-11,IER)
      DO 130 J=1,N
      V(J)=0.0D0
      DO 130 K=1,N
  130 V(J)=V(J)+COEFC(J,K)*Q(K)
      WRITE(6,140)
      DO 150 J=1,N
      WRITE(6,160) J,Q(J),V(J)
  150 CONTINUE
  140 FORMAT('1',15X,'CHARGES',20X,'POTENCIAL',//)
  160 FORMAT(' ',2X,I2,10X,F15.6,20X,F15.6)
C
C     COMPUTE CAPACITANCE OF CONDUCTOR
C
      QT=0.0D0
      DO 170 J=1,N
  170 QT=QT+Q(J)
      QTC=QT*2.0D0*PI*PER
      WRITE(6,180) QT,QTC
  180 FORMAT(///,' ',10X,'TOTAL CHARGE ON FOUR CONDUCTORS=',F15.3,/,10X,
     1'CAPACITANCE=',D15.8)
C     ..................................
C
C     COMPUTE POTENCIAL AT GRID POINTS AROUND SUBCONDUCTORS
C
C     ..................................
      NX=59
      NY=59
      XC=S-(A/2.0D0)-R-15.0D0
      DO 200 I=1,NX
      YC=H-(B/2.0D0)-R-15.0D0
      DO 210 J=1,NY
C
```

```
C
C
      IF(I.LT.17) GO TC 103
      IF(I.GT.19) GO TC 104
      IF(J.LT.17) GO TO 103
      IF(J.GT.19) GO TC 105
      GO TO 101
  105 IF(J.LT.41) GO TO 103
      IF(J.GT.43) GO TC 103

      GO TO 101
  104 IF(I.LT.41) GO TO 103
      IF(I.GT.43) GO TC 103
      IF(J.LT.17) GO TC 103
      IF(J.GT.19) GO TC 106
      GO TO 101
  106 IF(J.LT.41) GO TC 103
      IF(J.GT.43) GO TC 103
      GO TO 101
  103 VM(I,J)=0.0D0
      DO 220 K=1,N
      X1=XC-XQ1(K)
      Y1=YC-YQ1(K)
      X2=XC+XQ1(K)
      Y2=YC+YQ1(K)
      Z1=X1*X1+Y1*Y1
      Z2=X1*X1+Y2*Y2
      Z3=X2*X2+Y1*Y1
      Z4=X2*X2+Y2*Y2
      COEF=DLOG((Z2*Z3)/(Z1*Z4))/2.0D0
  220 VM(I,J)=VM(I,J)+COEF*Q(K)
      GC TO 102
  101 VM(I,J)=1.0D0
  102 YC=YC+1.0D0
  210 CONTINUE
      XC=XC+1.0D0
  200 CONTINUE
C
```

```
C
      DO 250 I=1,NX
      WRITE(6,260)(VM(I,J),J=1,NY)
  260 FORMAT(12F10.6)
  250 CONTINUE
C
      DO 251 I=1,NX
      DO 251 J=1,NY
  251 VMS(I,J)=VM(I,J)
      WRITE(7,333)((VMS(I,J),J=1,NY),I=1,NX)
  333 FORMAT(20A4)
C
C
      CALL CONTUR(VMS,58,58,0.90,0.02,0.98,1,10.0,1.0,90.0)
      NPT=21
      X(NPT+1)=0.0
      X(NPT+2)=5.8
      Y(NPT+1)=0.0
      Y(NPT+2)=5.8
      PI=3.141592653589793
      R=2.0
      DO 302 J=1,4
      DO 301 I=1,NPT
      BETA=(I-1)*(2.0*PI)/(NPT-1)
      X(I)=XX(J)+(R*COS(BETA))

  301 Y(I)=YY(J)+(R*SIN(BETA))
  302 CALL LINE(X,Y,NPT,1,0,1)
      CALL ENDPLT
C
      STOP
      END
```

IX. APPENDIX D

```
C      COMPUTER PLOTTING OF EQUIGRADIENT LINES FOR FOUR-BUNDLE
C      BIPOLAR TRANSMISSION LINES
C      ..........
       IMPLICIT REAL*8(A-H,O-Z)
       REAL*4 X(23),Y(23),BETA
       REAL*4 XX(4)/22.,22.,46.,46./,YY(4)/17.,41.,41.,17./
       REAL*4 DATE(7),PARM(11),EMS(81,81)
       CALL LABEL(DATE,PARM,NPARM)
       DIMENSION ALPHA(15),XC1(60),YC1(60),XQ1(60),YQ1(60)
       DIMENSION COEFF(60,60),COEFC(60,60),Q(60),V(60)
       DIMENSION EM(59,59)
       EQUIVALENCE (EMS(1,1),COEFF(1,1))
C
       DIMENSION L(60),M(60)
C
       READ(5,6) PER
     6 FORMAT(D15.4)
       READ(5,5) H,R,A,B,S
     5 FORMAT(5F10.2)
C
C      ..........
C
       PI=3.141592653589793
       SS=2.0D0*S
       P2=R/2.0D0
C
C      ..........
C
       WRITE(6,10) H,R,A,B,SS
       WRITE(6,11) PER
       WRITE(6,12) P2
    10 FORMAT('1',//,10X,'CONDUCTOR HEIGHT=',F10.2,//,10X,'CONDUCTOR RADI
      1US=',F10.2,//,10X,'SUBCONDUCTOR HORIZONTAL SEPERATION=',F10.2,//,1
      20X,'SUBCONDUCTOR VERTICAL SEPERATION=',F10.2,//,10X,'BUNDLE SEPERA
      3TION=',F10.2,//)
    11 FORMAT(' ',10X,'PERMITIVITTY=',E12.4,//)
    12 FORMAT(' ',10X,'CHARGE RADIUS=',F6.3,//)
```

```
C
      N=60
      NN=N/4
      DO 15 K=1,NN
   15 ALPHA(K)=((K-1)*2.0D0*PI)/NN
C     ..................................
C
C     COMPUTE COORDINATES OF POINTS ON CONDUCTOR SURFACE
C
C     ..................................
      DO 20 J1=1,NN
      XC1(J1)=S+(A/2.0D0)+(R*DCOS(ALPHA(J1)))

   20 YC1(J1)=H+(B/2.0D0)+(R*DSIN(ALPHA(J1)))
      DO 30 J1=1,NN
      J2=J1+NN
      XC1(J2)=S-(A/2.0D0)+(R*DCOS(ALPHA(J1)))
   30 YC1(J2)=YC1(J1)
      DO 40 J1=1,NN
      J2=J1+NN
      J3=J1+(2*NN)
      XC1(J3)=XC1(J2)
   40 YC1(J3)=H-(B/2.0D0)+(R*DSIN(ALPHA(J1)))
      DO 50 J1=1,NN
      J2=J1+NN
      J3=J1+(2*NN)
      J4=J1+(3*NN)
      XC1(J4)=XC1(J1)
   50 YC1(J4)=YC1(J3)
C     ..............................................
C
C      COMPUTE COORDINATES OF CHARGES INSIDE CONDUCTOR
C
C     ..............................................
      DO 60 K1=1,NN
      XQ1(K1)=S+(A/2.0D0)+(P2*DCOS(ALPHA(K1)))
   60 YQ1(K1)=H+(B/2.0D0)+(P2*DSIN(ALPHA(K1)))
      DO 70 K1=1,NN
      K2=K1+NN
```

```
      XQ1(K2)=S-(A/2.0D0)+(P2*DCOS(ALPHA(K1)))
   70 YQ1(K2)=YQ1(K1)
      DO 80 K1=1,NN
      K2=K1+NN
      K3=K1+(2*NN)
      XQ1(K3)=XQ1(K2)
   80 YQ1(K3)=H-(B/2.0D0)+(P2*DSIN(ALPHA(K1)))
      DO 90 K1=1,NN
      K2=K1+NN
      K3=K1+(2*NN)
      K4=K1+(3*NN)
      XQ1(K4)=XQ1(K1)
   90 YQ1(K4)=YQ1(K3)
C     ..........................................
C
C     COMPUTE CHARGE COEFFICIENT MATRIX
C
C     ..........................................
      DO 100 J=1,N
      DO 100 K=1,N
      X1=XC1(J)-XQ1(K)
      Y1=YC1(J)-YQ1(K)
      X2=XC1(J)+XQ1(K)
      Y2=YC1(J)+YQ1(K)
      Z1=X1*X1+Y1*Y1
      Z2=X1*X1+Y2*Y2
      Z3=X2*X2+Y1*Y1

      Z4=X2*X2+Y2*Y2
  100 COEFF(J,K)=DLOG((Z2*Z3)/(Z1*Z4))/2.0D0
C     ..........................................
C
C     SOLVE FOR CHARGES AND CHECK ACCURACY OF RESULTS
C
C     ..........................................
      DO 110 J=1,N
      DO 110 K=1,N
  110 COEFC(J,K)=COEFF(J,K)
```

```
      DO 120 J=1,N
  120 Q(J)=1.0D0
      CALL DGELG(Q,COEFF,N,1,1.E-11,IER)
      DO 130 J=1,N
      V(J)=0.0D0
      DO 130 K=1,N
  130 V(J)=V(J)+COEFC(J,K)*Q(K)
      WRITE(6,140)
      DO 150 J=1,N
      WRITE(6,160) J,Q(J),V(J)
  150 CONTINUE
  140 FORMAT('1',15X,'CHARGES',20X,'POTENCIAL',//)
  160 FORMAT(' ',2X,I2,10X,F15.6,20X,F15.6)
C
C     COMPUTE CAPACITANCE OF CONDUCTOR
C
      QT=0.0D0
      DO 170 J=1,N
  170 QT=QT+Q(J)
      QTC=QT*2.0D0*PI*PER
      WRITE(6,180) QT,QTC
  180 FORMAT(///,' ',10X,'TOTAL CHARGE ON FOUR CONDUCTORS=',F15.8,/,10X,
     1'CAPACITANCE=',D15.8)
C     ..................................
C
C     COMPUTE FIELD DISTRIBUTION AROUND CONDUCTOR SURFACE
C
C     ................................................
C
      NX=59
      NY=59
      XC=S-(A/2.0D0)-R-20.0D0
      DO 200 I=1,NX
      YC=H-(B/2.0D0)--R-15.0D0
      DO 210 J=1,NY
C
```

```
C       IF(I.LT.22) GO TC 103
        IF(I.GT.24) GO TO 104
        IF(J.LT.17) GO TO 103
        IF(J.GT.19) GO TC 105
        GO TO 101
  105 IF(J.LT.41) GO TO 103

        IF(J.GT.43) GO TC 103
        GO TO 101
  104 IF(I.LT.46) GO TC 103
        IF(I.GT.48) GO TO 103
        IF(J.LT.17) GO TO 103
        IF(J.GT.19) GO TC 106
        GO TO 101
  106 IF(J.LT.41) GO TO 103
        IF(J.GT.43) GO TO 103
        GO TO 101
  103 EX=0.0D0
        EY=0.0D0
        DO 220 K=1,N
        X1=XC-XQ1(K)
        Y1=YC-YQ1(K)
        X2=XC+XQ1(K)
        Y2=YC+YQ1(K)
        Z1=X1*X1+Y1*Y1
        Z2=X1*X1+Y2*Y2
        Z3=X2*X2+Y1*Y1
        Z4=X2*X2+Y2*Y2
        COEC=(X1/Z1)+(X2/Z4)-(X1/Z2)-(X2/Z3)
        COED=(Y1/Z1)+(Y2/Z4)-(Y2/Z2)-(Y1/Z3)
        EX=EX+COEC*Q(K)
  220 EY=EY+COED*Q(K)
        EM(I,J)=DSQRT(EX*EX+EY*EY)
        GO TO 102
  101 EM(I,J)=0.05D0
  102 YC=YC+1.0D0
  210 CONTINUE
        XC=XC+1.0D0
```

```
  200 CONTINUE
C
C
      DO 250 I=1,NX
      WRITE(6,260)(EM(I,J),J=1,NY)
  260 FORMAT(12F10.6)
  250 CONTINUE
C
      DO 251 I=1,NX
      DO 251 J=1,NY
  251 EMS(I,J)=EM(I,J)
      WRITE(7,333)((EMS(I,J),J=1,NY),I=1,NX)
  333 FORMAT(20A4)
C
      CALL CONTUR(EMS,58,58,0.0085,0.0020,0.0205,1,10.0,1.0,90.0)
C
      NPT=21
      X(NPT+1)=0.0
      X(NPT+2)=5.8
      Y(NPT+1)=0.0
      Y(NPT+2)=5.8
      PI=3.141592653589793

      R=2.0
      DO 302 J=1,4
      DO 301 I=1,NPT
      BETA=(I-1)*(2.0*PI)/(NPT-1)
      X(I)=XX(J)+(R*COS(BETA))
  301 Y(I)=YY(J)+(R*SIN(BETA))
  302 CALL LINE(X,Y,NPT,1,0,1)
      CALL ENDPLT
C
      STOP
      END
```

X. APPENDIX E

```
C     COMPUTATION OF ELECTRIC FIELD AND POTENCIAL ON CONDUCTOR SURFACE
C     FOR TWIN-BUNDLE UNIPOLAR STRANDED CONDUCTOR ABOVE GROUND
C
C     ..................................................................
      IMPLICIT REAL*8(A-H,O-Z)
      DIMENSION ALPHA(60),XC1(60),YC1(60),XQ1(60),YQ1(60)
      DIMENSION COEFF(60,60),COEFC(60,60),Q(60),V(60)
      DIMENSION COEFD(60,60),BETA(30),EX(60),EY(60),E(60),GAMA(60)
C
      DIMENSION L(60),M(60)
C
      READ(5,5) H,R,A,N
      READ(5,6) PER
    5 FORMAT(3F15.6,I2)
    6 FORMAT(D15.4)
C
C     ..................................................................
C
      PI=3.141592653589793
      AA=2.0D0*A
      A1=R*DSIN(PI/N)
      B1=1.0D0+DSIN(PI/N)
      SR=A1/B1
      P1=R-(SR/2.0D0)
      P2=R/2.0D0
C
C     ..................................................................
C
      WRITE(6,10) H,R,AA,SR,N
      WRITE(6,11) PER
      WRITE(6,12) P1,P2
   10 FORMAT('1',//,10X,'CONDUCTOR HEIGHT=',F10.4,//,10X,'CONDUCTOR RADI
     1US=',F10.4,//,10X,'BUNDLE SEPERATION=',F10.4,//,10X,'STRAND RADIUS
     2=',F10.4,//,10X,'NUMBER OF STRANDS IN OUTER LAYER=',I2,//)
   11 FORMAT(' ',10X,'PERMITIVITTY=',E15.4,//)
   12 FORMAT(' ',10X,'CUTER CHARGE RADIUS=',F15.8,//,10X,'INNER CHARGE R
     1ADIUS=',F15.8)
```

```
C
C     ..................................................................
C
      B=DSQRT(R*R-2.0D0*SR*R)
      NN=2*N
      DO 15 K=1,NN
   15 ALPHA(K)=((K-1)*2.0D0*PI)/NN
C     ..................................................................
C
C     COMPUTE COORDINATES OF POINTS ON CONDUCTOR SURFACE
C
C     ..................................................................
      DO 20 K=1,N
      J=2*K-1
      J1=J+1
      XC1(J)=R*DCOS(ALPHA(J))+A
      XC1(J1)=B*DCOS(ALPHA(J1))+A
      YC1(J)=R*DSIN(ALPHA(J))+H
   20 YC1(J1)=B*DSIN(ALPHA(J1))+H
C     ..................................................................
C
C     COMPUTE COORDINATES OF CHARGES INSIDE CONDUCTOR
C
C     ..................................................................
      DO 30 J=1,N
      K=2*J-1
      K1=K+1
      XQ1(K)=P1*DCOS(ALPHA(K))+A
      XQ1(K1)=P2*DCOS(ALPHA(K1))+A
      YQ1(K)=P1*DSIN(ALPHA(K))+H
   30 YQ1(K1)=P2*DSIN(ALPHA(K1))+H
C     ..................................................................
C
C     CCMPUTE CHARGE COEFFICIENT MATRIX
C
C     ..................................................................
```

```
      DO 40 J=1,NN
      DO 40 K=1,NN
      X1=XC1(J)-XQ1(K)
      Y1=YC1(J)-YQ1(K)
      X2=XC1(J)+XQ1(K)
      Y2=YC1(J)+YQ1(K)
      Z1=X1*X1+Y1*Y1
      Z2=X1*X1+Y2*Y2
      Z3=X2*X2+Y1*Y1
      Z4=X2*X2+Y2*Y2
   40 COEFF(J,K)=DLOG((Z2*Z4)/(Z1*Z3))/2.0D0
C     ..................................................................
C
C     SOLVE FOR CHARGES AND CHECK ACCURACY OF RESULTS
C
C     ..................................................................
      DO 50 J=1,NN
      DO 50 K=1,NN
   50 COEFC(J,K)=COEFF(J,K)
      DO 60 J=1,NN
   60 Q(J)=1.0D0
      CALL DGELG(Q,COEFF,NN,1,1.E-11,IER)
      DO 70 J=1,NN
      V(J)=0.0D0
      DO 70 K=1,NN
   70 V(J)=V(J)+COEFC(J,K)*Q(K)
      WRITE(6,80)
      DO 90 J=1,NN
      WRITE(6,100) J,Q(J),V(J)
   90 CONTINUE
   80 FORMAT('1',15X,'CHARGES',20X,'POTENCIAL',//)
  100 FORMAT(' ',2X,I2,10X,F10.6,20X,F10.6)
C
C     COMPUTE CAPACITANCE OF CONDUCTOR
C
      QT=0.0D0
      DO 95 J=1,NN
   95 QT=QT+Q(J)
```

```
      QTB=2.0D0*QT
      QTC=QTB*2.0D0*PI*PER
      WRITE(6,96) QTB,QTC
   96 FORMAT(///,' ',10X,'TOTAL CHARGE ON BOTH CONDUCTOR=',F15.8,/,10X,'
     1CAPACITANCE=',D15.8)
C
C     ***************************************************
C
      HH=2.0D0*H
      DD=DSQRT(R*AA)
      CC=DLOG(HH/DD)
      BB=1.0D0/CC
      QTT=BB*2.0D0*PI*PER
      WRITE(6,97) BB,QTT
   97 FORMAT(' ',10X,'TOTAL CHARGE BY THEORY=',F15.8,/,10X,'CAPACITANCE
     1BY THEORY=',D15.8)
C     ***************************************************
C
C     COMPUTE POTENCIAL AND FIELD DISTRIBUTION ON CONDUCTOR SURFACE
C
C     ***************************************************
      THETA=DARSIN(SR/(R-SR))
      PHI=THETA+(PI/2.0D0)
      PHIL=PHI/10.0D0
C
      I=1
      ANGLE=0.0D0
  170 H1=R-SR+(SR*DCOS(ANGLE))
      V1=SR*DSIN(ANGLE)
      HV1=H1*H1+V1*V1
      B1=DSQRT(HV1)
      T1=DATAN2(V1,H1)
C
C     ***************************************************
      DO 120 K=1,N
  120 BETA(K)=(K-1)*(6.28320D0/N)
```

```
C
C     COMPUTE COORDINATES OF POINTS ON CONDUCTOR SURFACE
C
      DO 125 K=1,N
      J=2*K-1
      J1=J+1
      XC1(J)=B1*DCOS(BETA(K)-T1)+A
      XC1(J1)=B1*DCOS(BETA(K)+T1)+A
      YC1(J)=H+(B1*DSIN(BETA(K)-T1))
  125 YC1(J1)=H+(B1*DSIN(BETA(K)+T1))
C
C     COMPUTE CHARGE COEFFICIENT MATRIX
C
C
      DO 130 J=1,NN
      DO 130 K=1,NN
      X1=XC1(J)-XQ1(K)
      Y1=YC1(J)-YQ1(K)
      X2=XC1(J)+XQ1(K)
      Y2=YC1(J)+YQ1(K)
      Z1=X1*X1+Y1*Y1
      Z2=X1*X1+Y2*Y2
      Z3=X2*X2+Y1*Y1
      Z4=X2*X2+Y2*Y2
      COEFF(J,K)=DLOG((Z2*Z4)/(Z1*Z3))/2.0D0
      COEFC(J,K)=(X1/Z1)+(X2/Z3)-(X1/Z2)-(X2/Z4)
  130 COEFD(J,K)=(Y1/Z1)+(Y1/Z3)-(Y2/Z2)-(Y2/Z4)
C
C
C
      DO 135 J=1,NN
      V(J)=0.0D0
      DO 135 K=1,NN
  135 V(J)=V(J)+COEFF(J,K)*Q(K)
C
      DO 140 J=1,NN
      EX(J)=0.0D0
```

```
      DO 140 K=1,NN
  140 EX(J)=EX(J)+COEFC(J,K)*Q(K)
C     ************************************************************
      DO 145 J=1,NN
      EY(J)=0.0D0
      DO 145 K=1,NN
  145 EY(J)=EY(J)+COEFD(J,K)*Q(K)
C     ************************************************
      DO 150 J=1,NN
      E(J)=DSQRT(EX(J)*EX(J)+EY(J)*EY(J))
      GAMA(J)=DATAN2(EY(J),EX(J))
  150 GAMA(J)=(180.0D0/3.14160D0)*GAMA(J)
C     ************************************************************
      ANGLED=(180.0D0/PI)*ANGLE
      WRITE(6,155) ANGLED
      WRITE(6,160)
      WRITE(6,165)(V(J),EX(J),EY(J),E(J),GAMA(J),J=1,NN)
  155 FORMAT('1',40X,'ANGLE=',F10.6,//)
  160 FORMAT(' ',4X,'POTENCIAL',13X,'EX',18X,'EY',18X,'E',18X,'GAMA',//)
  165 FORMAT(' ',2X,F10.6,10X,F10.6,10X,F10.6,10X,F10.6,10X,F12.6)
C
C     ************************************************************
C
      ANGLE=ANGLE+PHIL
      I=I+1
      IF(I.LE.11) GO TO 170
      STOP
      END
```

XI. APPENDIX F1

```
$JOB            I4229PAREKH,TIME=60,PAGES=100
C
C   ..............................................................
C
C     ELECTROSTATIC POTENCIAL OF A STRANDED CONDUCTOR-ANALYTICAL METHOD
C
C   ..............................................................
      IMPLICIT REAL*8(A-H,O-Z)
      REAL*4 XSIZE,YSIZE,XSF,XMIN,YSF,YMIN
      DIMENSION U(50),C(49),D(50),G(50),RJ(1225),A(50)
      COMMON /SFUM/ S(129)
      COMMON /FFFW/ F(129)
      COMMON /UMWUMN/ UM(129,50)
      COMMON /FFWUMN/ Y(129),Z(129)
      COMMON /BLK1/ IP
      COMMON /UMPAR/ PI,RC,RS,RF,BETA,AA,NS
      COMMON /ANGS/ BESRHS,IERTH
      COMMON /DEGRAD/ PIN180
      COMMON /BESANO/ BESN(50),ANO(50)
 1000 FORMAT(////50X,3HN =,I3//)
 4000 FORMAT(22X,1HN,20X,1HA,16X,'NORM. BESS. INEQ.')
 4100 FORMAT(44X,2HNO)
 4200 FORMAT(' ')
 5000 FORMAT(20X,I3,F25.7,F25.7)
 6000 FORMAT(1H1)
      IERTH=0
      PI=3.141592653589793
      PIN180=180.0D0/PI
      CALL STEP
      CALL PARM
      CALL SUBS
      CALL FCT
      CALL FF(BESRHS)
      NMAX=11
      KA=NMAX
```

```
     29          KAM1=NMAX-1
     30          KADIAG=(KA*KAM1)/2
     31          DO 30 M=1,NMAX
     32          NCAPP1=M
     33          CALL SUBW(W,M)
     34          CALL UMN(U,M)
     35          NO=M-1
     36          WRITE(6,1000) NO
     37          CALL  ORTH(U,W,C,D,G,RJ,A,NCAPP1,KA,KAM1,KADIAG,BESLHS,IER)
     38          IF(IER.EQ.0.AND.IERTH.EQ.0) GO TO 25
     39          CALL ERROR(IER,IERTH)
     40          GO TO 30
     41          WRITE(6,6000)
**WARNING**  UNNUMBERED EXECUTABLE STATEMENT FOLLOWS A TRANSFER
     42          WRITE(6,4000)
     43          WRITE(6,4100)
     44          WRITE(6,4200)
     45          M1=M-1
     46          DO 4 K=1,M1
     47          KK=K-1
     48          WRITE(6,5000) KK,ANO(K),BESN(K)
     49        4 CONTINUE
           C
     50          I=1
     51          DO 5 K=6,M1

     52          Z(I)=1.0D0/(I+4)
     53          BESN(I)=BESN(K)
     54          ANO(I)=ANO(K)
     55          I=I+1
     56        5 CONTINUE
           C
     57          XSIZE=4.01
     58          YSIZE=2.01
     59          XMIN=0.0
     60          YMIN=0.0
```

```
      XSF=0.0
      YSF=0.0
      NPTS=-(M1-5)
      ISYM=13
      MODE=3
C
      CALL GRAPH(NPTS,Z,BESN,ISYM,MODE,XSIZE,YSIZE,XSF,XMIN,YSF,YMIN,
     *' ;',' ;',' ;',' ;')
      CALL GRAPH(NPTS,Z,ANO,ISYM,MODE,XSIZE,YSIZE,XSF,XMIN,YSF,YMIN,
     *' ;',' ;',' ;',' ;')
C
      XSIZE=8.01
      YSIZE=4.01
C
      CALL GRAPH(NPTS,Z,ANO,ISYM,MODE,XSIZE,YSIZE,XSF,XMIN,YSF,YMIN,
     *' ;',' ;',' ;',' ;')
C
      ISYM=0
      MODE=4
C
      CALL GRAPH(NPTS,Z,ANO,ISYM,MODE,XSIZE,YSIZE,XSF,XMIN,YSF,YMIN,
     *' ;',' ;',' ;',' ;')
C
      GO TO 40
   25 CALL OUTPUT(A,BESLHS,BESRHS,M)
   30 CONTINUE
   40 STOP
      END
C
C  ..............................................................
C

      SUBROUTINE STEP
      IMPLICIT REAL*8(A-H,O-Z)
      COMMON /BLK1/ IP
      COMMON /BLK2/ SL,SU
```

```
      COMMON /BLK/ H,NDIM,NBIS
      COMMON /UMPAR/ PI,RC,RS,RF,BETA,AA,NS
      PI=3.141592653589793
      RC=1.0D0
      RF=2000.0D0
      NS=30
      BETA=PI/NS
      RS=(RC*DSIN(BETA))/(1.0D0+DSIN(BETA))
      AA=RC-RS
      SL=0.0D0
      SU=BETA
      IP=7
      NDIM=2**IP+1
      NBIS=NDIM-1

      H=(SU-SL)/NBIS
      RETURN
      END
C
C     ..................................................................
C

      SUBROUTINE PARM
      IMPLICIT REAL*8(A-H,O-Z)
      COMMON /BLK2/ SL,SU
      COMMON /BLK/ H,NDIM,NBIS
      COMMON /UMPAR/ PI,RC,RS,RF,BETA,AA,NS
 1000 FORMAT(1H1)
 2000 FORMAT(///40X,'ELECTROSTATIC POTENCIAL OF A STRANDED CONDUCTOR')
 3000 FORMAT(//20X,'CONDUCTOR RADIUS=',F5.2,//,20X,'STRAND RADIUS=',E15.
     18,//,20X,'FAR RADIUS=',F12.1,//,20X,'NUMBER OF STRANDS=',I2)
 4000 FORMAT(//10X,
     X'THE FOLLOWING VALUES WERE USED FOR THIS PROBLEM :')
 5000 FORMAT(/15X,29HLOWER BOUND OF THE INTERVAL =,D22.15)
 5100 FORMAT(/15X,29HUPPER BOUND OF THE INTERVAL =,D22.15)
```

```
111     5200 FORMAT(/15X,
            X45HSTEP SIZE USED IN THE NUMERICAL INTEGRATION =,D22.15)
112     5300 FORMAT(/15X,38HNUMBER OF BISECTIONS OF THE INTERVAL =,I4)
113          WRITE(6,1000)
114          WRITE(6,2000)
115          WRITE(6,3000) RC,RS,RF,NS
116          WRITE(6,4000)
117          WRITE(6,5000) SL
118          WRITE(6,5100) SU
119          WRITE(6,5200) H
120          WRITE(6,5300) NBIS
121          RETURN
122          END
       C
       C    ..................................................................
       C

123          SUBRCUTINE SUBS
124          IMPLICIT REAL*8(A--H,O-Z)
125          COMMCN /BLK2/ SL,SU
126          COMMCN /BLK/ H,NDIM,NBIS
127          COMMON /SFUM/ S(129)
       C
128          DO 1 J=1,NDIM
129        1 S(J)=SL+(J-1)*H
       C
130          RETURN
131          END
       C
       C    ..................................................................
       C

132          SUBROUTINE FCT
133          IMPLICIT REAL*8(A-H,O-Z)
134          COMMCN /BLK/ H,NDIM,NBIS
135          COMMON /SFUM/ S(129)
```

```
      COMMON /FFFW/ F(129)
C
      DO 1 J=1,NDIM
    1 F(J)=1.0D0
C
      RETURN
      END
C
C     ..................................................................
C

      SUBROUTINE FF(BESRHS)
      IMPLICIT REAL*8(A-H,O-Z)
      COMMON /BLK/ H,NDIM,NBIS
      COMMON /FFFW/ F(129)
      COMMON /FFWUMN/ Y(129),Z(129)
C
      DO 1 J=1,NDIM
    1 Y(J)=F(J)*F(J)
      CALL DGSF(H,Y,Z,NDIM)
      BESRHS=Z(NDIM)
C
      RETURN
      END
C
C     ..................................................................
C

      SUBROUTINE SUBW(W,M)
      IMPLICIT REAL*8(A-H,O-Z)
      COMMON /BLK/ H,NDIM,NBIS
      COMMON /FFFW/ F(129)
      COMMON /UMWUMN/ UM(129,50)
      COMMON /FFWUMN/ Y(129),Z(129)
C
      CALL UMFCT(M)
```

```
      C
159           DO 1 J=1,NDIM
160         1 Y(J)=UM(J,M)*F(J)
161           CALL DQSF(H,Y,Z,NDIM)
162           W=Z(NDIM)
      C
163           RETURN
164           END
      C
      C     ..................................................................
      C

165           SUBROUTINE UMN(U,M)
166           IMPLICIT REAL*8(A-H,O-Z)
167           DIMENSION U(M)
168           COMMON /BLK/ H,NDIM,NBIS
169           COMMON /UMWUMN/ UM(129,50)
170           COMMON /FFWUMN/ Y(129),Z(129)
      C
171           DO 6  N=1,M
      C
172           DO 1 J=1,NDIM
173         1 Y(J)=UM(J,M)*UM(J,N)
174           CALL DQSF(H,Y,Z,NDIM)
175           U(N)=Z(NDIM)
      C
176         6 CONTINUE
177           RETURN

178           END
      C
      C     ..................................................................
      C

179           SUBROUTINE UMFCT(M)
180           IMPLICIT REAL*8(A-H,O-Z)
```

```
      COMMON /BLK/ H,NDIM,NBIS
      COMMCN /UMPAR/ PI,RC,RS,RF,BETA,AA,NS
      COMMON /SFUM/ S(129)
      COMMCN /UMWUMN/ UM(129,50)
C
      MM=M-1
C
      IF(MM.EQ.0) GO TO 10
C
      EXP=MM*PI/BETA
      EXPN=-EXP
C
      DO 5 J=1,NDIM
      THETA=S(J)
      FOR=F(THETA)/RC
      UM(J,M)=(FOR**EXPN)*DCCS(EXP*THETA)
    5 CONTINUE
      RETURN
C
   10 CONTINUE
      TT=DLOG(RC/RF)
      CO 15 J=1,NDIM
      THETA=S(J)
      SS=DLOG(F(THETA)/RF)
      UM(J,M)=SS/TT
   15 CONTINUE
      RETURN
      END
C
C

      FUNCTICN F(THETA)
      IMPLICIT REAL*8(A-H,O-Z)
      COMMCN /UMPAR/ PI,RC,RS,RF,BETA,AA,NS
      CC=AA*DCOS(THETA)
      CD=AA*DSIN(THETA)
```

```
209           EE=DSQRT(RS*RS-DD*DD)
210           F=CC+EE
211           RETURN
212           END
      C
      C     ..................................................................
      C

213           SUBROUTINE ORTH(U,W,C,D,G,J,A,NCAPP1,KA,KAM1,KADIAG,BESLHS,IER)
214           IMPLICIT REAL*8(A-H,O-Z)
215           REAL*8 J(KADIAG),JTEMP
216           DIMENSION U(KA),C(KAM1),D(KA),G(KA),A(KA)
217           IF(NCAPP1-1) 1,2,2
218     1     IER=1
219           RETURN
220     2     IF(NCAPP1-KA) 4,4,3
221     3     IER=2

222           RETURN
223     4     IF(KA-1-KAM1) 5,6,5
224     5     IER=3
225           RETURN
226     6     IF((KA*KAM1)/2-KADIAG) 7,8,7
227     7     IER=4
228           RETURN
229     8     CONTINUE
230           IER=0
231           NCAP = NCAPP1-1
232           NCAPM1 = NCAP-1
233           IF(NCAPM1) 10,20,30
234     10    C(1) = U(1)
235           G(1) = W
236           E = G(1)/D(1)
237           A(1) = E
238           UANG = U(1)
239           CANG = D(1)
```

```
240           BESLHS =            E*E*DANG
241           CALL          ANGLES(BESLHS,DANG,UANG,W,IER)
242           RETURN
243     20    C(1) = U(1)/D(1)
244           C(2) = U(2)-C(1)*C(1)*D(1)
245           G(2) = W-C(1)*G(1)
246           E = G(2)/D(2)
247           J(1) = C(1)
248           A(1) = A(1)-E*J(1)
249           A(2) = E
250           UANG = U(2)
251           CANG = C(2)
252           BESLHS = BESLHS + E*E*DANG
253           CALL          ANGLES(BESLHS,DANG,UANG,W,IER)
254           RETURN
255     30    C(1) = U(1)/D(1)
256           NFORJ = 0
257           DO 120 N = 2,NCAP
258           CTEMP = U(N)
259           NM1 = N-1
260           DO 110 NN = 1,NM1
261           NFORJ = NFORJ+1
262     110   CTEMP = CTEMP-U(NN)*J(NFORJ)
263     120   C(N) = CTEMP/D(N)
264           DTEMP = U(NCAPP1)
265           GTEMP = W
266           DO 140 N = 1,NCAP
267           CTEMP = C(N)
268           DTEMP = DTEMP-CTEMP*CTEMP*D(N)
269     140   GTEMP = GTEMP-CTEMP*G(N)
270           D(NCAPP1) = DTEMP
271           G(NCAPP1) = GTEMP
272           E = GTEMP/DTEMP
273           NSTART = 0
274           DO 180 N = 1,NCAPM1
```

```
      JTEMP = C(N)
      NSTART = NSTART+N
      NFORJ = NSTART
      NP1 = N+1
      DO 170 NN = NP1,NCAP
      JTEMP = JTEMP-C(NN)*J(NFORJ)
  170 NFORJ = NFORJ+NN-1

      J(NFORJ) = JTEMP
  180 A(N) = A(N)-E*JTEMP
      NFORJ = NFORJ+1
      J(NFORJ) = C(NCAP)
      A(NCAP) = A(NCAP)-E*J(NFORJ)
      A(NCAPP1) = E
      UANG = U(NCAPP1)
      DANG = D(NCAPP1)
      BESLHS = BESLHS + E*E*DANG
      CALL       ANGLES(BESLHS,DANG,UANG,W,IER)
      RETURN
      END
C
C     ..................................................................
C

      SUBROUTINE ANGLES(BESLHS,DANG,UANG,W,IER)
      IMPLICIT REAL*8(A-H,O-Z)
      COMMON /ANGS/ BESRHS,IERTH
      COMMON /DEGRAD/ PIN180
 1000 FORMAT(' BESSEL''S INEQ.:',1PD22.15,'<',1PD22.15,
     1       ', D(N),U(N,N),W(N) =',1P3D17.10)
 2000 FORMAT(' IERTH =',I2,', IER =',I2,
     1', ANGBES,ANGNEW,ANGTGC =',0P3F15.10)
      WRITE(6,1000) BESLHS,BESRHS,DANG,UANG,W
      IERTH = 0
      IF(BESLHS.LT.0.D0) GO TO 10
      IF(BESLHS.GT.BESRHS) GO TO 20
```

```
304           ANGBES = DARCOS(DSQRT(BESLHS/BESRHS))*PIN180
305           IF(DANG.GT.UANG) GO TO 30
306           IF(DANG.LT.0.D0) GO TO 40
307           ANGNEW = DARCOS(DSQRT(1.D0-DANG/UANG))*PIN180
308           IF(UANG.LT.0.D0) GO TO 50
309           ANGTGO = DSQRT(BESRHS*UANG)
310           IF(CABS(W).GT.ANGTGO) GO TO 60
311           ANGTGO = DARCOS(W/ANGTGO)*PIN180
312           GO TO 70
313     10    IERTH = IERTH + 1
314     20    IERTH = IERTH + 1
315     30    IERTH = IERTH + 1
316     40    IERTH = IERTH + 1
317     50    IERTH = IERTH + 1
318     60    IERTH = IERTH + 1
319        70 WRITE(6,2000) IERTH,IER,ANGBES,ANGNEW,ANGTGO
320           RETURN
321           END
      C
      C     .....................................................
      C

322           SUBROUTINE ERROR(IER,IERTH)
      C     .....................................................
323      1000 FORMAT(///50X,'*****  W A R N I N G  *****')
324      1100 FORMAT(/10X,'NO FURTHER COMPUTATIONS ARE CARRIED OUT')
325      1200 FORMAT(10X,'BEYOND THE LAST VALUE OF N BECAUSE OF ERRORS.')
326      1300 FORMAT(/10X,'THE ERROR PARAMETERS ARE :')
327      2000 FORMAT(//30X,5HIER =,I3,30X,7HIERTH =,I3)
328           WRITE(6,1000)
329           WRITE(6,1100)
330           WRITE(6,1200)
331           WRITE(6,1300)
332           WRITE(6,2000) IER,IERTH
333           RETURN
334           END
```

```
C
C     ..................................................................
C
      SUBROUTINE OUTPUT(A,BESLHS,BESRHS,M)
      IMPLICIT REAL*8(A-H,O-Z)
      REAL*4 XSIZE,YSIZE,XSF,XMIN,YSF,YMIN
      DIMENSION A(50),XX(65)
      COMMON /SFUM/ S(129)
      COMMON /FFFW/ F(129)
      COMMON /UMWUMN/ UM(129,50)
      COMMON /FFWUMN/ Y(129),Z(129)
      COMMON /UMPAR/ PI,RC,RS,RF,BETA,AA,NS
      COMMON /BLK/ H,NDIM,NBIS
      COMMON /BESANO/ BESN(50),ANO(50)
  500 FORMAT(/2X,5HA'S  ,07D16.7/(' ',6X,07D16.7))
 2000 FORMAT(//11X,14HS - COORDINATE,15X,10HVALUE OF F,15X,15HAPP. VALUE
     1 OF F/)
 3000 FORMAT(F24.6,F25.6,F27.6)
 4000 FORMAT(22X,1HN,20X,1HA,16X,'NORM. BESS. INEQ.')
 4100 FORMAT(44X,2HNO)
 4200 FORMAT(' ')
 5000 FORMAT(20X,I3,F25.7,F25.7)
 6000 FORMAT(1H1)
 6500 FORMAT(25X,'POTENCIAL OF A STRANDED CONDUCTOR')
 6600 FORMAT('CONDUCTOR RADIUS=',F5.2,2X,'NUMBER OF STRANDS=',I2,2X,'FAR
     1RADIUS=',F7.1,2X,'N=',I2)
 7000 FORMAT(3D25.16)
      PI=3.141592653589793
      WRITE(6,500) (A(K),K=1,M)
      BESN(M)=BESLHS/BESRHS
      ANO(M)=A(1)
C
      NO=M-1
      IF(MCD(NO,5).EQ.0.OR.NC.EQ.1) GO TO 1
      GO TO 50
```

```
      1 CONTINUE
        XSIZE=2.01
        YSIZE=4.01
        XMIN=0.0
        YMIN=0.995
        XSF=0.50*(PI/NS)
        YSF=0.005
        ISYM=0
        MODE=4
        XX(1)=0.0D0
        XX(2)=PI/NS
        Z(1)=1.0D0
        Z(2)=1.0D0
        NPTS=-2
C
        CALL GRAPH(NPTS,XX,Z,ISYM,MODE,XSIZE,YSIZE,XSF,XMIN,YSF,YMIN,
     *' ;',' ;',' ;',' ;')
C
        I=1
        M3=8

        NPTS=NBIS/M3+1
        DO 2 J=1,NDIM,M3
        Z(J)=0.0D0
        DO 3 K=1,M
      3 Z(J)=Z(J)+A(K)*UM(J,K)
        Z(I)=Z(J)
        Y(I)=F(J)
        XX(I)=S(J)
        I=I+1
      2 CONTINUE
        WRITE (6,2000)
        WRITE (6,3000) (XX(J),Y(J),Z(J),J=1,NPTS)
        NPTS=-NPTS
        ISYM=1
```

```
      MODE=7
      CALL GRAPHS(NPTS,XX,Z,ISYM,MODE,' ;')
C
      IF(NO.NE.10) GO TO 50
C
C           PUNCH THE VALUES OF THE  A'S
      WRITE(7,6500)
      WRITE(7,6600) RC,NS,RF,NO
      WRITE(7,7000) (A(K),K=1,M)
C
      WRITE(6,6000)
      WRITE(6,4000)
      WRITE(6,4100)
      WRITE(6,4200)
      DO 8 K=1,M
      KK=K-1
      WRITE(6,5000) KK,ANO(K),BESN(K)
    8 CONTINUE
C
      I=1
      DO 9 K=6,M
      Z(I)=1.0D0/(I+4)
      BESN(I)=BESN(K)
      ANO(I)=ANO(K)
      I=I+1
    9 CONTINUE
C
      XSIZE=4.01
      YSIZE=2.01
      XMIN=0.0
      YMIN=0.99999
      XSF=0.05
      YSF=0.000005
      NPTS=-(M-5)
      ISYM=13
      MODE=3
```

```
      C
425         CALL GRAPH(NPTS,Z,BESN,ISYM,MODE,XSIZE,YSIZE,XSF,XMIN,YSF,YMIN,
           *' ;',' ;',' ;',' ;')
426         YMIN=0.997
427         YSF=0.001
428         CALL GRAPH(NPTS,Z,ANO,ISYM,MODE,XSIZE,YSIZE,XSF,XMIN,YSF,YMIN,
           *' ;',' ;',' ;',' ;')
      C
429         XSIZE=8.01
430         YSIZE=4.01

431         XMIN=0.0
432         YMIN=0.997
433         XSF=0.025
434         YSF=0.0005
      C
435         CALL GRAPH(NPTS,Z,ANO,ISYM,MODE,XSIZE,YSIZE,XSF,XMIN,YSF,YMIN,
           *' ;',' ;',' ;',' ;')
      C
436         ISYM=0
437         MODE=4
      C
438         CALL GRAPH(NPTS,Z,ANO,ISYM,MODE,XSIZE,YSIZE,XSF,XMIN,YSF,YMIN,
           *' ;',' ;',' ;',' ;')
      C
439      50 CONTINUE
      C
      C
440         RETURN
441         END
```

XII. APPENDIX F2

```
$JOB            I4229PAREKH,TIME=60,PAGES=100
C      ..........................................
C
C      COMPUTATION OF ELECTRIC POTENCIAL AND FIELD AROUND A STRANDED
C      CONDUCTOR INSIDE A CYLINDER- BY ANALYTICAL METHOD
C
C      ..........................................
 1          IMPLICIT REAL*8(A-H,O-Z)
 2          DIMENSION A(11),ALPHA(11),X1(11),Y1(11),THETA(11),R(11)
 3          DIMENSION ET(11,11),EP(11,11),EXP(10),EXPN(10),BB(11,10),CC(11,10)
 4          DIMENSION EE(11,10),ERF(11),ETF(11),EX1(11),EY1(11),EX2(11)
 5          DIMENSION EY2(11),EX3(11),EY3(11),E(11),GAMA(11)
 6          DIMENSION VC(11,11),V(11),FF(11,10)
      C
      C
 7          READ(5,5) RC,RF,N
 8          READ(5,6) PER
 9          READ(5,7) (A(K),K=1,11)
10        5 FORMAT(2F20.6,I2)
11        6 FORMAT(C15.4)
12        7 FORMAT(3D25.16)
      C
      C      ..........................................
      C
13          PI=3.141592653589793
14          C1=RC*DSIN(PI/N)
15          B1=1.0D0+DSIN(PI/N)
16          RS=C1/B1
17          AA=RC-RS
      C
      C      ..................................
      C
18          WRITE(6,10) RC,RF,N
19          WRITE(6,11) PER
```

```
      WRITE(6,12) RS,AA
      WRITE(6,13) (A(K),K=1,11)
   10 FORMAT('1',//,10X,'CONDUCTOR RADIUS=',F7.4,//,10X,'FAR RADIUS=',F1
     10.4,//,10X,'NUMBER OF STRANDS=',I2,//)
   11 FORMAT(' ',10X,'PERMITIVITTY=',E11.4,//)
   12 FORMAT(' ',10X,'STRAND RADIUS=',F9.6,//,11X,'AA=',F9.6,//)
   13 FORMAT(3D25.16)
C
C     ....................................
C     COMPUTE COORDINATES OF POINTS ON CONDUCTOR SURFACE
C
C     ............................................
      BETA=DARSIN(RS/AA)
      PHI=BETA+(PI/2.0D0)
      PHIL=PHI/10.0D0
C
      DO 15 K=1,11
   15 ALPHA(K)=(K-1)*PHIL
C
      DO 20 K=1,11
      X1(K)=AA+(RS*DCOS(ALPHA(K)))
   20 Y1(K)=RS*DSIN(ALPHA(K))
C
      DO 25 K=1,11
      THETA(K)=DATAN2(Y1(K),X1(K))
   25 R(K)=DSQRT(X1(K)*X1(K)+Y1(K)*Y1(K))

C     ..........................................
C
C     COMPUTE RADIAL FIELD AND FIELD IN THETA DIRECTION
C
C     ......................................
      DD=DLOG(RC/RF)
      K=1
      DO 30 J=1,11
      VC(J,K)=A(1)*DLOG(R(J)/RF)/DD
```

```
41          ET(J,K)=0.0D0
42       30 ER(J,K)=-A(1)/(R(J)*DD)
      C
      C
43          DO 40 J=1,11
44          DO 40 K=2,11
45          KK=K-1
46          EXP(KK)=(KK*PI)/BETA
47          EXPN(KK)=-EXP(KK)
48          BB(J,KK)=(R(J)/RC)**EXPN(KK)
49          CC(J,KK)=DCOS(EXP(KK)*THETA(J))/R(J)
50          EE(J,KK)=DSIN(EXP(KK)*THETA(J))/R(J)
51          FF(J,KK)=DCOS(EXP(KK)*THETA(J))
52          VC(J,K)=A(K)*BB(J,KK)*FF(J,KK)
53          ET(J,K)=A(K)*EXP(KK)*BB(J,KK)*EE(J,KK)
54       40 ER(J,K)=A(K)*EXP(KK)*BB(J,KK)*CC(J,KK)
      C
55          DO 45 J=1,11
56          V(J)=0.0D0
57          DO 45 K=1,11
58       45 V(J)=V(J)+VC(J,K)
      C
59          DO 50 J=1,11
60          ETF(J)=0.0D0
61          DO 50 K=1,11
62       50 ETF(J)=ETF(J)+ET(J,K)
      C
63          DO 60 J=1,11
64          ERF(J)=0.0D0
65          DO 60 K=1,11
66       60 ERF(J)=ERF(J)+ER(J,K)
      C
67          WRITE(6,65)
68       65 FORMAT('1',//,14X,'V',20X,'EX',20X,'EY',20X,'E',18X,'GAMA',//)
69          DO 70 J=1,11
70          EX1(J)=ERF(J)*DCOS(THETA(J))
```

```
71          EY1(J)=ERF(J)*DSIN(THETA(J))
72          EX2(J)=ETF(J)*DSIN(THETA(J))
73          EY2(J)=ETF(J)*DCOS(THETA(J))
74          EX3(J)=EX1(J)-EX2(J)
75          EY3(J)=EY1(J)+EY2(J)
76          E(J)=DSQRT(EX3(J)*EX3(J)+EY3(J)*EY3(J))
77       7C GAMA(J)=(180.0D0/PI)*DATAN2(EY3(J),EX3(J))
78          WRITE(6,80)(V(J),EX3(J),EY3(J),E(J),GAMA(J),J=1,11)
79       80 FORMAT(' ',5F20.6)
80          STOP
81          END

      $ENTRY
```

XIII. APPENDIX G

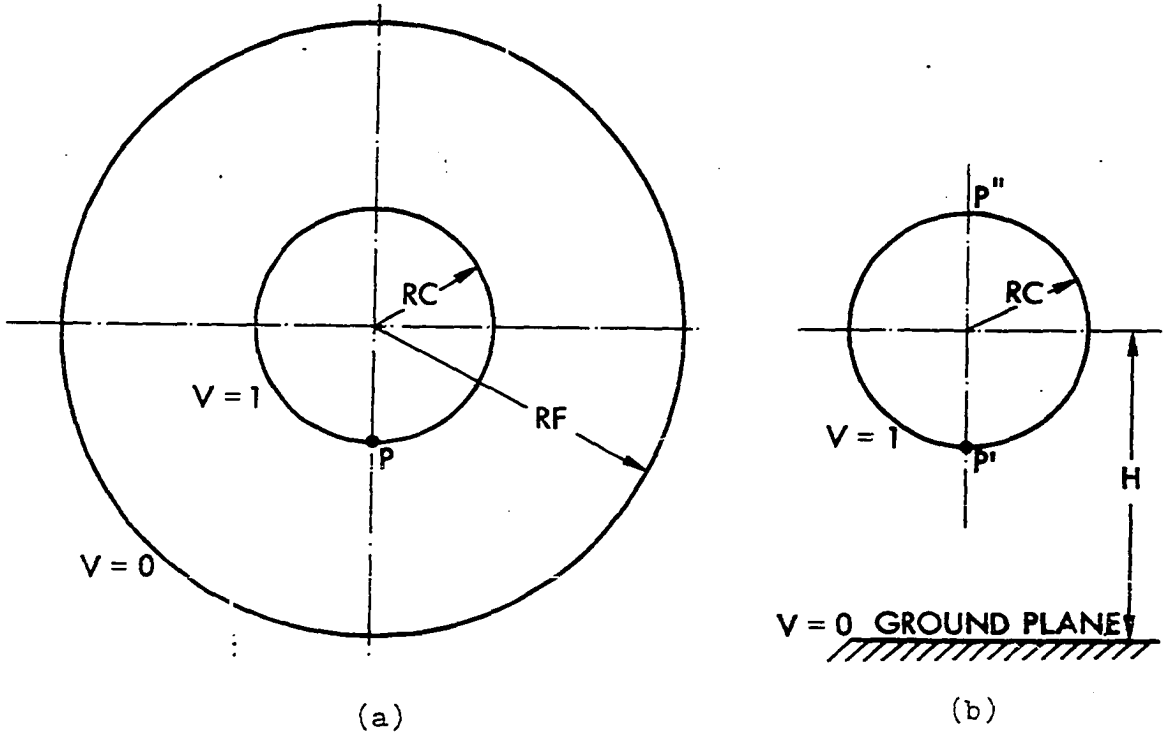

Figure 13.1. Equivalent configurations of transmission lines.
(a) Conductor inside a cylinder.
(b) Conductor above ground plane.

Electric field at any point P on the conductor surface of Figure 13.1 (a) is given by (36)

$$E_P = \frac{1}{RC \ln(RF/RC)} \qquad 13.1$$

Maximum electric field at point P' on the conductor surface of Figure 13.1 (b) is given by (36)

$$E_{P'} = \frac{1}{RC \ln(2H/RC)} \qquad 13.2$$

It can be shown that the ratio of electric field at P'' to that at point P' is given by

$$\frac{E_{P''}}{E_{P'}} = \frac{k - 1}{k + 1} \qquad 13.3$$

where

$$k = H/RC \qquad 13.4$$

For very high values of k, $E_{P'} \simeq E_{P''}$.

Comparing equations 13.1 and 13.2, $E_P = E_{P'}$ when

$$RF = 2H \qquad 13.5$$